A GENERALISED APPROACH TO EVALUATING VOLTAGE RISE IN NETWORKS EQUIPPED WITH DISTRIBUTED GENERATION

S.J. van Zyl

Thesis presented in fulfilment of the requirements
for the Degree of
MASTERS IN ELECTRICAL ENGINEERING
In the Department of Electrical Engineering
UNIVERSITY OF CAPE TOWN
March 2004

Contents

Acknowledgements

I am a part of all that I have met;
Yet all experience is an arch wherethro'
Gleams that untravell'd world, whose margin fades
For ever and for ever when I move.

Ulysses; Alfred, Lord Tennyson

I am grateful to my friends and colleagues for their insight, encouragement and support without which I could not have completed this thesis. My thanks are due to a few people and organisations in particular:

- to Eskom Distribution, and especially the Northern Region, for the opportunity to carry out a number of fascinating DG- and stand-by generator projects, and for the financial support of this research in the form of a study bursary. Elsie Fourie at the Menlyn Information Centre assisted me in obtaining copies of some of the references and proof-read the thesis. Funding of the project from Eskom's Research Group and the National Research Foundation's THRIP programme made it possible for me to present the findings of this thesis at the IEEE Powertech conference in Bologna, Italy. Eskom has also provided me with many interesting and diverse opportunities to develop as an engineer. For their mentorship, I am especially grateful to Patrick Arendse and Clinton Carter-Brown.

- to Clinton Vermeulen and Christo Oosthuizen at the TSB Malelane and Komati sugar mills for their experience and enthusiasm regarding the practical operation of co-generation schemes.

- to Prof. Gaunt at the University of Cape Town, not only for the guidance and encouragement that he offered on this project, but for the ongoing mentorship and inspiration he has provided me throughout my career.

- and especially to Pam and my two families: the Van Zyls and the Barclays who have shared the highs and lows of this project and play such an important role in my life.

Stuart van Zyl
March 2004

Declaration

I hereby declare that I have identified all work by others in this thesis. All other work presented in this thesis is my own.

Signed by candidate

Stuart van Zyl

Acronyms

The following acronyms are used in this thesis:

ACSR	Aluminium Conductor Steel Reinforced (conductor types)
AVR	Automatic Voltage Regulator
CCT	Critical Clearing Time (relating to generator stability)
DG	Distributed Generator, Distributed Generation
EHV	Extremely High Voltage (voltage levels greater than 132kV)
HV	High Voltage (voltage levels from 33kV up to and including 132kV)
LDC	Line-Drop Compensation (AVR control feature)
LV	Low Voltage (less than 1kV)
MV	Medium Voltage (voltage levels from 1kV up to and including 33kV)
NRC	Negative Reactance Compounding (AVR control feature)
OCTS	Off-Circuit Tap Switch
OLTC	On-Load Tap Changer
PF/VAR	Constant power factor or constant reactive power (synchronous generator control mode)
SCR	Short Circuit Ratio

Glossary

Active network. An electrical network that is equipped with at least one source of real-power generation. DG-installed feeders constitute active networks.

Co-generator, Co-generation. A source of electric power that is facilitated by, or is in addition to, some other manufacturing process. Sugar- and paper mills are the most common operators of co-generation in South Africa. In the case of sugar mills, waste cane fibre is used to produce steam that, in turn, is used in the sugar drying process and is available for the generation of electrical energy. Combined Heat and Power (CHP) schemes are common forms of co-generation in countries with colder climates [Jenkins et al., 2000, p.21]. Most co-generators fit the definition of DG, and some (as do sugar- and paper mills) constitute sources of renewable energy.

Distributed Generator, Distributed Generation, Dispersed Generation, DG. According to Gaunt et al. [2002]: "Any source of electric power that is interconnected with an electricty supply network at a system voltage level not exceeding 132kV. The generator is not centrally dispatched. It is probably not a trading participant in a power pool but usually responds to a tariff signal" (p.9).

Distribution networks. In South Africa, distribution networks typically constitute those at voltage levels up to and including 132kV. In the context of this thesis, however, these networks are subdivided into "distribution" systems (1 – 33kV) and "sub-transmission" (44 – 132kV) networks. The term "distribution" in the latter context is also referred to in South Africa as "*reticulation*" and refers specifically to 22kV and 11kV systems and those at lower voltage levels.

Passive network. An electrical network that does not include any sources of real power generation. Traditional distribution feeders, where power is derived only from the transmission system, are examples of passive networks.

Renewable energy. Energy derived from resources that are replaced over a short time period. Wind generators and photovoltaic cells are clear sources of renewable energy. Less obvious examples are generators that are fuelled by wood chips and waste cane fibre, as are commonly operated by paper- and sugar mills.

Reticulation network. See Distribution network.

Sub-transmission network. See Distribution network.

Summary

Reports have indicated a possibility of overvoltage problems that result when operating DG on lightly loaded feeders, and it was expected that the "weak" nature of South Africa's distribution networks might exaggerate these effects. This thesis considers the network parameters that determine the extent of voltage rise in radial networks that are equipped with synchronous DG, and develops a generalised approach to evaluating the phenomenon. The new approach is useful in understanding the relative influence of different network parameters on voltage rise and in evaluating the options for voltage rise mitigation. The research indicates that voltage rise is likely to form a key constraint to the widespread application of DG in South Africa and other African countries.

The application of DG in South Africa is currently limited to a few synchronous co-generation installations that are operated by sugar- and paper mills, and a number of small hydro power stations. The imminent de-regulation of the Electricity Supply Industry and mounting environmental awareness in the country may, however, be catalysts for increased DG penetrations into South African distribution networks. It is thus becoming increasingly important that the effect of these machines on aspects of network operation is well understood.

The application of DG to a distribution feeder tends to improve the voltage profile of the line. This occurs by way of the reduction in the magnitude of load current that must flow across the line impedance from the source substation, and hence reduces the voltage drop with respect to the substation busbar. This phenomenon indicates the potential for DGs to be used for network voltage support, although most DGs do not operate in this role. Rather, many DGs seek to make a profit from the sale of energy to the utility or network operator. Operation of these machines during periods of low system loading can, however, bring about a reversal in the direction of current flow on the feeder. In this event, the voltage profile of the feeder will be seen to rise from the level at the source substation to a maximum value at the DG's point of connection and, in some cases, may exceed statutory voltage regulation limits. This "voltage rise effect" has been encountered with DG applications in Europe and has previously been identified as a key constraint to the widespread application of DG.

The DG-initiated voltage rise effect occurs in a similar manner to the voltage drop phenomenon that occurs in traditional passive electrical networks. Passive distribution networks in South Africa are commonly constrained by voltage drop considerations and it is thus likely that the voltage rise phenomenon will be exaggerated under local network conditions.

Two generalised methods for the evaluation of DG-initiated voltage rise are in use in other countries. The first method is based on the voltage level at which the DG is connected and the location of the machine, while the second method considers the three-phase fault level at the DG's point of connection. Both methods tend to be overly conservative, however, and neither is useful in ascertaining which network parameters most affect the voltage rise phenomenon. It is proposed in the thesis that a better understanding of voltage rise can be obtained using an improved generalised method. Such a method could also facilitate informed decision-making regarding the options for the mitigation of voltage rise. These options include upgrading the conductor, installing a voltage regulator, varying the DG's control mode, lowering the source voltage, and constraining the generator.

A number of published studies use a simple 2-node model to understand the basic mechanism of voltage rise. This approach was used to identify eleven broad factors that were expected to influence the extent of voltage rise in DG applications. Amongst others, these factors included:

(i) *The source impedance seen from the upstream substation busbar.* A survey of the three-phase fault levels at busbars in the Eskom network provided an indication of the busbar source impedances, and confirmed the relative weakness of South African distribution systems. Source impedances are nevertheless small relative to the impedance of typical feeders, and the substation source impedance was subsequently found to have little impact on the constraint imposed on DG by the voltage rise effect.

(ii) *The presence and operation of transformer tap changers and/or voltage regulators on the DG feeder.* Voltage control in MV networks in South Africa is achieved through the predominant application of transformer On-Load Tap Changers (OLTCs), although line-installed voltage regulators are also commonly used. Voltage regulators and OLTCs using fixed setpoint control will operate correctly irrespective of the direction of power flow. Advanced control algorithms such as Line-Drop Compensation (LDC) and Negative Reactance Compounding (NRC) will, however, be negatively affected by the presence of DG. The latter method is commonly used for parallel control of transformers.

    A busbar whose voltage is regulated by OLTC or voltage regulator action can be modelled as an infinite source fixed at the controller's setpoint voltage. In contrast, the source impedance seen from a line-installed regulator cannot be neglected. Rather, voltage studies on regulator-installed networks must be considered in two parts: one study on the network downstream of the regulator location and a second study on the network between the OLTC-regulated busbar and the voltage regulator.

(iii) *The allowable limit for overvoltages on the network.* Statutory regulations and design philosophies in South Africa restrict MV busbar voltages to a maximum of 105% of nominal. This figure, coupled with typical OLTC/voltage regulator setpoint settings, gives rise to an allowable range of DG-initiated voltage rise of between 0.01pu and 0.02pu in

South African DG applications. Significantly, however, a new approach to voltage drop apportionment and MV/LV transformer Off-Circuit Tap Switch (OCTS) setting in Eskom's distribution system will restrict the extent of the allowable voltage rise in some MV networks.

(iv) *The (synchronous) DG control mode.* Through variation of its control mode or controller settings, a synchronous DG can be made to operate at leading or lagging power factors. The choice of operating mode – usually between constant power factor, constant reactive control and voltage feedback control – and operating point is determined by consideration of tariffs, losses and stability. These factors indicate that, when not participating in network voltage control, DGs should be operated at or near unity power factor.

Six assumptions were made to allow a 4-node network model to be used for the generalised analysis of voltage rise. These assumptions included: (i) assuming a uniform distribution of feeder load, (ii) the DG is connected directly onto the backbone of the feeder, and that (iii) a single conductor type is used along the entire feeder length. The 4-node model allows for the representation of a wide range of radial networks, including those at different voltage levels, using different conductor types, and with DGs situated at different locations.

A simple algebraic method, based on the 2-node network theory of other studies, was used to derive an expression for the maximum DG penetration that can be accepted at a particular location on the model DG feeder before the upper voltage regulation limit is exceeded. This method required three simplifying assumptions to facilitate solution in a direct (non-iterative) manner and a Microsoft Excel-based application, using the traditional Gauss-Seidel load-flow method, was written to assess the effect of these on solution accuracy.

The mathematical form of the algebraic solution equation indicates that DG penetration limits can be considered as the sum of three terms:

1) a term that is independent of feeder load and which varies in proportion to the allowable voltage rise and inversely with the conductor resistance. The "No-load" term is hyperbolic with respect to "d", the distance of the DG from the source substation.

2) a "Load" term that is linear with respect to d, and which varies with the load magnitude, location, power factor and the X/R ratio of the feeder.

3) a "Reactive Power Generation" term that is constant with respect to d and which varies with the reactive power generation by the DG, and the X/R ratio of the feeder. For a DG operating at a fixed power factor, this term is transformed into a multiplier of the "No-load" and "Load" terms.

Analysis conducted using the algebraic solution equation indicates that the constraint imposed by the voltage rise effect increases dramatically in the event that the DG is connected to feeders at lower voltage levels. This is compounded in the event that high resistance conductor types are used and where the DG is located far from the source

substation. Feeder load has a significant effect on penetration limits, particularly in weak systems where the no-load penetration limits are small. Loading on weak feeders is, however, limited by voltage drop considerations during times that the DG is out of service. Reactive power absorption by the DG is an effective means of reducing voltage rise only on higher voltage, higher capacity networks. This option gives rise to increased network losses, however, and is difficult to evaluate, owing to the absence of a reactive power pricing tariff for DGs and a procedure for loss allocation between network customers.

The algebraic method can also be used to study the relative efficiencies of other options for voltage rise mitigation. This analysis indicates that a network upgrade is only appropriate in applications on higher voltage networks and for DGs located close to the source substation on distribution feeders. Voltage regulators are a viable option for DGs located at intermediate distances from the source on distribution feeders, while constraining the generator may be the only option for small DG installations and for those located far from the source substation. Methods to increase feeder loading such as using the DG feeder to back-feed an adjacent network are effective in mitigating voltage rise, but could lead to undervoltage problems with the DG out of service.

Comparison of the results from the algebraic solution method with those from the Gauss-Seidel load-flow indicate an inaccuracy less than 7% under most network conditions. Significantly, the algebraic method is most accurate when used on highly resistive and lightly loaded feeders – properties of those networks that are most constrained by the voltage rise phenomenon. The accuracy of the algebraic method is diminished in simulations with heavy reactive power loading on the DG feeder. The decrease in accuracy appears, however, to be related to a sharp increase in line losses on the feeder and should not form a constraint to the method's application.

Despite the assumptions that were made in the derivation of the network model, the algebraic solution equation can be easily modified to accommodate networks with non-uniform load distributions and "tapering" conductors on the backbone and spurs of the feeder. The method is also applicable in cases where the DG is connected to the feeder via a generator transformer, and where the source substation voltage is not regulated by OLTC action.

The algebraic solution method is used as the basis for a generalised process for the evaluation of voltage rise in DG-installed networks. The process is simple to implement and relies on data that is readily available, yet should be sufficiently accurate for most planning studies. The "new" generalised method is more accurate than the two existing generalised techniques and can be used to understand the origin of the fault-level based method. The application of the "new" method is demonstrated in two South African DG case studies.

The thesis concludes that voltage rise is likely to be a key constraint to the widespread application of DG in South Africa and other African countries. It is stressed that voltage rise studies should be performed when evaluating all proposals for DG. The simple analysis technique that was developed in this research may be useful in this regard.

Chapter 1
DG and Network Voltage Regulation

1.1 Introduction

There has been a worldwide increase in the practice of using generators – be it windmills, solar panels or diesel engines – to supply power to distribution networks. Reasons for this trend include the maturation of small generator technologies and difficulties in acquiring funding or land for the construction of larger power stations. The de-regulation of electricity markets has also encouraged the application of DG, as have politically-motivated subsidies for environmentally friendly generation that are provided in many countries. DG has also been seen to thrive in countries with relatively high costs for bulk power generation [Cigré, 1999, p.1].

Given the findings of the 1999 Cigré report, it is not surprising that the application of DG in South Africa is presently very limited. Grid-supplied electricity from the country's coal-fired power stations is among the cheapest in the world. This, coupled with high fuel costs, makes it difficult for diesel engines to compete successfully in the energy market, as has occurred in the United States [Sellick, 1998], and novel generation technologies are prohibitively expensive to import or develop. The latter statement was borne out with the commissioning of South Africa's first wind farm at Klipheuwel in the Western Cape in February 2003 at the cost of R45-million for a total generation capacity of only 3.2MW[1]. Environmental pressures in South Africa are also lenient relative to those in "developed" countries, and local utilities presently have little incentive to adopt such "green" forms of power generation on a large scale.

The high price of fuel and technology has limited DG applications in Southern Africa to a handful of schemes that operate synchronous generators and which utilise a "free" source of fuel. Bagasse - waste cane fibre - is a ready fuel source that is available from the sugar refining process, and is used in at least four co-generation applications in the Mpumalanga and KwaZulu-Natal provinces, as well as a 20MW scheme in Zimbabwe[2]. A number of paper mills in South Africa use wood shavings to fuel embedded generators, with one plant in Mpumalanga possessing generation to the capacity of 117MW. At least six hydro power stations are also in operation in Southern Africa: four stations in the Transkei region generate

[1] In *Eskom News*, April 2003, p.4-5.

[2] In *Energise*, the power journal of the SAIEE, March 2003, p.37.

up to a total of 61MW onto the local electricity networks, and although operated by Eskom, fit the accepted definition of DG. Two hydro stations in Lesotho also operate as DG [Gaunt et al., 2002].

Even though the outlook for DG in South Africa is presently limited, there is reason to believe that this may change in the near future. Possible catalysts for change include the gradual transition of the country's electricity supply industry towards de-regulation and the steadily increasing environmental awareness in the country. With regard to the latter aspect, it may be significant that the South African government acceded to the United Nation's "Kyoto Protocol" in July 2002 and has thus undertaken to reduce the levels of greenhouse gas emissions by its heavy industry. This may create future opportunities for increased generation using the "renewable" resources of the country's sugar- and paper mills.

The potential for increased penetrations of generators into the country's distribution networks makes it increasingly important that the effect of these machines on aspects of system operation is clearly understood.

1.2 Impact of DG on Distribution Networks

Documentation from those schemes that currently operate in parallel with distribution networks in South Africa indicate that each application was extensively evaluated in terms of its influence on safety and on generator and intertie protection. All concerns in this regard appear to have been effectively handled through the application of detailed switching and isolation procedures, and the provision of synchronism check and "live-line close-blocking" functionality on selected circuit breakers in the network. Further considerations regarding safety and protection aspects are also well documented in the Eskom guideline on the interconnection of DG [Topham, 1995]. Similar documents also exist from other countries, for example the UK's "G59/1" described in Jenkins et al. [2000, p149-188] and the American standard IEEE P1547 [2001].

Apart from safety and protection issues, the application of DG is also known to have an influence on equipment ratings and on aspects of network voltage quality and voltage regulation. Surprisingly, no record exists of detailed studies having been performed in these areas with respect to local DG projects. In reality, however, it is unlikely that equipment ratings have been compromised by DG in this country, because fault levels on South Africa's distribution networks are generally low with respect to equipment rupturing capacities. Also,

while it is acknowledged that DGs operating on weak electrical systems[3] may cause unacceptable transient voltage variations when switched, Cigré Task Force 38.06.04 [2002, p.11] comments that such problems are unlikely in applications with synchronous machines, provided that they are synchronised correctly and they are not disconnected at full-load. No such mitigating factors exist to lessen the influence of DG on the regulation of steady-state voltage levels in DG-connected networks. In fact, it is seen from the following discussion that voltage regulation problems may form the primary barrier to the widespread application of DG in South Africa.

1.3 Impact of DG on Network Voltage Regulation

The inclusion of DG on a distribution feeder tends to improve the voltage profile of the line. This occurs by way of the reduction in the magnitude of load current that must flow across the line impedance from the source substation, and hence reduces the voltage drop with respect to the substation busbar [Masters, 2002]. This effect indicates potential for DG to be applied for the purposes of network voltage support. In fact, Sellick [1998] reports that diesel generators have been applied in this role on long distribution feeders in the United States since at least 1985, and discusses the possibility of using DG in the same manner in South Africa. Actually, several small hydro-generators in the Transkei area have been providing network support for a number of years and, in recent times, have become a pre-requisite for maintaining voltage stability in the area. The widespread application of DG in a network supporting role is, however, constrained by the high price of fuel and the lack of an effective pricing- or scheduling mechanism for the service. As a result, applications of DG in this role are generally limited to select machines that are owned and operated by power utilities.

Many DGs do not specifically provide network voltage support, although the application of "time of generation" tariffs does encourage their operation during periods of heaviest network loading. Ultimately, however, the decision on whether on not to generate at a particular time remains at the discretion of the DG operator and this, as in the case of co-generators, may be aligned more with the requirements of a core manufacturing process rather than with the offered electricity price. As a result, some DGs may export power to the network during periods of low system loading and, instead of merely reducing the magnitude of current flowing from the source, may bring about a reversal in the direction of current flow. In this event the voltage profile of the feeder will be seen to rise from the level at the source substation to a maximum value at the DG's point of connection, and in some cases may

[3] A "weak" network is defined in this thesis as one that is constrained by voltage-related aspects rather than by the thermal capacity of the components, or by aspects of waveform quality. In Chapter 2 is it seen that "weak" networks are also characterised as being those with high source impedances.

exceed statutory voltage regulation limits. This "voltage rise effect" has been encountered with DG applications in Europe and is described by Cigré Task Force 38.06.03 [2002, p.8-9] and Masters [2002] as a key constraint to the widespread application of DG.

Cigré Task Force 38.06.03 [2002, p.41-2] identifies three options for the mitigation of the voltage rise phenomenon:

1. Reactive power compensation achieved by altering the generator control mode (in the case of synchronous DGs),
2. Co-ordinated voltage control achieved using On-Load Tap Changers (OLTCs) on substation power transformers, and
3. Constraining the generator.

Masters [2002] also discusses the above mitigation options and describes two others:

4. Installing a voltage regulator on the DG feeder, and
5. Upgrading the network.

Each of the five options for the mitigation of the effect will have cost implications for DG operators, and may themselves form a constraint to the application of DG technologies.

It is possible that the voltage rise effect will be of special significance for DG applications in South Africa. This is because the country's rural distribution networks are normally constrained by voltage considerations, albeit undervoltage rather than overvoltage scenarios [Carter-Brown and Gaunt, 2003]. The previous discussion identified that the mechanism for network voltage rise is similar to that which causes voltage drops in passive networks, and it is thus possible that the voltage rise effect will be exaggerated under local system conditions.

Generalised evaluation of the voltage rise effect

Cigré Task Force 38.06.03 [2002, p.10] describes two generalised rules for the evaluation of the extent of the voltage rise problem in different applications. The generalised methods prescribe maximum limit for power export by DGs at different network locations so as to avoid steady-state overvoltage conditions. In fact, these methods also attempt to include the effect of DG on power quality in a single parameter. The first method involves the application of standard generator capacity limits based on the voltage level of the DG-feeder and the electrical location of the machine. Typical values used in this approach are given in Table 1.1 below.

Table 1.1. Standardised penetration limits for DGs based on their electrical location.

[Cigré, 2002, p.10]

DG location	*Maximum DG capacity*
Anywhere on a 63kV – 90kV network	10-40MVA
Anywhere on a 15kV – 20kV	6.5-10MVA
At an 11kV or 11.5kV busbar	8MVA
Elsewhere on an 11kV or 11.5kV network	2-3MVA
At a 400V busbar	200-250kVA
Elsewhere on a 400V network	50kVA

The second general method uses the three-phase fault level at the DG's point of connection as an indication of the allowable DG penetration limit[4]. A common stipulation in this regard is that the three-phase fault level at the generator location must be at least a given number of multiples of the DG's rating. A multiple of 10 is used in evaluating DG projects in Spain [Cigré, 1999, p.42], whilst multiples as high as 25 have been specified in other countries [Cigré, 2002, p.10].

Cigré Task Force 38.06.03 [2002] comments that the generalised methods must cater for the worst case of a number of network parameters and that they tend to be overly conservative as a result. In this regard the Task Force comments that: "if such rules were to be [widely] applied they would lead to a very conservative and restrictive approach to the connection of dispersed generators" (p.10). As a result, many countries opt to perform detailed studies per DG application. An accurate, generalised method would, however, be useful in understanding the mechanism by which voltage rise occurs. Also, a generalised method might provide an answer to the question:

- Which network parameters are most important in determining the extent of the voltage rise problem in DG applications?

In the absence of an answer to this question, it is not possible to evaluate, in general, the extent of the voltage rise problem that will occur with increased DG penetrations into South African distribution networks. An answer to the above question is also important on account of the fact that it will improve the understanding of the mechanism by which the five mitigation options achieve a reduction in network voltage rise and may suggest alternative solution methods. The first question also provides a basis for a second question:

- Which is the optimal method for the mitigation of network voltage rise in typical DG applications?

---

[4] Both methods consider only single-generator applications, or applications that can be modelled as a single installation (for example, wind farms).

1.4 Hypothesis and Research Methodology

This research addresses the following basic hypothesis:

> *It is possible to improve the existing generalised methods for the evaluation of the influence of synchronous DGs on the steady-state voltage regulation of radial distribution networks to which they are connected. By design, the improved process should remain simple to implement; relying on data that is readily available, yet its results should not be overly conservative. The method should be useful in seeking realistic solutions to the voltage rise problem.*

The hypothesis describes the derivation of an improved evaluation method of voltage rise in *synchronous* DG applications on *radial* distribution networks. The two evaluation methods described by the Cigré Task Force are not limited to a particular generator technology, or to a particular network topology. These limitations are applied in the present study in an effort to simplify the analysis. It may occur, however, that the results of the present study can be generalised to include alternative generator technologies and meshed networks.

Evaluation of the hypothesis requires that an understanding of the mechanism of network voltage rise be developed. The phenomenon is not particular to South African networks, however, and it is expected that an amount of research would have already been completed in this regard. This work should provide a good basis for understanding methods by which the voltage rise effect can be studied and will also serve to identify the limits of allowable voltage rise in different electrical systems. These methods might then be adapted and applied to local network conditions.

The discussion in Section 1.3 indicated that there is a correlation between voltage rise effects in DG-installed networks and voltage drops in passive systems. An understanding of network voltage rise might thus be obtained using similar methods to those used for traditional voltage studies. Such studies are commonly performed using established load-flow techniques. This research seeks to apply these methods to the evaluation of the main hypothesis. The studies use parameter values typical of local network conditions and the concepts are demonstrated using two South African DG case studies.

The five options for the mitigation of DG-initiated voltage rise presented by Cigré Task Force 38.06.03 [2002] and Masters [2002] indicate that traditional voltage regulation methods and options for synchronous DG control are key elements in the study of the phenomenon. The second voltage rise evaluation method described by the Cigré Task Force uses the fault level at the DG location as a measure of the anticipated problem. The application of fault levels as a gauge of steady-state voltage problems is another key element that will be addressed in this research.

Possible voltage regulation problems arising from the introduction of generators to distribution networks and the proposed derivation of a generalised evaluation method lead to the following research questions:

- Which methods can be used to study the voltage rise effect?
- What is the limit of allowable voltage rise in electrical networks?
- To what extent can the fault level at a busbar be used to determine the degree of the voltage rise problem arising from DGs installed at that location?
- How is adequate regulation of voltage attained in passive distribution systems?
- To what extent are classical voltage regulation methods applicable for the mitigation of voltage rise in DG-installed networks?
- What control mode options are available to synchronous DG operators?
- What factors influence the choice of DG control mode?

Answers to the above questions are sought in published material in the literature survey of Chapter 2. This information is developed further in subsequent chapters to provide an insight into the feasibility of the basic hypothesis.

1.5 Relevance of this Research

In considering single-machine synchronous DG applications on radial distribution networks, the present research is particularly relevant to the study of possible overvoltage conditions arising from the operation of co-generators. In South Africa, sugar- and paper mills are the principal operators of DGs whose purpose is other than the provision of network support. These operators are likely to benefit most from future changes in environmental regulations and are thus the most likely to request permission for new generator installations or increased levels of penetration from existing facilities.

The hypothesis on which the research is based is not limited to voltage rise only in South African DG applications. While the examples and case studies will draw on data that is typical of South African systems, the method should be applicable to DGs on any distribution network.

1.6 Structure of the Thesis

The structure of this thesis is guided by the objectives of the research and the process that must be followed in order to evaluate the hypothesis. The chapters that follow are briefly outlined below.

Chapter 2 includes a review of available literature on network voltage regulation and, in particular, the DG-initiated voltage rise effect as pertaining to the objectives of the hypothesis.

Chapters 3, 4 and 5 include more detailed discussions of three broad aspects arising from the literature survey. Chapter 3 examines the voltage rise phenomenon in detail, whilst Chapters 4 and 5 discuss voltage regulation in distribution networks and the operation and control of synchronous machines respectively.

The information from the previous chapters is consolidated in Chapter 6 with the derivation of a network model and, ultimately, a method for the evaluation of network voltage rise.

In Chapter 7, the evaluation method is applied to typical network scenarios to determine the relative influence of network parameters on the voltage rise effect, and establish the usefulness of the approach.

Chapter 8 investigates the extent to which a number of assumptions that were made in the derivation of the method influence the accuracy of the results it delivers.

The developed method is applied to the evaluation of the voltage rise mitigation options in Chapter 9. The method is also used in this chapter as the basis for a logical process for the evaluation and mitigation of voltage rise in DG projects. The application of the process is demonstrated using two South African DG case studies.

Chapter 10 summarises the findings of the research, evaluates the hypothesis and reviews the voltage rise problem in South African DG applications.

1.7 Chapter in Perspective

The DG-initiated voltage rise effect has been identified as a key constraint to the widespread application of generators on distribution networks. It is likely that the phenomenon will be exaggerated by network conditions in South Africa, yet this is difficult to analyse in the absence of a simple, accurate evaluation approach. Such an approach would lead not only to a better understanding of the effect, but would also facilitate informed decision-making regarding the application of mitigation options.

Key questions have been identified whose solution will facilitate the evaluation of the hypothesis. The next chapter includes a review of relevant literature relating to these questions, with the intention of establishing the existing base of knowledge on which the present research can be founded.

Chapter 2

Published information on Network Voltage Rise

Chapter 1 identified a number of questions related to the hypothesis that an improved generalised method for the evaluation of DG-initiated network voltage rise could be developed. The present chapter includes a review of published information that provides solutions for, or further insight into, these questions.

The questions in Chapter 1 can be grouped into four broad topics; a framework that is used in the present chapter to structure the literate survey. These topics and the purpose of the corresponding sections of the literature survey are as follows:

1. *The study of the DG voltage rise effect.* Identify studies that have been performed to establish the extent of the voltage rise problem in different types of networks. Examine the methods used and the network parameters that are considered. This discussion must establish the limits for voltage rise on different types of network that define the point at which the phenomenon will impose constraints on DG operation.

2. *Fault levels.* Determine the scope of application of fault level studies for the analysis of voltage regulation problems in electrical networks. This discussion seeks to ascertain the principle on which the fault level-based generalised method is founded.

3. *Voltage regulation methods.* Establish the methods that are used to achieve voltage regulation on passive distribution networks. Determine the extent to which these methods are affected by the presence of DG, and the extent to which they will be effective in mitigating against the voltage rise effect.

4. *Operation and control of synchronous generators.* Identify references on aspects of the operation and control of synchronous DGs. Establish the control mode options for DGs and identify the parameters that influence control mode selection.

2.1 The Study of DG-initiated Network Voltage Rise

Three studies concerning the voltage rise effect in DG-installed networks use a simple 2-node network comprising a single branch impedance to understand the mechanism by which the phenomenon occurs [Pandiaraj et al., 2000; Salman et al., 1996; and Masters, 2002]. The same method is used in engineering textbooks such as Weedy [1994, p.79–81] and Glover and Sarma [1994, p.214-6] to understand the relationship between busbar voltages and network power flows in traditional passive networks. This method is referred to in Glover and Sarma as the "short line approximation" of a transmission line and, in neglecting the shunt admittance, is stated to be accurate for the representation of transmission lines that are less than 80km long. McCann [1950, p.265] comments that this method is appropriate for the analysis of voltage problems on all lines of voltage less than 40kV.

McCann [1950, p.270] also describes how the 2-node analysis method can be used to calculate the sending-end busbar voltage with respect to the receiving-end quantities. The method cannot, however, be used to calculate the receiving-end busbar voltage with respect to the sending-end parameters without employing an iterative solution method or applying a number of assumptions [Pandiaraj et al., 2000]. This limitation of the 2-node method has restricted its application in most studies to that of placing the voltage rise effect in context.

Detailed studies

Detailed study of the effect of different network parameters on network voltage rise is accomplished in many studies through the use of a model network. Studies such as those by Pandiaraj et al. [2000] and Repo et al. [2003] use models based on real-life networks, while others by Salman et al. [1996], Persaud et al. [1999], Masters [2002] and Kiprakis and Wallace [2003] use hypothetical systems. These studies typically assume constant values for most network parameters and vary selected parameters according to the objectives of the research. In this regard, Table 2.1 summarises the objectives of each of these studies, as well as the models used and the variables that were considered.

Table 2.1. Summary of detailed studies relating to DG-initiated network voltage rise.

Study	Purpose	Network model used	Variables considered
Salman et al. [1996]	Investigate the effect of different control strategies for synchronous DGs on the voltage rise effect.	9-bus network, including two 33kV busbars upstream of two 33/11kV transformers. Feeder load is applied at three busbars on the 11kV network.	- Load magnitude. - Generator control mode. - Automatic variation of the transformer tap position.
Persaud et al. [1999]	Investigate the influence of DG location and power output on the operation of an advanced tap change control strategy.	20-bus 11kV network, including six lateral feeders. Different conductor types are used on the backbone and spurs. The source substation transformer is discretely modelled with a tap changer that uses an advanced control algorithm.	- Feeder load magnitudes exhibit voltage dependency. - Load magnitude and generator output. - DG location. - Automatic variation of the transformer tap position.
Masters [2002]	Generalised study of network voltage rise and its mitigation.	6-bus, 11kV network of a single conductor type and uniformly distributed load.	- Generator output. - Generator location. - Conductor type. - Voltage at the source substation. - Application of a voltage regulator. - Operation of DG at a leading power factor.
Pandiaraj et al. [2002]	Investigate the optimal control mode for synchronous DGs that operate for network voltage support.	4-bus 11kV network. Total feeder load is distributed between the nodes.	- Feeder load magnitude and power factor vary according to a typical daily load profile. - Generator control mode.
Repo et al. [2003]	Investigate methods to increase the allowable DG output in a wind farm application without exceeding voltage limits.	27-bus network including discrete representation of the 110/20kV power transformers. The network is based on a real-life system. Load is located at 13 busbars and magnitudes are based on metered data.	- Generator control mode. - Voltage at the source substation. - Network configuration (operation as a ring network).
Kiprakis and Wallace [2003]	1. Develop a hybrid control strategy for synchronous DGs.	5-bus network with an infinite source. The model includes representation of a "tapered"[1] feeder backbone. Load is uniformly distributed between busbars.	- Generator control mode.
	2. Investigate the potential application of a voltage regulator with a custom control algorithm for voltage rise mitigation.	Conductor between Buses 2 and 3 is replaced by a representation of a voltage regulator for a second series of studies. Load is lumped at the DG busbar	- Feeder load magnitude varies according to a typical daily load profile. - Automatic variation of the regulator tap position.

[1] "Tapering" refers to the common practice of using successively thinner-gauge conductors further from the source substation on account of the reduced loading and hence voltage drops encountered.

The results of Table 2.1 indicate that at least ten different network parameters have an influence on the voltage rise effect. The individual studies consider a number of different combinations of these variables, yet it is difficult to generalise their overall findings, or to determine the relative influence of different variables on the voltage rise effect. The study by Masters [2002] considers the broadest range of variables of all of the studies, but the discussion is of a more qualitative nature and the relative influence of the different variables on the voltage rise phenomenon is not explored in detail.

Voltage regulation limits

All of the studies listed in Table 2.2 originate from European countries where the extent of allowable voltage rise is limited to 6% above nominal voltage. Persaud et al. [2002] and Salman et al. [1999] comment, however, that a stricter limit of +2% is applied on 11kV networks in Northern Ireland. On a similar note, Masters [2002] comments that voltage rise is often limited to +3% during the planning stage of 11kV networks in Britain and Scotland.

Voltage regulation limits in South Africa are specified in the South African Electricity Act (Act 41 of 1987) and NRS 048 as described by Carter-Brown [2002c, p.13-5]. NRS 048 requires that the highest voltage on a MV system lies within +5% of nominal, although contractual agreements between Eskom and customers sometimes stipulate a +7.5% limit. Interestingly, Carter-Brown describes a new philosophy for the apportionment of voltage drops between MV and LV reticulation systems that can impose more strict limits on overvoltages in MV networks. This topic is discussed in detail in Section 4.3.

Direct and indirect approaches to the study of network voltage rise

Most of the references listed in Table 2.1 use a direct approach to study the influence of different network parameters on the busbar voltages in the model networks. In these studies, the busbar voltages are calculated as a function of the chosen network variables and the results are presented as a series of graphs where the busbar voltages (as the dependent variables) are plotted on the y-axis. Examples of this occur in Masters [2002] and Kiprakis and Wallace [2003], where the voltage rise phenomenon is studied for particular applications by considering the voltage profile of the line: a plot of busbar voltage as a function of busbar location. Other studies such as those by Persaud et al. [1999] and Salman et al. [1996] consider busbar voltages as a function of feeder load magnitude and transformer tap position. Network voltage regulation limits appear as horizontal lines in these graphs, allowing violations to be readily identified.

A study by Masters [2002][2] into the effect of two parameters on the extent of network voltage rise does not consider the actual values of the busbar voltages. Rather, the study determines the maximum real-power output by DGs at different locations that can be accepted before the onset of overvoltage conditions at any location on the line. In this way, Masters's results are presented as a series of curves with "DG penetration" as the dependent variable. This alternative approach to studying network voltage rise is unique in that it considers the *constraint* that will be imposed on DGs by the phenomenon, rather than considering the effect directly. This approach incorporates network voltage regulation limits into the solution algorithm.

Techniques for the solution of model networks

None of the studies described in Table 2.1 are clear as to the methods used to solve the network models. It is probable, however, that many studies employ commercial load-flow programs for this purpose. Weedy [1994, p.221-35], however, describes a number of numerical methods that might equally have been used. Two of the most widely used methods include the Gauss-Seidel and Newton-Raphson iterative techniques.

Weedy [1994, p.227] comments that the modern trend in load-flow solution is to apply the Newton-Raphson technique that offers greater assurance of convergence and economy of computation time when compared to the more traditional Gauss-Seidel method. The former method involves the application of partial differential equations, however, and is thus more complex than the Gauss-Seidel technique. The speed of convergence of the Gauss-Seidel method can be increased through the application of acceleration factors. This method also readily allows for the representation of transformer tap changers [Weedy, 1994, p.225-6]. Of the two solution methods, the Gauss-Seidel algorithm appears best suited to the solution of relatively small, simple networks described in Table 2.1.

[2] Masters describes a number of different voltage rise studies, including those that study voltage rise using direct and indirect methods.

2.2 Fault Levels

The fault level at a particular location in a network is calculated according to the expression:

$$\text{Fault Level (MVA)} = \sqrt{3} \times V_{Nom} \times I_f \qquad (2.1)$$

Where: V_{Nom} = the nominal voltage (kV), and
I_f = the current drawn by a three-phase fault at the point of interest (kA).

Jenkins et al. [2001, p.68-9] explain that, when expressed in the per-unit system[3], the fault level is equal to the per-unit three-phase fault current at that location. Further, if it is assumed that the pre-fault voltage at the fault location is equal to the nominal voltage, then:

$$\text{Fault Level (pu)} = I_{f(pu)} = \frac{1}{|Z_{th(pu)}|} \qquad (2.2)$$

Where: $I_{f(pu)}$ = the per-unit three-phase fault current, and
$Z_{th(pu)}$ = the Thevenin impedance of network as seen from the fault point (pu).

In this way, Jenkins et al. describe how the fault level gives an indication of the electrical proximity of a particular point to the source of the system. The fault level can thus be used as a measure of the "strength" or "stiffness" of a network from a given location. By Eq. 2.2, larger fault levels correspond to smaller Thevenin impedances. This, Jenkin et al. explain, indicates that "the voltage drop caused by a given load will be smaller at busbars where the fault level is high" (p.69). This discussion establishes a connection between fault level and voltage regulation, and begins to explain the basis for the fault level-based approach to DG capacity limitation.

Beukes et al. [2001, p.11.7] comment that the relative strength of a system can be expressed relative to the loading on the network by considering the Short Circuit Ratio (SCR). This is given by the expression:

$$SCR = \frac{\text{Fault level (MVA)}}{\text{Connected Load (MVA)}} \qquad (2.3)$$

In a draft Eskom planning guideline, Ferguson [2003] describes how SCRs have a major influence on voltage dips and flicker in electrical systems. The guide prescribes minimum SCRs at the points of connection of different flicker and dip-producing load types. The requirements include a minimum SCR of between 12 and 73 for crushers, 50 for an AC arc furnace, and 150 for a direct on-line motor that is switched less frequently than once an hour.

[3] The Per-Unit System is discussed in more detail in Appendix A.

There is a close similarity between the SCR approach to ensuring voltage quality in passive networks and the fault level-based rule described by Cigré Task Force 38.06.03 [2002] for the limitation of voltage rise and quality problems in DG-installed networks. No clarity could, however, be found in the literature regarding the selection of limit values for either approach.

The previous discussion indicates that a comparison of busbar fault levels in different countries can be used as a measure of the comparative strength of their electrical networks. In this regard, Weedy [1994, p.268] lists typical maximum fault levels for the British system. No references were found that described typical fault levels in South Africa's or other countries' networks.

2.3 Voltage Regulation Methods

Weedy [1994, p.182-188] describes two broad methods of achieving voltage control in electrical systems: injection or absorption of reactive power, and transformer tap changing. The former method includes the application of series- and shunt capacitors or reactors, and variation of the control mode of synchronous machines that operate on the network (the latter topic being discussed in Section 2.4).

Series- and shunt capacitors/reactors

Series- and shunt capacitors have traditionally been used to provide compensation for lagging power factor loads, decreasing the extent of voltage drops. Reactors are used for loads at leading power factors and serve to restrict voltage rise [Weedy, 1994, p.184]. This suggests that reactors may be appropriate for the mitigation of voltage rise in DG applications.

Repo et al. [2003] consider the application of shunt reactors to reduce the voltage rise in a wind farm application. In this case, the reactor compensates not for the voltage rise caused by a leading power factor load – a lightly loaded cable, for example – but mitigates that caused by real power export by the DG. Repo et al. note, however, that "use of the reactor doubles the active power losses of the whole distribution network." It is possibly for this reason that none of the other studies in Table 2.1 consider the application of shunt reactors for the mitigation of voltage rise. This topic is likely to be similar to that of having a synchronous DG operate at a leading power factor[4], however, and could be considered as an

[4] As is common practice in industry, reference to DG power factors in this thesis are made using the generator convention where "leading" refers to the absorption, and "lagging" to the sourcing of reactive power. Reference to the power factor of a load, for example that which flows through a utility transformer, is made using the load convention where "leading" and "lagging" have opposite meanings to those of the generator convention.

extension of that discussion. The possible application of shunt reactors in DG-installed networks is thus not considered further in this thesis.

Salman et al. [1996] comment that connecting the DG to the network via a generator transformer (essentially a series reactor) increases the efficiency of reactive power absorption by the DG as a mitigation option. None of the studies in Table 2.1 consider the application of a dedicated series reactor for the mitigation of voltage rise. This is most probably a result of the fact that a series reactor would give rise to increased voltage drops in the presence of lagging power factor load, and would thus have to be switched in the event that the DG is out of service. This is in contrast to a voltage regulator that can remain in service irrespective of the direction of power flow.

Transformer tap changing

Step voltage regulating transformers can be described in terms of two categories of devices [Carter-Brown, 2002b]:

1. Variable ratio power transformers - units that transform between different voltage levels (eg. 132/22kV), but which are also equipped to regulate the secondary voltage, and

2. Regulating transformers - devices whose primary function is to regulate the secondary voltage and which do not change voltage levels.

In this thesis, as is common in industry, variable ratio power transformers are referred to as "tap changing transformers" and regulating transformers are termed simply "voltage regulators". The former category can be further sub-divided into units that can automatically vary their transformation ratio while on-load, termed "On-Load Tap Changers" (OLTCs), and those which must be manually altered while disconnected from the load: "Off-Circuit Tap Switches" (OCTSs).

In two publications, Thomson [2000a&b] describes the fundamentals of OLTC operation and control. Two advanced control techniques, Line Drop Compensation (LDC) and Negative Reactance Compounding (NRC), are described, and Thomson discusses how the accuracy of these methods is reduced with the introduction of DG to the network. Salman et al. [1996] also describe the negative effect of DG on the accuracy of the LDC control algorithm, while Carter-Brown [2002a] describes the scope of application of this technique in passive distribution networks.

Carter-Brown [2002b] discusses many aspects of voltage regulator application to distribution networks, including their theory of operation, technical information and considerations for their sizing and placement. The use of voltage regulators in DG applications is not specifically considered. In her discussion of these applications, however, Masters [2002] makes no reference to any special conditions that are specific to DG-installed networks.

2.4 Operation and Control of Synchronous Generators

The theory of operation of synchronous DGs is described by Jenkins et al. [2001, p.97-131]. This discussion is similar to that presented in classical textbooks on electrical machines, such as Sen [1989] and Weedy [1994, p.88-110].

Jenkins et al. [2001, p.103-4] describe the options for the excitation control of synchronous DGs. A "quadrature droop characteristic" is used for excitation control of large synchronous generators, but Jenkins et al. comment that: "[this] control scheme may not be appropriate for small embedded synchronous generators" (p.104). Instead, the control strategy for synchronous DGs is most often based on reactive power output rather than on the network voltage. In this regard, the studies listed in Table 2.1 consider DGs operated in fixed reactive power or fixed power factor control mode as the base case. Many of the studies, for example those by Salman et al. [1996], Pandiaraj et al. [2002], Repo et al. [2003] and Kiprakis and Wallace [2003], also consider the operation of DGs in voltage control mode. Pandiaraj et al. [2002] find, however, that the DG is incapable of maintaining the busbar voltage within statutory limits by using voltage control mode, although voltage fluctuations are reduced when compared with operation at a fixed power factor. This is related to the capability curve or performance chart of the machine, as described by Weedy [1994, p.101-3].

The choice of control mode for DGs is influenced by the tariff for reactive power generation or absorption. Cigré Task Force 38.06.03 [2002, p.22] comments, however, that "VAR management as a means of reducing the voltage fluctuations in distribution networks is not supported by appropriate pricing mechanisms" (p.22). Guidance on pricing for DGs in Eskom's networks is given in Crous [2001], although no decision is made regarding the policy for reactive power absorption by DGs.

The choice of control mode and operating point of DGs has an effect on network losses. In this regard, Cigré Task Force 38.06.03 [2002, p.42] comments that absorption of reactive power by DGs leads to an increase in network losses, and that evaluation of DGs operating in this mode should include loss assessment. This is similar to the finding by Repo et al. [2003] regarding the increased losses that are brought about with the application of shunt reactors to reduce voltage rise.

Cacioli et al. [2001] describe how DGs that are made to absorb reactive power from the network are more prone to instability than those which generate reactive power. Selection of the control mode for a synchronous DG is thus seen to have an effect on the stability of the machine. This is especially significant given the finding of Mabuza and Gaunt [2002] that DGs connected to weak distribution networks are prone to instability.

2.5 Chapter in Perspective

The literature survey has provided preliminary answers to many of the research questions from Chapter 1. These answers are developed further in the detailed analysis of later chapters. In particular, Chapter 4 considers fault levels, voltage regulation methods and limits for voltage rise in the South African context and Chapter 5 considers the operation and control of synchronous generators in more detail.

None of the previous studies identified in the literature survey have attempted to perform a generalised analysis of DG-initiated voltage rise. These studies have, however, suggested an approach by which this can be achieved: develop a network model that is representative of typical network conditions, and determine the penetration limit for DGs at different network locations. This task is pursued in Chapter 6. Prior to that, Chapter 3 uses the simple 2-node analysis method that was identified in Section 2.1 to develop a better understanding of the voltage rise effect.

Chapter 3

The DG Voltage Rise Effect

The DG-initiated voltage rise effect can be understood in its simplest form by applying basic engineering principles to a simple 2-node network model. In Section 2.1 it was seen that many authors on the topic of network voltage rise have used this method of analysis to place their work in context. The simple analysis technique is used for the same purpose in the present study, and is described in detail in Sections 3.1 and 3.2 to follow. It is seen that, despite its simplicity, the approach provides valuable information regarding the network parameters likely to affect voltage rise and is useful for analysing the methods by which the effect can be mitigated.

3.1 Understanding Voltage Regulation

The simple technique for analysing the voltage rise phenomenon on DG-installed networks is not a new concept. In fact, the technique has traditionally been used to understand voltage regulation in passive networks. The technique is, however, equally useful when applied to active distribution systems.

3.1.1 Voltage regulation - simple network analysis [Weedy, 1994, p.79-81]

The principle of voltage regulation in electrical systems is understood in its simplest form by considering two nodes that are interconnected by a conductor of given impedance (R+jX), and across which real (P_1) and reactive (Q_1) power is transferred (refer to Fig. 3.1 below).

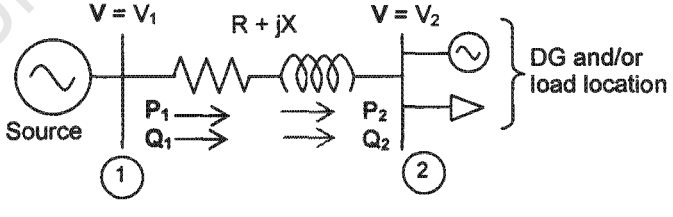

Note: P_1 and Q_1 are positive when flowing *away* from bus 1, whilst P_2 and Q_2 are referenced as positive *into* bus 2.

Fig. 3.1. Simple network model used to understand voltage regulation on a radial network.

In Fig. 3.1, power flow across the branch impedance is expressed in terms of both sending-end (P_1, Q_1) and receiving-end (P_2, Q_2) quantities. These quantities differ by the branch losses. For the initial discussion, we are concerned only with the power flow expressed with respect to the sending-end.

An expression for the voltage difference between nodes 1 and 2 in Fig. 3.1 is derived in terms of the given system parameters using two fundamental engineering principles: Ohm's laws and the definition of apparent power.

From Ohm's law, it is possible to state that[1]:

$$\overline{V}_1 = \overline{V}_2 + \overline{I}_{12} \times (R + jX) \tag{3.1}$$

and from the definition of apparent power we have:

$$\overline{S}_1 = \overline{V}_1 \times \overline{I}_{12}^{*} \Rightarrow \overline{I}_{12} = \frac{\overline{S}_1^{*}}{\overline{V}_1^{*}} \tag{3.2}$$

In Eq. 3.2, it is assumed that the parameters are expressed in per-unit values and hence the customary root-three coefficient has been neglected. Note also that, since $\overline{I}_{12}$ is the power flowing from bus 1 to bus 2, $\overline{S}_1$ represents the complex power that flows away from bus 1.

Substituting Eq. 3.2 into Eq. 3.1, we have:

$$\overline{V}_1 = \overline{V}_2 + \frac{\overline{S}_1^{*}}{\overline{V}_1^{*}} \times (R + jX) = \overline{V}_2 + \frac{(P_1 - jQ_1)(R + jX)}{\overline{V}_1^{*}}$$

Taking $\overline{V}_1$ as reference, $\overline{V}_1 = \overline{V}_1^{*} = V_1$ and we obtain:

$$V_1 = \overline{V}_2 + \left(\frac{RP_1 + XQ_1}{V_1}\right) + j\left(\frac{XP_1 - RQ_1}{V_1}\right)$$

or (expressed in terms of $\overline{V}_2$): $\overline{V}_2 = V_1 + \Delta V_1 + j\delta V_1$ (3.3)

where $$\Delta V_1 = -\frac{RP_1 + XQ_1}{V_1} \tag{3.3a}$$

and $$\delta V_1 = -\frac{XP_1 - RQ_1}{V_1} \tag{3.3b}$$

Equation 3.3 represents the voltage change between the sending- and receiving-end busbars. It can be visualised as a simple vector diagram where the voltage difference between nodes 1 and 2 is expressed in terms of two orthogonal vectors: ΔV_1 and $j\delta V_1$ (given by Eqs. 3.3a and 3.3b respectively). The voltage vector diagram for a traditional passive distribution network is included as Fig. 3.2a below. It is described in Section 3.1.3 how it is normal in this type of system for ΔV_1 and δV_1 to be negative, indicating a negative voltage change (or voltage drop) from the sending- to the receiving-end busbar.

[1] Vector quantities are expressed with a bar above the variable. Scalars are expressed without bars.

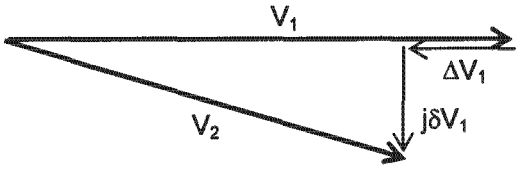

Note: ΔV_1 and $j\delta V_1$ are **negative,** indicating a **voltage drop** across the feeder.

Fig. 3.2a. Vector diagram illustrating the orthogonal voltage-change parameters ΔV_1 and δV_1 for a passive distribution feeder.

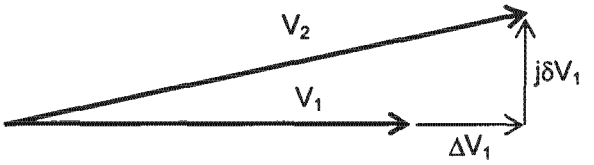

Note: ΔV_1 and $j\delta V_1$ are **positive,** indicating a **voltage rise** across the feeder.

Fig. 3.2b. Vector diagram illustrating the orthogonal voltage-change parameters ΔV_1 and δV_1 for a DG-installed distribution feeder.

The vector diagram for a feeder in which the direction of real and reactive power flow is reversed (i.e. P_1 and Q_1 flowing *into* bus 1) is included as Fig 3.2b above. In this case, the voltage change vectors ΔV_1 and $j\delta V_1$ are positive, indicating a net voltage rise of the receiving-end busbar with respect to the sending-end. It is seen from the discussion of Section 3.1.3 to follow that vector diagrams of this type are realised in some DG-installed networks.

The voltage vector diagrams of Figs. 3.2a-b are drawn using the vector $\overline{V}_1$ as reference. This is a result of having assigned $\overline{V}_1$ as reference in the derivation of Eq. 3.3. In fact, it is also possible to derive an expression for voltage regulation on an electrical system, using the receiving-end busbar voltage, $\overline{V}_2$, as reference.

Following a similar derivation to that shown above, but using receiving-end quantities (referenced *into* bus 2) in Eq. 3.2, and $\overline{V}_2$ as the reference voltage, Eq. 3.3 can be alternatively expressed as:

$$\overline{V}_1 = V_2 - \Delta V_2 - j\delta V_2 \qquad (3.4)$$

where

$$\Delta V_2 = -\frac{RP_2 + XQ_2}{V_2} \qquad (3.4a)$$

and

$$\delta V_2 = -\frac{XP_2 - RQ_2}{V_2} \qquad (3.4b)$$

Using this form of the analysis equation, the vector diagrams of Figs. 3.2a-b appear as shown in Figs. 3.3a-b below.

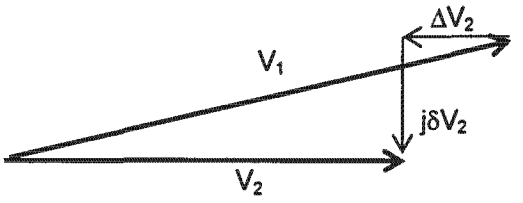

Fig. 3.3a. Voltage vector diagram for a passive distribution feeder, using the receiving-end busbar voltage as reference.

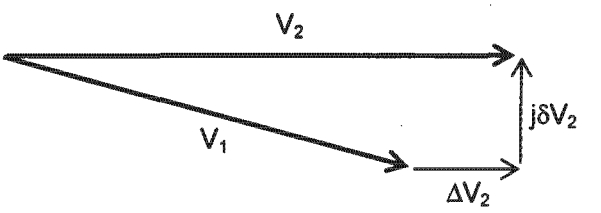

Fig. 3.3b. Voltage vector diagram for a DG-installed distribution feeder, using the receiving-end busbar voltage as reference.

The analysis equation expressed in terms of receiving-end quantities (i.e. Eq. 3.4) is used in Chapter 6 as the basis of a generalised tool for the evaluation of DG-initiated voltage rise. From the onset, however, it must be noted that Eq. 3.4 (and indeed Eq. 3.3) cannot normally be used to solve network power flows. This is because application of Eq. 3.3 requires knowledge of the branch losses (included in the terms P_1 and Q_1) that are unknown in an unsolved network, whilst the use of Eq. 3.4 requires that the receiving-end busbar voltage is known (and a load-flow is often required to ascertain this). In Chapter 6, three assumptions are made to facilitate the application of this approach as a means to solve a model network.

The original form of the analysis equation (Eq. 3.3) is used in Section 3.1.3 to investigate the origins of the voltage rise effect and, in Section 3.2.1, to identify those network parameters that are expected to affect the phenomenon. First, however, Section 3.1.2 discusses further simplifications that can be made to the analysis equations when studying voltage regulation in electrical networks.

3.1.2 Simplifications to the analysis equations

It is important to notice from Figs. 3.2a-b and 3.3a-b that the difference in magnitude between $\overline{V}_1$ and $\overline{V}_2$ is governed almost entirely by the vector ΔV, whilst the difference in phase angle between the busbar voltages is largely due to $j\delta V$. In fact, it is common for the term $j\delta V$ to be neglected when studying voltage regulation on electrical networks. This is because regulation studies are usually only concerned with the magnitude of the voltage at different nodes in the network. To good approximation, this effect can be understood using Eq. 3.3a alone, and Eq. 3.3 can be stated more simply as:

$$\left|\overline{V}_2\right| \approx V_1 + \Delta V = V_1 - \frac{RP_1 + XQ_1}{V_1} \qquad (3.5)$$

This form of the regulation equation is used in the discussion of voltage regulation in passive and active systems in Section 3.1.3.

A second commonly-applied simplification to the voltage regulation equations is to neglect the terms that are dependent on the branch resistance, R. This approach is adopted in many engineering textbooks[2] for the study of voltage regulation in transmission networks, and is justified on account of the high X/R ratios of typical transmission lines. The same assumption cannot, however, be used in voltage regulation studies on sub-transmission and distribution networks, owing to the lower X/R ratios that are encountered. To this end, line impedances used for network modelling purposes indicate an average X/R ratio of 5.4 for 132kV lines and a ratio of 13.5 for 400kV lines. At 11kV and 22kV, the X/R ratios of the line impedances average 0.8 and 1.9 respectively. It is thus clear that in sub-transmission and distribution networks, voltage regulation must be studied in terms of both branch resistance and reactance.

3.1.3 Simple network analysis applied to passive and active systems

Passive distribution networks are characterised by unidirectional real power flows with the power P_1 in Fig. 3.1 flowing from the source towards the load. Depending on the particular network configuration and level of loading, the reactive power flow, Q_1, may be directed either as shown in Fig. 3.1, or in the reverse direction. In almost all rural feeder applications using overhead lines and supplying loads at lagging power factors, however, the direction of Q_1 will be towards the load. Under normal operating conditions, Eq. 3.3a indicates that there will be a negative voltage change (or voltage drop) between the sending- and receiving-end busbars. This condition is indicated in the vector diagram of Fig. 3.2a.

The introduction of DG to a feeder reduces the amount of real power, P_1, that must be supplied from the source, with the remainder of the load being supplied by the DG. This reduces the magnitude of the term "RP_1" in Eq. 3.3a and thus also reduces the voltage drop between busbars 1 and 2 in Fig. 3.1.

In the event that the real power generation by the DG exceeds the local demand (either as a result of excessive generation or minimal feeder load) it will reverse the direction of P_1 in Fig. 3.1. If the reverse flow of real power is of sufficient magnitude, it can overcome the voltage-drop caused by the "XQ_1" term in Eq. 3.3a and will give rise to a net voltage rise between busbars 1 and 2. Under these conditions, the network voltage will be highest at the DG busbar as given by Eq. 3.5. This represents a significant departure from traditional passive networks where the network voltage is almost always highest at the source busbar.

It is thus seen how Fig. 3.1 and Eq. 3.3a can be used not only in understanding voltage drops on passive distribution systems, but also to understand the voltage rise phenomenon that occurs in some DG applications. The mechanism by which the voltage rise effect occurs is seen to be similar to that which causes voltage drops in passive systems.

[2] For example, Weedy [1994, p.80] and Jenkins et al. [2000, p.54].

3.2 Understanding the Voltage Rise Effect

In this section, the voltage regulation equations from Section 3.1 are analysed in more detail to identify those network parameters that affect the severity of the phenomenon. Thereafter, the discussion of Section 3.2.2 indicates that typical parameter values from distribution networks in South Africa are of a nature so as to aggravate the voltage rise phenomenon. In Section 3.2.3, the simple voltage regulation formulae and the discussion of the previous sections are used to identify actions that can be undertaken to mitigate the voltage rise effect.

3.2.1 Network parameters that influence the voltage rise phenomenon

The form of Eq. 3.3a suggests that feeder power flows (P_1 and Q_1) and network impedance (R and X) are the most important factors when considering the voltage rise phenomenon. As we do not expect the substation voltage, V_1, to vary significantly from 1pu, the effect of this term in Eq. 3.3a can be neglected. Slight variances in V_1 will, however, have a significant effect on the measured voltage at the DG installation (as described by Eq. 3.5), and the source voltage is thus also an important study variable. Branch power flows, network impedance and source voltage, in turn, are influenced by different network parameters and operating conditions. These parameters and operating conditions are introduced in the discussion below.

Branch power flows (P_1 and Q_1). Branch power flows are determined by the magnitude and location of network load relative to the DG. It is clear from Fig. 3.1 and Eq. 3.3a that load of sufficient magnitude downstream of the generator will prevent the DG's real power output from being exported towards the source. In fact, even load that is situated upstream of the DG will reduce the extent of voltage rise at the DG busbar. This will occur as a result of the DG's output power not having to flow across the length of the feeder that connects the DG to the source. It is, however, expected that upstream load will be more effective in reducing the voltage rise effect the closer it is located to the generator.

The load power factor is also expected to be an important variable in the study of network voltage regulation. By Eq. 3.3a, inductive loads give rise to voltage drops along the feeder length. This effect is undesirable in passive distribution networks, but in DG-installed networks will counteract the voltage rise phenomenon. Equally, a DG that operates at a leading power factor will increase the level of reactive power supplied from the source, and will thus limit the extent of voltage rise encountered. By the same mechanism, DGs operating at lagging power factors will give rise to more extreme voltage increases.

Branch power flows are dependent on the voltage characteristics of the loads. These, in turn, are closely linked to the type of load. Weedy [1994, p.137], for example, comments how the real power drawn by heating loads varies with the square of the supply voltage, whilst for lighting loads this relationship is closer to (voltage)$^{1.6}$. These types of loads will help to counteract the voltage rise effect, since increases in the supply voltage are met with increased real-power load magnitudes. The real power that is consumed by induction motors remains constant with slight increases in supply voltage, although their reactive power consumption can increase considerably. These devices will thus also tend to suppress the voltage rise phenomenon in DG applications.

The magnitude, power factor, type, and location of load relative to the DG are thus important factors when considering the DG voltage rise effect, as are the magnitude and power factor of the generator's output.

Branch impedance (R and X). Branch impedances are governed by the line length/s between the substation and DG busbars and the network loads. As with branch power flows, branch impedances are dependent on the relative locations of the DG and loads with respect to the source substation.

Branch impedances are determined by the impedance per-unit length of the line conductor. The resistance per-unit length of a conductor is mainly determined by its cross-sectional area and the resistivity of alloy/s used. Conductor resistance is thus specific to a particular conductor type with higher capacity/thicker conductors having lower resistances than thinner ones. The series inductance of a line (per-unit length) varies logarithmically with increased phase spacing and is thus dependent on the voltage level. This is because phase clearances are generally increased at higher voltage levels so as to achieve an adequate level of insulation [Weedy, 1994, p112-117].

The increased inductance of overhead lines at higher voltages has a significant effect on the X/R ratio of the line impedance. For example, an 11kV line strung with ACSR "Hare" conductor has an X/R ratio of 1.16 while the same conductor at 88kV has an impedance ratio of 1.47. By Eq. 3.3a, the line's X/R ratio affects the degree to which voltage regulation is dependent on real or reactive power flows. Regulation on high voltage networks is thus normally influenced more by reactive power flow than that of real power. The converse of this is that reactive power flow has less influence on voltage regulation in lower voltage networks although, as described in Section 3.1.2, its effect is still significant.

The branch impedances "R" and "X" in Eq. 3.3a are dependent on the network voltage level. This is because the variables are expressed as per-unit quantities. In Appendix A it is seen that the per-unit impedance base varies with the square of the voltage level. Branch impedances for a given line/transformer thus decrease with the square of an increase in voltage level.

The line impedance that is seen from the DG location is reduced in the event that the network is interconnected: operated in a ring configuration. Distribution networks, especially at 66kV and below, are seldom interconnected, however, and the present study focuses only on radial networks as a result.

Source Voltage (V_1). Voltage variations at the source substation busbar occur in a similar manner to those at the DG busbar – as a result of real and reactive power flow across the source impedance. This being the case, Eq. 3.3a indicates that the magnitude and angle of the source impedance and the magnitude and power factor of HV and MV network loads (including the DG feeder and adjacent feeders) will be important factors determining the voltage at the source substation. On-Load Tap Changer (OLTC) action of the substation transformer, where installed and enabled, will affect the voltage level at the source substation and must also be considered. Equally, the presence of a voltage regulator between the DG- and source substation busbars will affect the "source" voltage seen by the generator.

In summary, the above discussion indicates that the following ten factors are expected to be of primary importance when considering the voltage rise effect on DG-installed feeders:

Factors affecting source voltage:

1. Presence and method of control of source transformer OLTC and/or voltage regulator/s;
2. Source impedance (magnitude and angle);
3. Substation HV and MV busbar loads (magnitude and angle);

Factors pertaining to the DG:

4. Location relative to the source substation;
5. Power generated (magnitude and power factor);

Factors relating to the DG feeder:

6. Network voltage level;
7. Conductor type or types used;
8. Locations of specific loads;
9. Magnitude and power factor of load; and
10. Load type.

Although not apparent from the simple equations of Section 3.1, the study of the voltage rise phenomenon must also include consideration of an eleventh factor:

11. Network limits for steady-state overvoltages.

This last factor is important, as it describes the extent to which the voltage rise phenomenon can be tolerated.

The eleven factors described above were identified from an analysis of Eq. 3.5 under the assumption that a generator is installed on the feeder. In fact, as described in Section 3.1.2, the same analysis is applicable to voltage regulation studies on traditional passive distribution networks. It can thus be concluded that the first ten factors that were identified above as influencing the voltage rise phenomenon in active networks will give rise to voltage drop effects in passive systems. When performing voltage drop studies, the eleventh factor, the network limit for overvoltages, must be replaced by the network undervoltage limits.

Distribution networks in South Africa were described in Chapter 1 as being most often constrained by voltage-drop considerations. The "weak" nature of the country's distribution systems is investigated in more detail in Section 3.2.2 to follow. This discussion is important in view of the interrelationship between voltage drop and voltage rise phenomena that was described in Section 3.1.3.

3.2.2 The voltage rise effect in South African distribution networks

The majority of rural distribution networks in South Africa are constrained by voltage-related issues rather than capacity, waveform quality or electrical loss considerations. These networks can be described as being electrically "weak".

The weakness of South Africa's networks can most often be attributed to the sparsity of load. This, in turn, arises from the low population densities in most of the country and translates into average rural load density figures of the order of 100kVA/km^2. This is in contrast to a study from Italy [Ippolito et al., 2003] that assumes load densities upwards of 10MW/km^2.

The magnitudes of loads (i.e. load per customer) on rural networks in South Africa are also low. This is evidenced by individual customers commonly being supplied through relatively small (16-200kVA) distribution transformers [Carter-Brown and Gaunt (2003)].

The distributed nature of network load dictates that rural distribution feeders in South Africa are long, with typical lengths ranging between 20km and 100km. By Eq. 3.3a, long feeders are prone to voltage-drop problems on account of their high resistance, and conductor sizing is thus usually based on the limitation of this effect rather than on capacity or loss considerations. Nevertheless, the economics of these lightly loaded networks is such that relatively high resistance ACSR "Hare" or "Mink" conductors are commonly applied at voltages up to 66kV. ACSR "Wolf" conductor is used widely at 88kV and 132kV voltage levels.

The above discussion has serious implications for DG in South Africa. As described in Section 3.1.3, the same factors that lead to voltage drop problems on "heavily" loaded networks will give rise to voltage rise concerns on lightly loaded, DG-installed feeders. Thus, voltage rise problems must be expected with increased penetrations of DG on local

distribution networks. Further, given that local networks are significantly more sparsely- and lightly-loaded than typical systems in other countries, it is to be expected that the voltage rise problem will be more severe in South Africa than elsewhere.

Another effect of the low loading on rural feeders in South Africa is that HV/MV substation transformer capacities are low, ranging from 750kVA. This gives rise to high source impedances as seen from substation busbars and, by the analysis of Section 3.2.1, is also expected to affect the degree of the voltage rise phenomenon in local DG applications.

The qualitative description of local distribution systems indicates that the nature of the network parameters is such as to cause an exaggeration of the voltage rise phenomenon as compared to experiences from other countries. It is thus increasingly important that the factors affecting the voltage rise phenomenon are well understood, and that effective solutions to the problem are found. In this regard, Section 3.2.3 extends the simple analysis of the previous section to evaluate the options for the mitigation of the voltage rise effect.

3.2.3 Mitigation of the voltage rise effect

A number of authors describing DG-initiated voltage rise (for example, Masters [2002] and Cigré [2002, p.41-2]) list five standard options for the mitigation of the problem. These include:

(i) reducing the sending-end substation voltage,
(ii) having the DG operate at a leading power factor,
(iii) installing a voltage regulator on the DG feeder,
(iv) upgrading the feeder to a conductor of larger cross-section, or
(v) constraining the generator.

It is seen in the present section that the means by which each of these options brings about a reduction in the voltage rise effect can be understood from Eq. 3.5. The form of this equation suggests that the possible solutions must influence at least one of the variables: "R", "X", "P", "Q" or "V_1", as described in Table 3.1 below:

Table 3.1. Voltage rise mitigation options evaluated in terms of the voltage regulation equation (Eq. 3.5).

Option	*Influence on Eq. 3.5*
Reducing the sending-end voltage.	Reduces V_1 and allows for increased voltage rise before regulatory limits are exceeded.
Operating the DG at a leading power factor.	Increases Q_1.
Installing a voltage regulator.	Affects V_1 and X. Details of this option are not clear from the simple analysis.
Up-rating the conductor.	Reduces R.
Constraining the generator.	Limits the extent of real power export, P_1, towards the source substation. This may be achieved by limiting the DG output, or stipulating that the DG can operate only during times of heavier network loading.

The modes of operation of two further solutions to network voltage rise problems are also apparent from Eq. 3.5:

Option	*Influence on Eq. 3.5*
Operate the DG feeder as a ring network.	Reduces R and X. The feasibility of this solution will depend on the physical layout of the network. It may also create complexities with regard to feeder protection and is not considered further in this study
Use the DG feeder to "back-feed" an adjacent network via a tie-point.	Reduces magnitude or prevents P_1 flowing towards the source.

The form of Eq. 3.5 provides an indication of the effectiveness of some of the solution methods. It is clear that the option of having the DG absorb reactive power will be more effective on higher reactance networks. Conversely, as described also by Cigré [2002, p.9], this solution will be less effective on cable networks as a result of their low series inductances.

From the discussion of this section, the simple voltage regulation equations are found to be useful in understanding the means of operation of each of the voltage rise mitigation options. In some cases, the equations also provide an indication of the efficiency of the method, but this cannot be extended to evaluate the relative efficiencies of the different options. The promising results of this section indicate, however, that the method might be extended to fulfil such a function. This is developed further in Chapter 6.

3.3 Chapter in Perspective

Voltage regulation in electrical networks can be understood using simple linear expressions that describe the voltage drop or rise between sending- and receiving-end busbars in terms of branch impedances and power flows. Application of the voltage regulation equations appears limited, however, since they cannot normally be used on unsolved networks (i.e. networks whose busbar voltages are not know). Nevertheless, the simple mathematical form of the equations provides for easy analysis of the voltage rise phenomenon and hence fulfils one of the requirements for a generalised analysis tool. In Chapter 6 it is seen that, by drawing some assumptions regarding network conditions, it is, in fact, possible to apply Eq. 3.5 to solve a model network. In this way, Eq. 3.5 is used as the basis for a generalised approach to evaluating voltage rise in DG-installed networks.

Chapter 4 explores two of the factors that were identified in the present chapter as affecting the extent of the voltage rise effect: busbar source impedance and methods of voltage control in distribution networks. The former topic is based on a study of three-phase fault levels at busbars in South Africa and is used later in further discussions regarding fault-level-based approach to evaluating DG penetration limits.

Chapter 4 also includes a discussion of voltage regulation limits in South Africa. In later chapters these will form a basis for defining a penetration limit for DG in terms of the voltage rise phenomenon.

Chapter 4

Voltage Control and Regulation Limits in Distribution Networks

Chapter 3 identified eleven factors that are expected to affect the voltage rise phenomenon in DG-installed networks. The effect of one factor, the presence and method of control of substation transformer OLTCs and/or voltage regulators, was not clear from the simple analysis of voltage regulation and was identified as a topic for further investigation. This discussion is included in Section 4.2 of the present chapter.

Section 4.3 explores a second factor: the regulatory limits for voltage regulation in South Africa. This section also includes a review of current Eskom planning philosophies that will influence the extent of the allowable voltage rise on selected DG-installed feeders.

First, however, Section 4.1 includes a study of busbar source impedances in South Africa. These were identified in Chapter 3 as a third factor of influence when studying network voltage rise. This topic is closely related to that of busbar fault levels that were identified in Chapter 2 as being indicators of allowable DG penetration.

4.1 Busbar Source Impedances in South Africa

The source impedance seen from a point in an electrical system is the result of an often-complicated network of series and parallel impedances. Referring to Fig. 4.1 below, transformers and lines are represented as series impedances, whilst loads are described as parallel impedances.

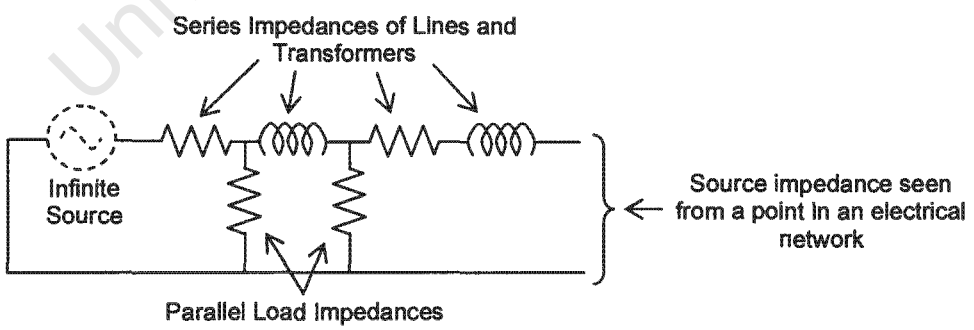

Fig. 4.1. Source impedance seen from a point in an electrical network.

Accurate source impedance statistics are seldom available for busbars in distribution networks. This is most often due to a lack of information regarding network loading, as up-to-date records of network series impedances are usually kept. The latter information is required for the calculation of busbar fault levels that are used in a number of engineering applications, including network planning and protection co-ordination.

It was mentioned in Chapter 3 that distribution networks in South Africa are generally lightly loaded. Load impedances - especially those near to the distribution substations - will thus be high. These impedances decrease at higher voltages, corresponding to increased levels of loading, but so too do the series impedances of the higher capacity lines and transformers. This being the case, the source impedance at a busbar can be estimated reasonably accurately even if load impedance is neglected. The source impedance at a particular busbar can be approximated by considering the three-phase fault level at that point. In neglecting the influence of upstream load, this approach will provide a worst-case estimate of the source impedance.

Each of Eskom's Distribution regions compiles an annual report of calculated fault levels at all MV and HV busbars in their area. These reports were used to compile the cumulative percentile fault level distributions in Figs. 4.2 and 4.3 below. The first figure describes the fault level distributions at source busbars for voltage levels from 11kV to 88kV. Source busbars are defined here as busbars on the secondary side of HV/MV transformers. These busbars are typically "sources" for radial sub-transmission and distribution feeders to which DGs could be connected.

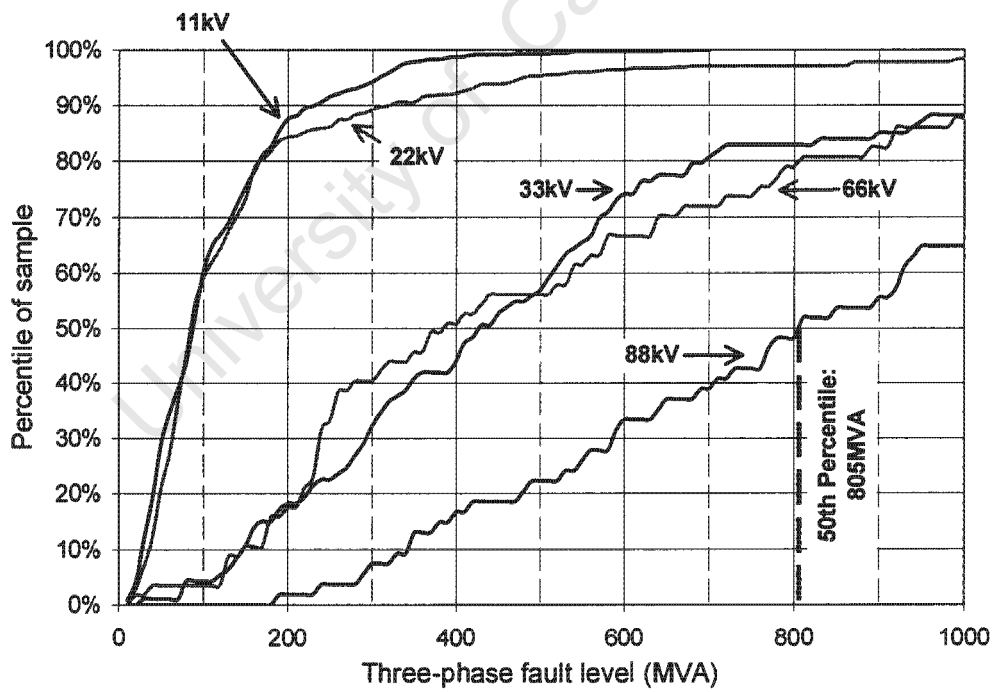

Fig. 4.2. Cumulative percentile distribution of source-busbar fault levels in South Africa.

The "88kV" curve in Fig. 4.2 indicates that 50% of all 88kV source busbars in the Eskom system have three-phase fault levels below 805MVA. This corresponds to source impedances greater than or equal to 0.124pu[1].

The 20th, 50th and 80th percentile fault levels for each voltage level (derived from Fig. 4.2) are shown in Table 4.1 below. The table lists the number of busbars in each voltage level that were considered in the survey. Typical rupturing capacities of outdoor circuit breakers, based on information received from two international breaker manufacturers[2], are also presented in Table 4.1 for comparison with the local fault level data.

Table 4.1. Percentile source-busbar MVA fault levels per voltage level.

Voltage Level	No. of Busbars	Percentile Fault level (MVA)			Typical Breaker ratings (MVA)
		20%	50%	80%	
11kV	713	41	88	167	476†
22kV	446	49	84	166	952†
33kV	93	224	425	697	1428†
66kV	57	219	387	807	2857†
88kV	54	482	805	1233	6096‡

† Calculated using a 25kA breaker rating

‡ Calculated using a 40kA breaker rating

The fault level data presented in Fig. 4.2 and Table 4.1 demonstrates a marked decrease in fault levels at lower voltage levels. This is to be expected, given the lower capacity (and hence high impedance) feeders and transformers that are typical of lower voltage systems. The increasing number of source busbars at lower voltages that is apparent from Table 4.1 is also typical of distribution networks that become more dispersed nearer the customer supply voltages.

Comparison of the busbar fault level statistics with international breaker ratings in Table 4.1 indicates the relative weakness of South African networks with respect to world standards. The table indicates that in 80% of applications on 11kV, 22kV, 66kV and 88kV networks, the fault level falls below thirty percent of the switchgear rating. In Section 1.1 it was described how the fault current contributions by DGs in some countries can cause switchgear to operate

[1] The fault level data that is presented in Fig. 4.2 and Table 4.1 can be expressed as an equivalent per-unit source impedance using Eq. 2.2.

[2] The IEC specifications for current ratings of switchgear include a wide range of options including: 1, 1.25, 1.6, 2, 2.5, 3.15, 4, 5, 6.3 and 8A and their multiples of ten up to 80kA [IEC60059, 2002, p.71]. Telephonic discussions with switchgear manufacturers ABB and Alstom (on 19 Feb 2004) indicate, however, that 40kA ratings are preferred at 132kV and 88kV voltage levels (although Eskom Distribution specifies 31.5kA), whilst 20kA or 25kA ratings are most often used at voltage levels of 11kV to 66kV.

beyond its limits. The results of Table 4.2 indicate that this is unlikely to occur with DG applications in South Africa.

The low fault levels at source busbars in South Africa are significant since these represent the *highest* fault levels on the respective networks. Particularly at lower voltage levels, fault levels are expected to decrease rapidly along rural feeders on account of the high line impedances. In this regard, Fig. 4.3 shows a comparison of percentile fault level distributions for 33kV and 88kV source and load busbars. Load busbars are defined as those fed via a sub-transmission or distribution line and typically comprise the HV busbar of a downstream substation.

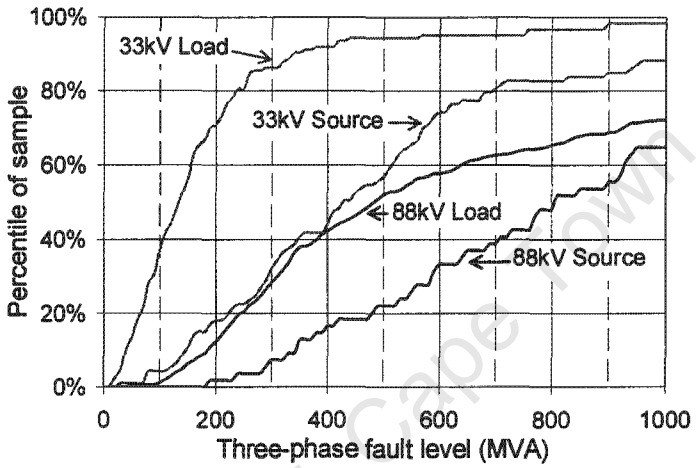

Fig. 4.3. Comparison of source- and load-busbar fault levels in South Africa.

Fig. 4.3 indicates that there is a greater variation between source- and load-busbar fault levels at the lower voltage level. The "33kV load" distribution is approximately 60% lower than the distribution for source busbars, and indicates that the fault level at the connection points for DGs will often be significantly lower than at a source substation.

A better understanding of the nature of busbar source impedances is derived from an analysis of the source impedance angles. To this end, histograms of the source impedance angles for 11kV, 33kV, 66kV and 88kV busbars were calculated from X/R ratio data provided in the Eskom fault level reports. These are presented as Figs. 4.4a-d below. The source impedance angles for source and load busbars are displayed separately at each voltage level. No data was available for fault levels at 11kV load busbars, since very few of these are modelled. The histograms in Figs. 4.4a-d have been normalised for ease of comparison.

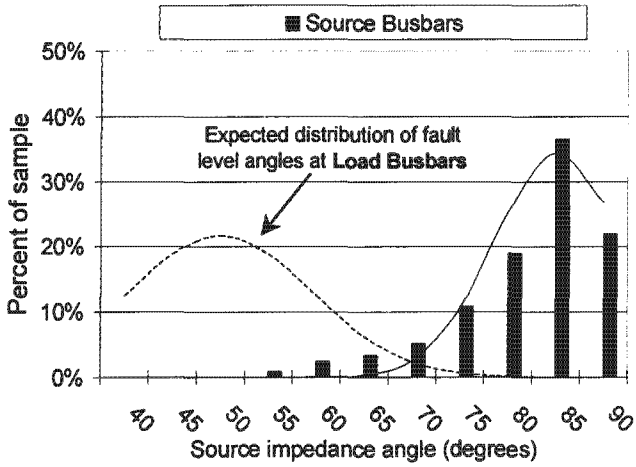

Fig. 4.4a. Normalised histogram of source impedance angles of 11kV busbars in South Africa.

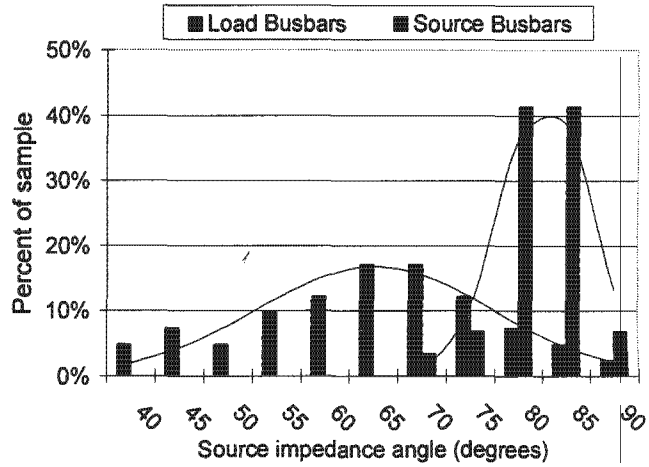

Fig. 4.4b. Normalised histogram of source impedance angles of 33kV busbars in South Africa.

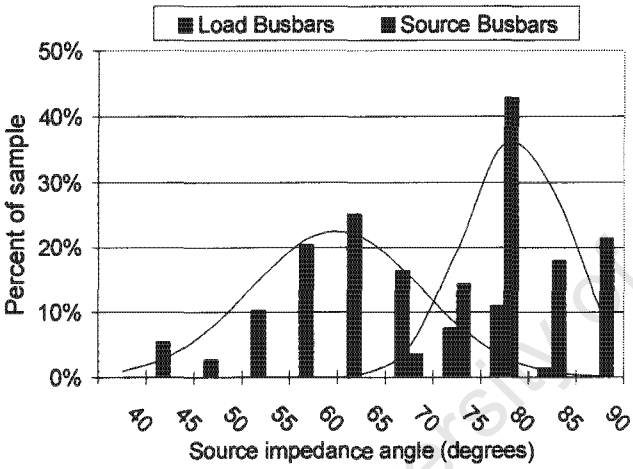

Fig. 4.4c. Normalised histogram of source impedance angles of 66kV busbars in South Africa.

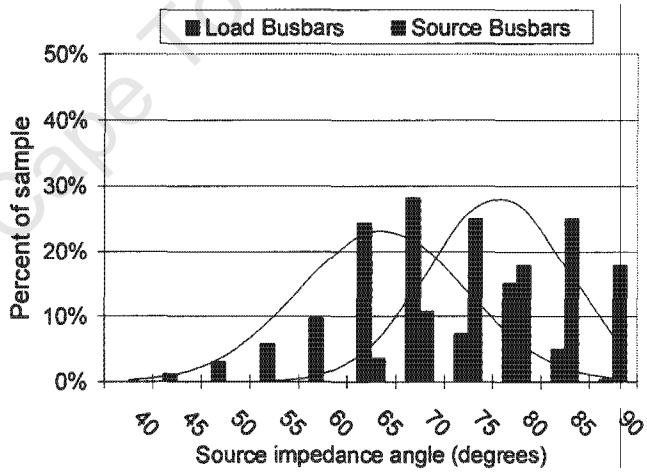

Fig. 4.4d. Normalised histogram of source impedance angles of 88kV busbars in South Africa.

Two important trends are apparent from the histograms of Figs. 4.4a-d:

1. The source impedance angles at source busbars are high, and tend towards ninety degrees as the voltage level is reduced. This indicates that source impedances at source busbars are dominated by the impedances of the upstream transformers. Transformer impedances are almost entirely reactive, and are often modelled as pure inductances. The increase in source impedance angles for source busbars at lower voltages is thus indicative of small (and hence high impedance) transformers at distribution substations.

2. The source impedance angles for load busbars are distributed around the impedance angles of lines. Lines at 33kV and 66kV have impedance angles in the region of 55°, while 88kV line angles are of the order of 60° or 65°. The load-busbar distributions in

Figs. 4.4a-d are thus seen to be dominated by the contribution to the impedance angle of the line, rather than the source transformers. This trend will be applicable also to 11kV load busbars as indicated by the dashed-line distribution in Fig. 4.4a.

The highly reactive nature of source busbar impedances in South Africa is of importance for DG applications in this country. The discussion of Section 3.1 indicated that voltage drops/rises are dependent on the product of branch resistance and real power flow and branch reactance and reactive power flow. It can be deduced from this that DGs operating at relatively high power factors will not drastically alter the substation busbar voltages, even in the event that its output is exported back through the substation's power transformer/s. In Section 4.2, it is found that the action of a transformer OLTC, in any case, compensates for the effect of busbar source impedance on the DG-initiated voltage rise.

4.2 Voltage Control in Distribution Networks

For many years, voltage control in distribution networks has been achieved predominantly through the use of On-Load Tap Changing (OLTC) of the substation-installed power transformers. In more recent times, line-installed voltage regulators are also being used to support the voltage on weak networks at times of heavy loading. This section includes a description of both types of devices and a discussion of their controller settings. Details regarding the modelling of these devices for planning purposes are also included.

4.2.1 Basics of Step Voltage Regulating Transformers

Transformer Tap Changers - OLTCs and OCTSs

A tap changer is a mechanical switching device that is used to alter the number of turns on either the primary or secondary windings of the power transformer to which it is fitted. In three-phase transformers, a single mechanism is provided that alters the turns ratio of all three phases in equal increments at the same time. The most basic type of tap changer, designed for operation only under no-load conditions, is called an Off-Circuit Tap Switch (OCTS). This type of tap changer provides limited (fixed) support of secondary voltages, as it is unable to react to changes in voltage that occur as a result of load fluctuations. It is, however, common for MV/LV distribution transformers to be fitted with OCTSs and it will be seen in Section 4.3.2 how judicious setting of these devices can influence on the voltage regulation limits on the MV system.

An On-Load Tap Changer is more versatile than an OCTS. The tap change mechanism is motorised and is fitted with current diverter switches that permit the alteration of winding ratios without interrupting supply or creating short circuits in the transformer windings. An OLTC can be automatically controlled using a suitable relay to support the MV network voltage

during periods of heavy loading and, if required, can buck (i.e. reduce) the voltage during off-peak times [Thomson, 2000a].

Heathcote [1998, p.170-2] describes how power transformers operated on HV networks with ±5% regulation limits[3] are normally provided with ±10% tapping ranges, but with an offset nominal voltage ratio to provide an effective -5%/+15% buck/boost capability. The increased MV voltage boosting capability is provided so as to allow the MV voltage to be regulated at a value above nominal even during times of minimum HV voltage. The tapping range is normally divided into 17 equal tap steps of 1.25% each and with tap 5 corresponding to nominal voltage. Transformers with fifteen 1.43% tap steps also are available to implement (non-offset) ±10% tapping ranges [Thomson, 2002a]. Both varieties of tap changer are used in South Africa, although the 17-tap version is by far the more common (and is the current industry standard).

Tap changers are usually installed on the HV winding of a transformer so as to exploit the lower current (compared to that in the secondary winding) that must be "diverted" during a tapping operation [Heathcote, 1998, p.35]. Increments in HV turns in 1.25% steps give rise to voltage increments on the secondary winding of between 1.15% and 1.71% per tap: minimum variation for a transition from tap 1 to 2 and maximum variation between taps 16 and 17.

Transformer/tap changer combinations are generally cheaper than similarly-rated voltage regulators. They also take up less space and are thus generally preferable to voltage regulators in substation environments. Voltage regulators are favoured for installations "out on the line".

Voltage regulators [Carter-Brown, 2002b]

Voltage regulators are auto-transformers that are fitted with a tapped series (secondary) winding (or windings) so as to provide ±10% regulation of the secondary voltage with respect to the primary. On three-phase systems, either a single-unit three-phase regulator or a combination of single phase units can be used.

Three-phase voltage regulators are similar to transformer tap changers in that they include a ganged mechanism that alters the ratio of all three phase windings at the same time. These units are, however, much more expensive than an equivalent installation using single-phase units[4] and this type of unit is unlikely to find future application in South Africa. Nevertheless, a number of older three-phase regulators are in use on South African reticulation systems.

[3] Voltage regulation limits in South Africa are described in detail in Section 4.3.

[4] Carter-Brown comments that a three-phase regulator typically costs the same as four equivalently rated single-phase units.

The industry standard for single-phase voltage regulators, often termed "cans" as a result of their appearance, is ±10% regulation in 32 steps (16 up and 16 down). This equates to tap steps of 0.625%. Single-phase regulator cans can be combined in three different configurations for use on three-phase systems. Two of these configurations are applicable to the delta-connected (three-phase with no neutral conductor) systems that are typical of reticulation networks in South Africa: Open Delta and Closed Delta configurations. Open Delta applications use two regulator cans to provide ±10% regulation on all three phases, while a three-can Closed Delta configuration allows for ±15% regulation. Open Delta applications are commonly used in South Africa with a possible upgrade to a three-can installation if needed.

4.2.2 Basic Tap Changer & Voltage Regulator Controller Settings

The automated control of transformer OLTCs and voltage regulators is achieved using Automatic Voltage Regulating (AVR) relays of very similar design. In fact, the fundamental features of these controllers are identical and are described below. Some additional relay features, one particular to OLTC controllers, are described in Section 4.2.3 to follow.

In their most simple form, AVR relays monitor the voltage of the transformer secondary against a setpoint and initiate up- or down tap operations as required. The voltage setpoint is an adjustable relay setting that is normally calibrated as a percentage of system rated voltage.

It is common for controlled busbar/node voltages to be maintained at values above nominal - typically 103% - so as to ensure adequate regulation at the most remote end of the feeder. Higher setpoint voltages (up to 104%) are also commonly applied in South Africa, although Carter-Brown [2002c] comments that: "the operation of MV networks with sending voltages in excess of 105% is only to be considered in extreme emergency conditions, and then only for a limited time (typically a maximum of a 48 hour period)" (p.20).

Owing to the discrete nature of the winding taps, it is not possible for the regulating device's secondary voltage to be maintained exactly at the setpoint value. To accommodate this, AVR relay designers have defined a "dead-band" around the voltage setpoint inside which the MV voltage is deemed to be acceptable and the tap changer/regulator is not required to operate. The dead-band is centred at the setpoint voltage, and its "width" is governed by a relay setting termed the "bandwidth" (refer to Fig. 4.5 below). As with the reference voltage setting, bandwidth is normally specified as a percentage of nominal voltage.

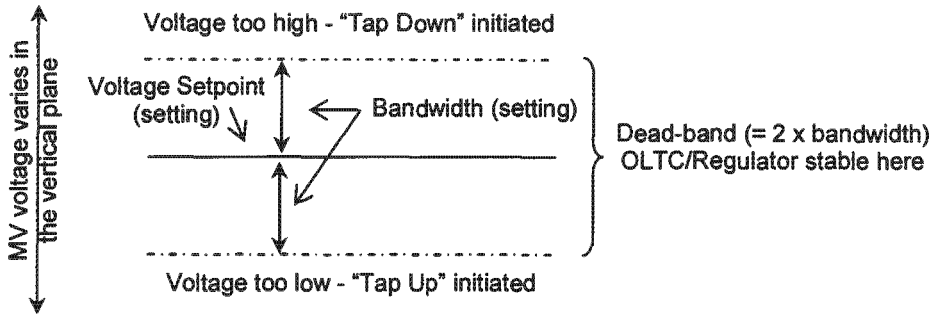

Fig. 4.5. AVR parameters – voltage setpoint, bandwidth and dead-band.

It is common for AVR relay bandwidths on distribution transformer OLTCs to be set to 1.4% or 1.5%. This setting in chosen to accommodate two considerations:

1. It must be ensured that the OLTC *dead-band* is larger than the maximum voltage step for a transition from one tap to another (given in Section 4.2.1 as 1.71% for a 17 tap transformer) so as to prevent a phenomenon termed "hunting". Here the device successively taps up and down, as it is unable to reach a stable operating point in any tap position [Thomson, 2000a].

2. The bandwidth setting must be higher than that of the upstream OLTC transformers[5] to ensure that the optimal device reacts first for any given change in network voltage [De Jongh, 2001]. For example, a change in the transmission system voltage should be regulated for the sub-transmission and distribution networks by the EHV/HV OLTCs and not those on the HV/MV transformers. This concept is similar in principle to that of grading the pick-ups of overcurrent relays that are in series (as well as providing time grading).

To accommodate the above considerations, a bandwidth setting of 1.6% is typically used on AVR relays for voltage regulators.

It is important to notice that the basic algorithm of AVR relays is unaffected by the direction of power flow or the load power factor. These devices will thus continue to regulate the chosen busbar voltage irrespective of the presence or absence of DG on the feeder. This is because the network voltage remains referenced to the grid (a near-infinite source) rather than to that at the DG bushings.

4.2.3 Advanced AVR relay features

The previous discussion of tap change/regulator control focused only on the most basic methodology, whereby the transformer secondary voltage is held at a constant setpoint and,

[5]EHV/HV transformers in South Africa typically use bandwidth settings of 1.2% [De Jongh (2001)].

in the specific case of OLTCs, the transformer is not operated in parallel with another unit. In practice, a number of more advanced control features are available. Detailed discussion of these features is beyond the scope of this study, but, for completeness, those features that will be affected by the introduction of DG are briefly described under two sub-headings to follow.

4.2.3.1 Line Drop Compensation

The Line Drop Compensation (LDC) method allows the AVR relay to regulate the voltage at a point downstream of the OLTC/regulator's location. It achieves this by calculating the voltage-drop/rise to the remote busbar using phase-current measurements at the OLTC/regulator installation and information regarding the branch impedance to the remote node. This voltage drop/rise is then added to the measured local voltage value and the resultant is assumed to be the actual voltage at the remote location. The AVR relay then controls the OLTC/regulator in such a manner that the remote (calculated) voltage is maintained at the relay setpoint. It is seen from Fig 4.6 below that the effect of LDC is to raise the local busbar voltage as the load increases.

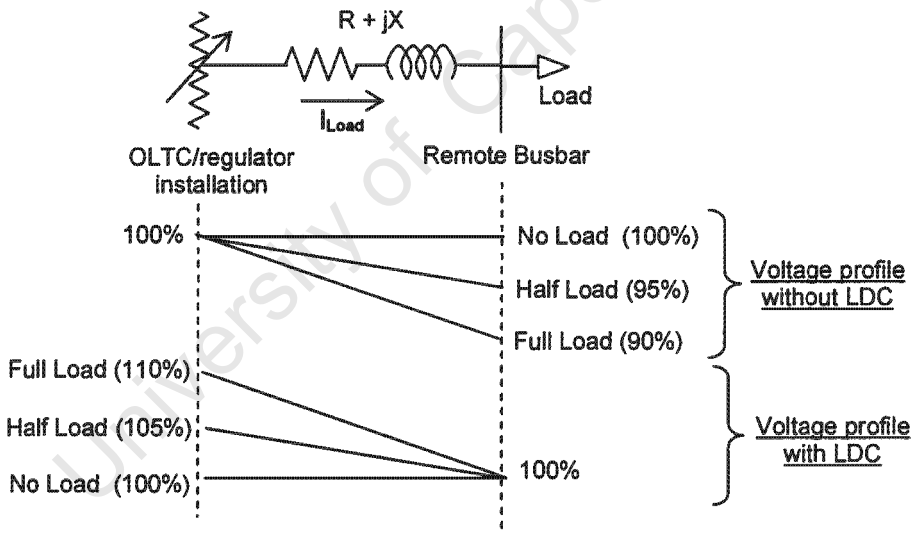

Fig. 4.6. The effect of LDC on the voltage profile of a distribution line.

[Carter-Brown, 2002b, p.22]

Application of LDC to OLTC and regulators on distribution networks can give rise to large increases in effective network capacity. This is because the technique helps to maintain the voltage profile "centred" within the allowable voltage band and hence allows for greater voltage drops before statutory regulations are violated [Carter-Brown, 2002c, p.9-10]. The theory by which LDC operates, however, is dependent on the transformer/s being the only source of power to the MV network in question. It is well documented by Thomson [2000a], Persaud et al. [1999] and Salman et al. [1996] that the inclusion of DG on such a network can at best reduce the effectiveness of LDC, or, in the worst case, make the technique completely

unviable. In any event, LDC is difficult to apply at substations that supply multiple feeders, and as a result is not commonly used on OLTC controllers in South Africa. The LDC technique is also seldom used on voltage regulators.

4.2.3.2 Negative Reactance Compounding (NRC) for Parallel Control of Transformer OLTCs

OLTC-enabled transformers that operate in parallel must be prevented from running on widely differing taps. This is because tap differences give rise to circulating currents between the transformers. Circulating currents lead to premature insulation ageing and limit the units' load-carrying capacities. In the past, transformers operating in parallel were maintained on the same tap through the use of the "master-follower" technique. While this method of parallel control was effective, it was found to limit the flexibility of some substations as it restricted the possible different groupings of parallel transformers. To overcome this, AVR relay designers developed a technique called "Negative Reactance Compounding" (NRC), whereby a transformer could independently determine whether or not it was the sink or source of circulating current (and hence whether it was out of step with a parallel unit). Although the method of application differs between relay manufacturers, the essence of NRC is that each AVR relay calculates how much reactive current its transformer should be carrying, assuming that the load current is at a pre-defined power factor. The relay compares this value with the measured value for reactive current and deduces that the difference in the two values is due to circulating current. Where necessary, corrective tapping instructions can then be issued by the tap change relay.

The effective operation of NRC is reliant on the actual load power factor being relatively constant and its average value being near to the pre-set relay setting. The introduction of DG to a distribution feeder (especially one operating at unity or a leading power factor) tends to reduce the power factor seen by the source transformers. Thomson [2000b] describes further how the accuracy of NRC relays is negatively affected by DG. The results are significant because certain electronic AVR relays (for example, the SuperTapp relay from Reyrolle) use NRC as their only algorithm for parallel control. Modern microprocessor-based AVR relays offer alternative parallel control algorithms that are unaffected by the presence of DG, but NRC techniques remain the only option when paralleling transformers that use AVR relays from different manufacturers.

4.2.4 Modelling of Voltage-Controlled busbars for planning purposes

Voltage studies on passive distribution networks have traditionally been completed under the assumption that the voltage of an OLTC-regulated substation busbar remains constant at the OLTC setpoint value [Carter-Brown, 2002c, p.31]. This is equivalent to assuming that the regulated busbar is an infinite source of zero impedance and neglects the effect of the OLTC bandwidth. The former assumption, however, bears further justification given the findings of

Section 4.1 regarding the *high* source impedances that are encountered at busbars in South Africa.

From the simple analysis of Section 4.2, the actual voltage of the regulated busbar will vary within the OLTC dead-band in accordance with changes in load across the source impedance. For a setpoint of 103% and bandwidth of 1.4%, this corresponds to a stable band of operation between 101.6% and 104.4%. The instantaneous busbar voltage is, however, almost impossible to model accurately, as it is dependent on the instantaneous network loading both upstream and downstream of the substation busbar. In the absence of a more detailed model, the assumption of a busbar voltage that is fixed at its most likely value is used as the best alternative. Here, it must be noted that the actual magnitude of the busbar source impedance does not affect the validity of the infinite source assumption. Rather, it will only affect the rate at which the busbar voltage changes within the OLTC dead-band with changing load (and hence the number of tap operations per day/month).

In Section 4.1 it was seen that, owing to the highly reactive nature of substation source impedances, DG is unlikely to give rise to voltage problems on the HV terminals of step-down transformers. This, combined with the above discussion, indicates that substation source impedances can be completely neglected when studying the DG voltage rise effect.

Application of the infinite source model for planning purposes gives rise to a window of uncertainty around the predicted voltage values. This window corresponds to the dead-band of the OLTC controller. Carter Brown [2002c, p.31] comments, however, that this effect can be neglected, because steady-state voltage limits and those for transformer fluxing are linked to the average value of the voltage supplied, and that this corresponds to the OLTC setpoint figure.

The discussion above indicates that the planning practice of modelling a regulated substation busbar as a fixed-voltage infinite source is adequate for voltage studies, even in weak networks (provided a substation OLTC is installed). In fact, a similar argument can be made for the modelling of nodes whose voltage is controlled by a voltage regulator. In the case of voltage regulator installations, however, the effect of source impedance cannot be completely neglected. This is because the source impedance seen by a voltage regulator will be much higher than that encountered in a substation, and "back generation" through a regulator may well give rise to overvoltages on the regulator's primary bushings. This indicates that voltage studies on regulator-installed networks must be considered in two parts: one study on the network downstream of the regulator location and a second study on the network between the OLTC-regulated busbar and the voltage regulator. This is a significant finding in the context of voltage rise studies with DG on radial networks, as it indicates that the effect of a voltage regulator can be studied using a simple, infinite source model that does not specifically include a model for the regulator. In fact, it is seen in Chapter 9 that it is possible to infer the

influence of a voltage regulator on the DG voltage rise problem from the results of studies performed on networks that are not fitted with these devices.

4.3 Voltage Regulation Limits in South Africa

The emphasis of this study is on DG connected to distribution networks at medium (1kV – 33kV) and high voltages (33kV – 132kV). It will be seen presently, however, that practical voltage regulation limits for MV networks are closely linked to the regulations for low voltage supplies. As a result, this section begins with a discussion on regulatory limits for HV, MV and LV networks in South Africa. The current network planning philosophies as applied by Eskom Distribution are described thereafter, and it is seen that compliance with these philosophies may be more of a constraint to DG applications than the statutory limits.

4.3.1 Statutory voltage regulation limits

Voltage regulation limits for LV networks in South Africa are defined in the South African Electricity Act (Act 41 of 1987) and NRS048:2. The standard for new customers is 400/230V (three-phase/single-phase) with an allowable variation of ±10%. Prior to 1990, however, the Electricity Act specified limits of 380/220V ±5%, although Eskom designed and contracted to 380/220V ±7.5% in supply agreements during this time [Carter-Brown, 2002a].

In Eskom, the voltage regulation limit for direct supplies to customers at medium and high voltages is normally contracted as a default value of ±7.5%, although Carter-Brown [2002c, p20] stipulates that the actual voltage must fall within +5%, -7.5% under normal network conditions. In the absence of a contractual agreement, NRS048:2 stipulates that the maximum voltage regulation range for MV and HV supplies is limited to ±5%.

The above discussion might lead to a conclusion that, in terms of voltage regulation, the maximum permissible penetration of DG onto a distribution network must, in the worst case, cause the MV or HV network voltage to rise to a maximum of 105% of nominal. Indeed, this is true of HV networks, and would be true of MV systems were it not for the newly-adopted planning strategy in Eskom Distribution regarding the apportionment of voltage drops between MV and LV networks. It will be seen presently that in certain DG applications, the maximum prescribed voltage at MV-connected DG locations may be less than 105%.

4.3.2 Voltage Apportionment in Eskom Distribution

In distribution networks, voltage apportionment for a particular LV service point (or zone of service points), refers to the act of prescribing the maximum voltage drop to the MV and LV networks such that the nominal ±10% statutory limit is maintained at the customer's installation. Until recently, there was no standard in Eskom regarding the apportionment of volt drops when planning, designing and operating distribution networks. This situation has changed with the approval of an Eskom Distribution Standard entitled "Distribution voltage regulation and apportionment limits" in October 2002.

The new Eskom standard is based on research by Carter-Brown [2002c] into the substantial cost savings that can be realised by assigning voltage apportionment limits to different types of distribution feeders. The standard considers traditional passive distribution feeders only, but will have a significant impact on certain DG applications.

The application of voltage apportionment in distribution feeders can be considered in terms of two options, although variations of these are also described in the Eskom standard. The first case refers to urban networks or rural/electrification networks with good MV voltage regulation, whilst the second is used for longer rural lines typical of many South African feeders.

4.3.2.1 Voltage apportionment on urban-type networks and its affect on DG

For urban-type networks where the load density is relatively high, research has shown that significant cost savings can be achieved by specifying a smaller range of variation for voltage drops on the MV system, and allowing greater voltage drops over "weaker" LV systems. Examples given in the standard show that in many cases (specifically in electrification projects), the savings on LV connections that are brought about through the use of this design philosophy can normally more than justify the expenditure on voltage regulators that may be required to adhere to the MV volt drop limits.

The application of this planning philosophy is significant for possible DG applications, as large fluctuations in MV voltage will not be tolerated. This is because the design philosophy relies on the MV voltage being stable. Considering the network as a traditional passive system, the Eskom standard stipulates that the highest MV voltage on this type of feeder must be limited to under 104%. It is reasonable to assume that a similar limit would apply to a DG busbar on such a feeder.

4.3.2.2 Voltage apportionment on rural networks and the philosophy of OCTS tap zones

It was seen in Section 4.1 that rural distribution networks in South Africa are generally long, with relatively low load densities. In the Eskom system, customers are often supplied from dedicated MV/LV transformers and the meter is commonly installed on the same structure as the transformer. As a result, LV volt drops on such feeders are generally small. This phenomenon enables planners to apply wider voltage regulation limits on the MV system and still maintain the LV voltage within 10% of nominal.

A new method of applying OCTS settings for MV/LV distribution transformers on rural feeders allows for even greater MV voltage drops in some networks [Carter-Brown, 2002c]. Previously, the tap changers of these transformers would be set to the same nominal boost, irrespective of the their specific locations on the feeder. The new approach involves the division of a feeder into "tap zones". These zones are defined according to the maximum MV voltage during normal network conditions and represent a section of the feeder in which the MV/LV transformer taps are set the same. The division of a feeder into more than one zone allows different transformer tap settings to be applied for units at different locations: less boost near the source, and successively greater boost in areas where the voltage is always below certain set thresholds. The concepts described above are illustrated in Fig. 4.7a and Fig. 4.7b.

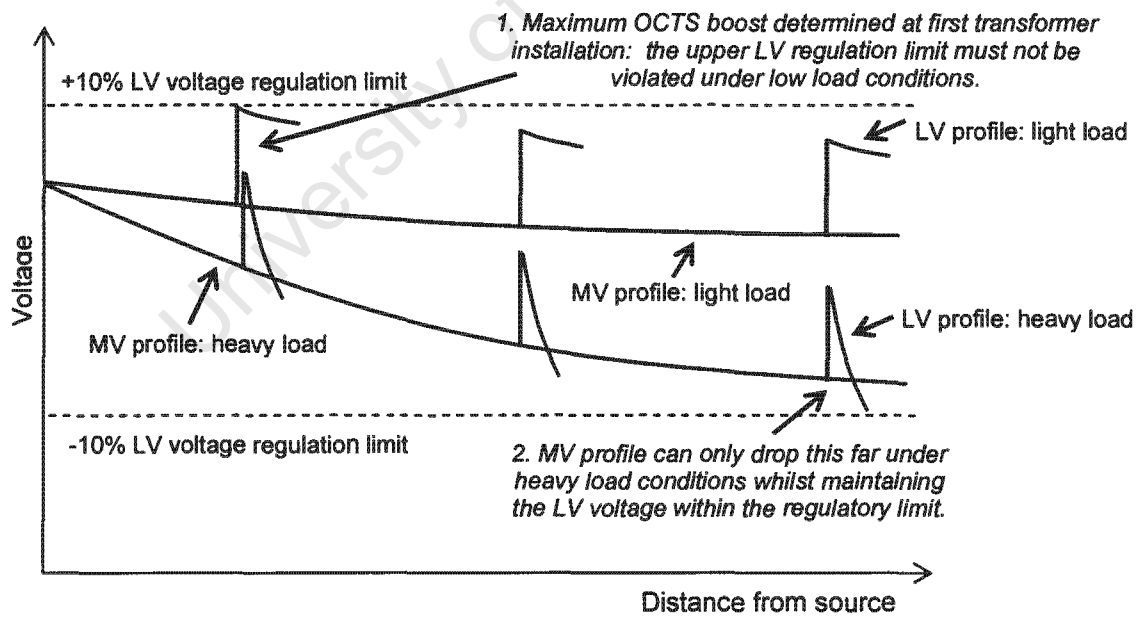

Fig. 4.7a. Voltage profile of a MV feeder indicating the previous approach to setting MV/LV transformer OCTS boost settings - all transformers set with equal boost.

[Carter-Brown, 2002c, p.10]

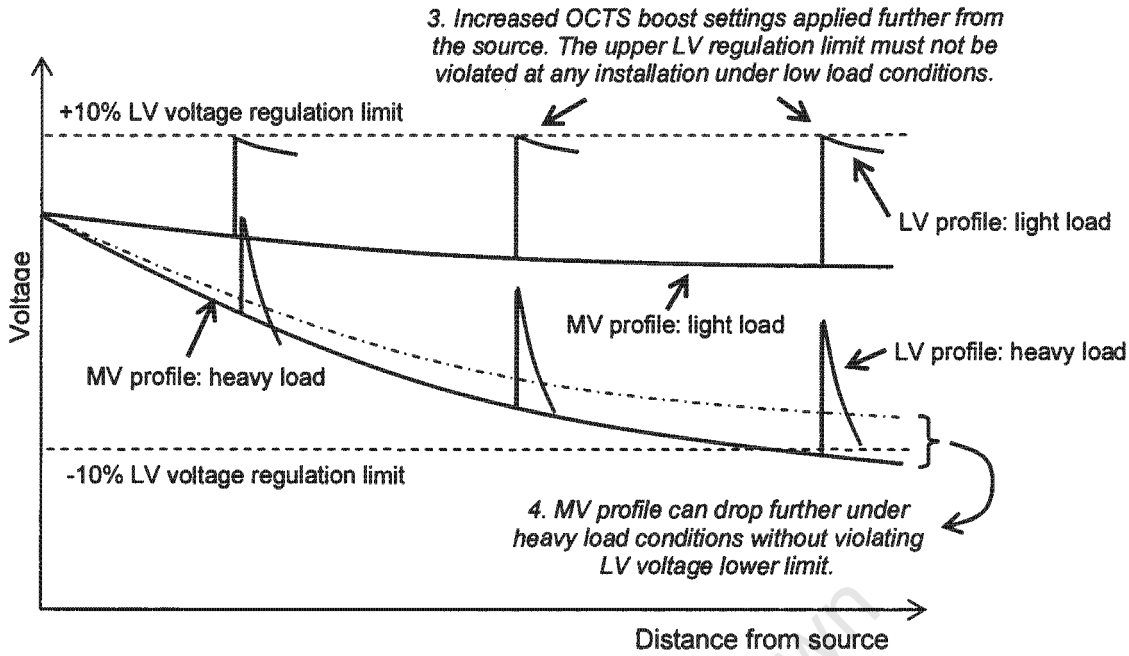

Fig. 4.7b. Voltage profile of a MV feeder indicating the new approach to setting MV/LV transformer OCTS boost settings - settings increased further from the source.

[Carter-Brown, 2002c, p.10]

Carter-Brown [2002c] shows that in the best case, the application of different tap zones on a feeder will increase the allowable MV voltage drop (during periods of peak loading) in one zone by 2.5% and in the zone most remote from the source by 5% of nominal. This, in turn, can be related to a significant increase in the carrying capacity of the feeder or a significant saving in network upgrade costs.

It is important to notice from Fig. 4.7b and the discussion above that the application of the zone approach to applying OCTS settings is dependent on the *maximum* MV voltage at the transformer location. The introduction of DG on a distribution network will almost always give rise to an increase in voltage at the point of generator installation. The inclusion of any DG on a feeder could thus be expected to raise the maximum voltage in a portion of the network and limit the opportunity for applying OCTS tap zones. In the worst case, DG that raises the voltage on a significant portion of the network to above 103% could prevent the OCTS tap zone philosophy from being used at all. In this way, the inclusion of DG onto such a feeder could be seen to actually reduce the carrying capacity of the feeder (or give rise to extra capital costs for network upgrades).

At this point, it must be stated that the benefits of setting MV/LV transformer OCTSs using tap zones may not be as great in all applications. For example, on feeders with customers taking supply at MV, planners will have to ensure that the MV voltage is always greater than 92.5% (nominal minus 7.5%). In this case, it may not be possible to fully utilise the OCTS tap zones whose application could possibly allow the MV voltage to deviate even below 90% whilst still

maintaining satisfactory LV regulation. Significantly, in this study we are primarily concerned with DG connected at MV and HV voltage levels, and it may be that the negative effect of DG application on the standard Eskom approach to OCTS setting can be overlooked in some cases.

4.4 Voltage Rise Factors Revisited

The discussion of Section 3.2 identified eleven factors that were expected to influence the voltage rise effect in DG-installed networks. The discussion of the present chapter has identified three amendments that can be made to this list. These include:

1. *Source impedance can be neglected if the substation busbar voltage is regulated by OLTC action.* The effect of source impedance can be neglected despite the discussion of Section 4.1 that indicated relatively high impedances at many busbars in South Africa.

2. *Substation HV and MV busbar loads (excluding load on the DG feeder) can be neglected* if an OLTC is in operation at the source substation. An OLTC-regulated busbar is equivalent to an infinite source of fixed voltage. Voltage regulation on the DG feeder is thus unaffected by the presence or absence of adjacent feeders at the source substation.

3. *Voltage regulators need not be modelled* for their influence on the voltage rise effect to be studied. This simplification stems from the assertion in Section 4.2.4 that the load-side bushings of a voltage regulator can be modelled as an infinite source at the setpoint voltage. Networks fitted with voltage regulators must, however, be studied in terms of the effect of the DG on the voltage on the network downstream *and* upstream of the regulator installation.

4.5 Chapter in Perspective

The overall effect of considering voltage control and limits on MV networks is that some restrictions to the connection of DG are established by the regulations defining acceptable voltage variations, the practical performance of voltage regulating relays and the utility's approach to voltage control along the length of a radial feeder. The extent of the restrictions that are placed on DGs as a result of these factors will be examined further in Chapter 7 using a network model that is derived in Chapter 6. First, however, Chapter 5 examines the operation and control of synchronous generators. The purpose of this discussion is to identify the most likely operating regime for synchronous DG. In Chapter 3 it was described how a DG that operates at a leading power factor can help to lessen the degree of the voltage rise effect. The practicality and implications of this are explored in Chapter 5.

Chapter 5

Operation and Control of Synchronous Generators

Although some of the results will be applicable to other types of DG, this study is primarily concerned with the effect of synchronous generators on voltage regulation in distribution networks. This chapter begins with a discussion of the fundamental concepts of synchronous generators, including the widely accepted equivalent circuit model and machine output power characteristics. Aspects of synchronous generator stability are discussed thereafter.

Methods of excitation control for synchronous generators are described in the second section of this chapter, while topics in the final section include the influence of tariffs, network and machine losses and generator stability on the selection of DG control mode.

5.1 Fundamentals

A synchronous generator consists of an armature winding that is connected to the three phases of the network and a rotor winding that is supplied by a source of direct current[1], and which is driven at a fixed rotational speed by a prime mover. Steam- and hydro turbines are commonly-used prime movers for DG in South Africa, but it is also possible to use diesel engines, although the fuel cost is prohibitive. The direct current supply for the field winding is derived from the so-called excitation system of the generator. Jenkins et al. [2001, p.107] explain how a synchronous generator's excitation system falls into one of two broad categories:

1. *Self excited*: where the power for the exciter is taken from the main terminals of the generator, or
2. *Separately excited*: where excitation is provided by a separate source, a permanent magnet generator, for example.

The type of excitation employed by a generator has a strong influence on the transient and dynamic performance of the unit, and particularly affects the generator's ability to source fault current. This study focuses on the steady-state performance of synchronous DG and, as a result, the details regarding the *source* of field current for the generator will not be discussed further. It is seen in Section 5.1, however, that a synchronous generator's steady-state (and

[1] In the theory of electrical machines, the winding in which voltage is induced is termed the armature. In the case of synchronous machines, the armature winding is also referred to as the stator winding, as it does not move. The winding on the rotor is the primary source of flux in the machine and is also termed the field winding [Sen, 1989, p.132-3].

transient) performance is governed by the *amount* of excitation current provided and the torque that is applied to the rotor shaft. Different methods by which the excitation current can be varied are described in Section 5.2 to follow.

5.1.1 Equivalent circuit of a synchronous generator [Sen, 1989, p.322-327]

For the purposes of this study it is sufficient to consider the behaviour of a synchronous generator in terms of the widely accepted per-phase equivalent circuit model that is included as Fig. 5.1 below.

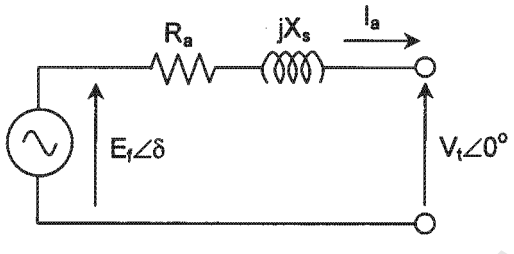

Fig. 5.1. Per-phase equivalent circuit of a synchronous generator.
[Sen, 1989, p.327]

The voltage source in Fig. 5.1, E_f, is representative of the no-load excitation voltage which in turn is governed by the field current. The relationship between the field current and excitation voltage for a particular machine is dependent on the magnetic properties of the machine's core and the width of the air gap, but for steady-state operation is often assumed to be linear.

In Fig. 5.1, the excitation voltage is phase shifted from the terminal voltage, V_t, by the "power angle", δ. The power angle is proportional to the torque that is applied to the rotor shaft by the prime mover, and consequently is also sometimes referred to as the "torque angle".

The term X_s in Fig. 5.1 represents the synchronous reactance of the machine. This is used to model the effect of leakage flux and the flux associated with the armature reaction on the terminal voltage of the machine. From data presented in Weedy [1994, p.324], it is clear that the per-unit synchronous reactance of a generator varies in proportion to the machine capacity.

The final component in the equivalent circuit of Fig. 5.1 is the series resistance term that represents the AC resistance of the stator winding. This term is small in comparison to X_s and is often neglected.

5.1.2 Power characteristics of synchronous generators

The equivalent circuit model presented above can be used to derive an expression for the complex power that is delivered to the system by a synchronous generator. The simple derivation is based on the definition of apparent power and is presented in full in Weedy [1994, p.332-3]. If the stator resistance of the machine is neglected, the three-phase electromagnetic power delivered to the system is given by the expressions:

$$P_{3\phi} = \frac{3 \times V_t \times E_f}{X_s} \times \sin(\delta) \tag{5.1}$$

and

$$Q_{3\phi} = \frac{3 \times V_t \times E_f}{X_s} \times \cos(\delta) - \frac{3 \times V_t^2}{X_s} \tag{5.2}$$

Equations 5.1 and 5.2 considered together can be visualised as a circular locus in the Q-P plane with its centre at $\left(-\frac{3 \times V_t^2}{X_s}, 0\right)$ and radius $\frac{3 \times V_t \times E_f}{X_s}$ as illustrated in Fig. 5.2 below.

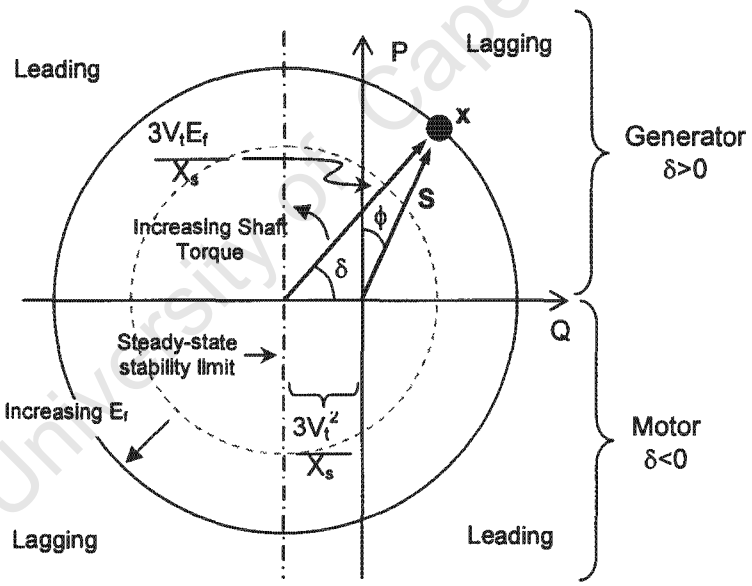

Fig. 5.2. Complex power locus of a synchronous machine showing an arbitrary operating point x. [Sen, 1989, p.343]

An arbitrary operating point, x, is shown in Fig. 5.2 above. If we assume that the machine is connected to an infinite busbar, the terminal voltage, V_t, is fixed[2] and the point x is defined uniquely by the machine's excitation voltage E_f, and by the power angle, δ. Further, by changing the field current and/or the applied torque (and hence the excitation voltage and/or

power angle), it is possible to operate the machine at a variety of different points in the Q-P plane. Specifically, for a fixed real power output, the *power factor* angle, ϕ, can be altered and the machine can be made either to source or sink reactive power.

It will be seen in the sub-section to follow that a synchronous generator is unstable when operated in the steady-state at torque angles greater than 90°. This limitation means that the generator cannot be operated in the left hemisphere of the circle in Fig. 5.2 and dictates that the machine's ability to sink reactive power is less than that for supplying reactive power.

From Fig. 5.2, it is seen that the maximum amount of reactive power that can be sunk by a synchronous generator before instability is proportional to the square of the terminal voltage and inversely proportional to the machine's synchronous reactance. In Section 5.1.1, it was described how the reactance of a synchronous machine decreases with decreased capacity and it is thus expected that smaller generators will be able to sink more per-unit reactive power than larger units. In the sections to follow, however, it is seen that smaller generators are more sensitive to dynamic instability, so their increased capacity for sinking reactive power may not be used in practice.

A final point of interest in Fig. 5.2 is that of the definition of "leading" and "lagging" currents with respect to the generator and motor conventions. It is seen that a positive (sourced) reactive current in the generator convention is termed "lagging", whilst in the motor convention it is "leading". This can lead to misunderstandings between generator operators (using the generator convention) and utility engineers (using the traditional motor convention). As a rule, any power generation by a DG is referred to in the generator convention, whilst the network load power factor is referenced in the motor convention.

5.1.3 Synchronous generator stability

A full discussion of synchronous generator stability is beyond the scope of this study, but some of the basic principles are required in the analysis to come. As a result, this sub-section includes a brief introduction to important aspects of steady-state and dynamic stability.

5.1.3.1 Steady-state stability of a synchronous generator

Equation 5.1 from Section 5.1.2 represents the electromagnetic power developed by a synchronous machine operating at a given level of excitation. The expression for electromagnetic power is shown in graphical form as a function of torque angle, δ, in Fig. 5.3

[2] Recall from Chapter 4 that MV and HV voltage regulation limits specify a maximum variation of ±5%, so the assumption of a fixed V_t will not give rise to appreciable errors. The excitation voltage E_f can vary to a much greater extent.

below. Also included in Fig. 5.3 is a horizontal line that represents the mechanical input power to the generator by the prime mover[3].

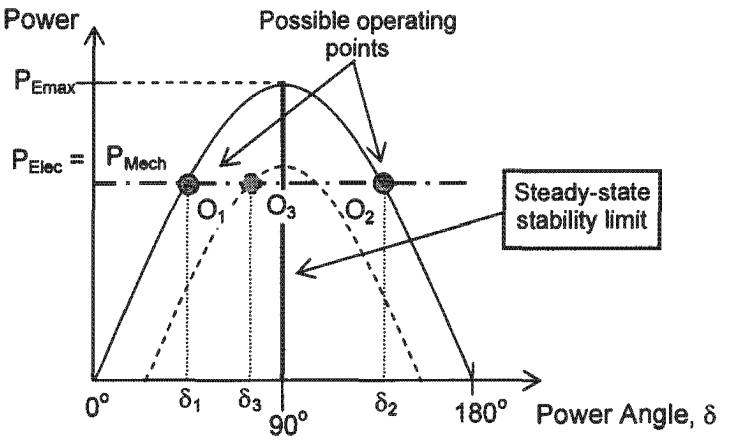

Fig. 5.3. Power - power angle characteristic of a synchronous generator.
[Weedy, 1994, p.99]

In the steady-state (and neglecting losses), the mechanical input power to the generator will be matched by the electromagnetic output power, and the machine will be seen to operate at either point O_1 or O_2 corresponding to power angles δ_1 or δ_2 in Fig. 5.3. In fact, the generator is said to be unstable if made to operate at point O_2, or at any point where the power angle is greater than 90°. This is because an increase in input power to the generator increases the power angle, δ, but for $90° < \delta < 180°$ this increase in angle will lead to a decrease in the electromagnetic output power. The mismatch in input and output power will tend to accelerate the rotor and a phenomenon called "pole-slipping" will occur. This may result in damage to the machine as a consequence of winding overheating or mechanical stress [Redfern and Checksfield, 1989]. It is for this reason that the line, $\delta = 90°$, shown in Fig. 5.2 and Fig. 5.3 is termed the "steady-state stability limit", and operation at power angles in excess of 90° is not possible.

5.1.3.2 Dynamic stability of a synchronous generator

Dynamic stability refers to a generator's ability to remain synchronised with the network during transient network disturbances. In its simplest form it is understood using the "Equal Area Criterion" as presented by Weedy [1994, p.314] and Jenkins et al. [2000, p.83-5]. The equal area criterion indicates that a generator is more prone to transient instability when operated at power angles near the steady-state stability limit. For the same output power as considered previously, O_3 in Fig. 5.3 represents such an operating point.

[3] Note that in Fig. 5.3, as we have assumed that the machine is operating as a generator, the power delivered by the machine is positive and $0° < \delta < 180°$.

With reference to Eq. 5.1, operation of a generator at point O_3 in Fig. 5.3 instead of point O_2 for a given power output is a result of one or more of the following factors:

1. Operating the generator on a system where the voltage is below nominal, i.e. reducing V_t,
2. Increased system impedance, say with the removal from service of parallel lines in the network, or
3. Operation of the generator at low excitation, i.e. reducing E_f.

The second of these factors has serious implications for DG. This is because the per-unit impedance of distribution networks is generally higher than that for sub-transmission and transmission systems. Consequently, for a given power output, a generator connected to a distribution system will be inherently more unstable than one connected at a higher voltage level[4].

According to point 3 above, a synchronous DG operated on a MV network with low excitation (also termed "under-excited") will be more unstable for transient disturbances than those operated with higher excitation levels. From Fig. 5.2, for a given real power output, under-excitation of a generator corresponds to operation at a leading power factor (absorbing reactive power).

Transient stability of a synchronous machine is often specified in terms of a "Critical Clearing Time" (CCT) for disturbances at different points in the network. A generator will lose synchronism with the grid if a particular fault persists on the network for longer than its given CCT [Mabuza and Gaunt, 2002]. In a study on generators connected to a 132kV network in Italy, Cacioli et al. [2001] noted that, as predicted above, the CCTs for faults on the network were shorter (approximately 350 milliseconds) when the machines were operated under-excited and longer when the excitation was increased (400 milliseconds).

5.1.4 Synchronous generator capability curves

In Section 5.1.2, it was seen how a synchronous generator may be made to operate at a number of different points in the Q-P plane depending on the level of excitation and the applied rotor torque. In the previous section, it was found that steady-state stability constraints prevent the generator from being operated in one section of the power plane. This section includes a discussion regarding three further "capability curves" that, together with the stability criterion, demarcate the allowable operating region of a generator in the Q-P plane.

[4] Mabuza and Gaunt [2002] conclude that DGs connected to weak distribution networks are especially prone to instability and that this is exacerbated by the low rotational inertias typical of small generators.

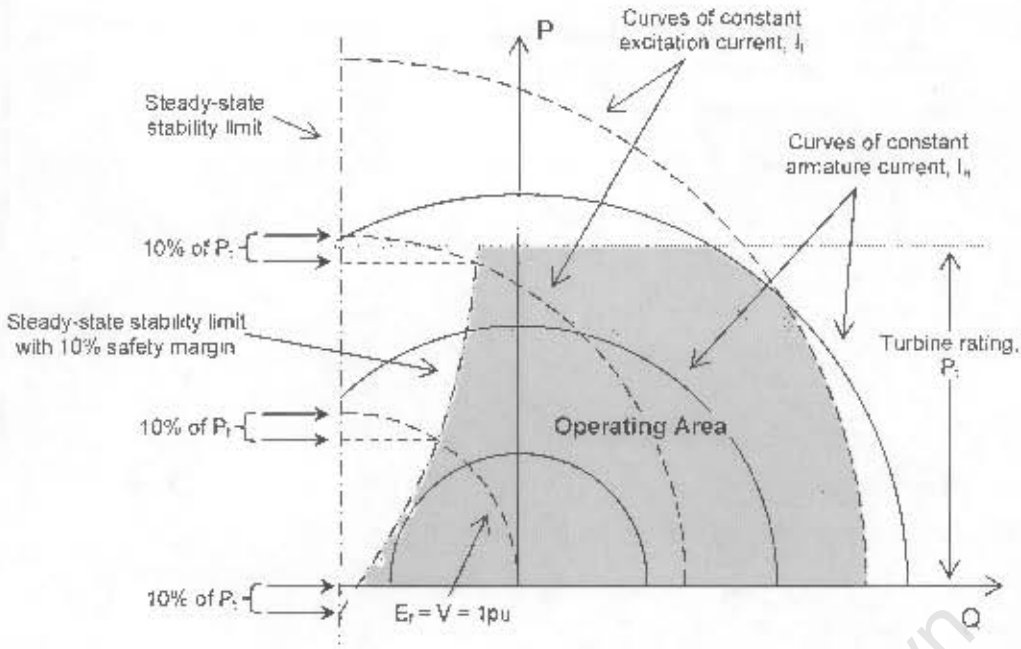

Fig. 5.4. Performance chart of a synchronous generator indicating the operating area (bounded by the capability curves of the machine). [Weedy, 1994, p.102]

With reference to Fig. 5.4, the capability curves of a synchronous generator are as follows:

1. Turbine rating. This is the rated output of the prime-mover and is normally expressed as a three-phase power. The turbine rating capability curve is a horizontal line in the Q-P plane.

2. Armature heating limit. This is related to the I^2R losses in the stator and is thus a function of the armature current, I_a, or alternatively the apparent power generated. The armature heating capability curve is a circle centred at the origin in the Q-P plane, and its radius is given by the apparent power rating of the alternator.

3. Field heating limit. Similar to the armature heating limit, this capability curve is related to the I^2R losses in the rotor winding. For a particular generator, this limit is governed by the maximum allowable field current. As discussed in Section 5.1.2, this capability curve is a circle in the Q-P plane with its centre at $\left(-\frac{3\times V_t^2}{X_s}, 0\right)$ and radius of $\frac{3\times V_t \times E_f}{X_s}$ where V_t and E_f are the nominal and maximum-rated values respectively.

4. Stability limit. In the previous section, it was discussed how a synchronous generator is unstable when operated at a torque angle greater than 90°. This criterion gives rise to the steady-state stability limit shown as a vertical line in Fig. 5.4. In practice, a safety margin is introduced to allow for an increase in load of either 10% or 20% of the turbine rating before the machine becomes unstable. The safety margin is realised on each

locus of constant excitation current by subtracting a percentage of the turbine rating from the maximum electromagnetic power at that excitation level. The power angle corresponding to this operating point is then set as the upper limit for that excitation level. This procedure is illustrated in Fig. 5.4, assuming that a 10% safety margin is to be applied.

5.2 Methods of Excitation Control

In the previous section, it was described how the reactive power output of a synchronous generator is controlled using the machine's excitation system - specifically through the variation of the current in the field winding. By (manually) varying the field current, it was seen that the generator could be made to operate at different points within its performance chart, and for a given power input could be made to operate at leading or lagging power factors. This method of controlling generator field current is termed "manual control", and is discussed further in the present section. Also discussed are two alternative methods of automatic field current control whereby the reactive power output of the machine or the generation power factor or terminal voltage can be kept constant.

In practice, the basic methods used for the control of generator excitation systems have not changed much over the years. The advent of micro-processor based control relays within the last ten years has, however, given rise to a number of more advanced "extra" control features that may prove very beneficial, particularly with respect to small generators. Some of these features are described towards the end of the present section. Methods to model generators operating in different control modes are also presented.

5.2.1 Manual excitation control

Manual control is the most basic method by which a synchronous generator's field current can be regulated. In this case, the current is varied directly by the operator, using a rheostat, for example, until the desired generator output is attained. In setting the field current, the operator would typically consider the effect of field current variation on generator output power and/or terminal voltage via power- and voltmeters mounted on the control panel. That is to say, the operator would be interested in the end-state of the excitation control and not in the magnitude of the field current itself.

The disadvantage of manual excitation control is that it requires operator intervention for any change in generator output power, or worse (in the case of manual control of the terminal voltage) changes in network load, and it is for this reason that excitation control is normally automated.

5.2.2 Power factor and reactive power control

Automatic reactive power and power factor control operate on very similar principles, and are normally discussed as a single control mode (and are termed PF/VAR mode in this study). In this control mode, an excitation controller is employed to perform the function of the operator in manual control mode: to regulate the field current such that the reactive power output or power factor of the generator is maintained at a set value. A schematic diagram of this control mode is included as Fig. 5.5a below and the operating loci in the Q-P plane are shown in Fig. 5.5b.

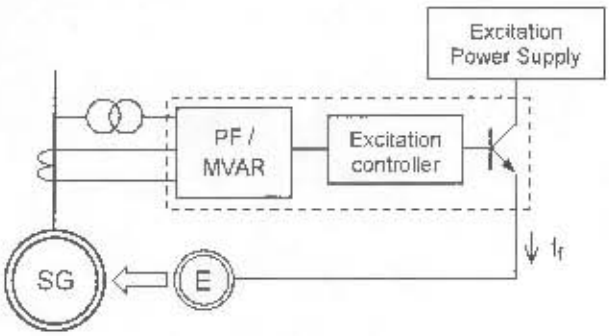

Fig. 5.5a. Schematic diagram of PF/VAR excitation control mode. [Moor, 2001, p.18]

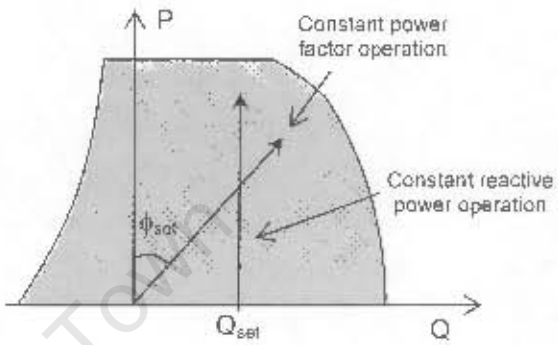

Fig. 5.5b. Operating loci of a PF/VAR controlled generator in the Q-P plane.

Notice from Fig. 5.5b that in PF/VAR mode, the reactive power output of the generator is a constant or linear function of the real power output. As a result, this mode of control is unsuitable for single generators operating on networks that are independent of the grid supply, as here the MW and MVAr components of the loads do not vary linearly. It will be seen in the discussion of Section 5.3 and the analysis of latter chapters, however, that this mode of excitation control is well suited for small and medium-sized DG applications. In fact, PF/VAR control will be the first choice for excitation control in most DG applications.

5.2.3 Voltage feedback control

As its name suggests, this mode of excitation control involves the variation of the field current so as to maintain the generator terminal voltage at a preset value. The basic method by which this is achieved is illustrated in the schematic of Fig. 5.6a. The mechanism by which this control mode operates can be understood using the phasor diagram of Fig. 5.6b.

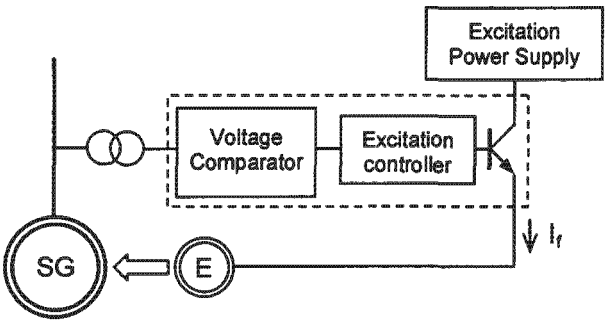

Fig. 5.6a. Schematic diagram of voltage control mode. [Moor, 2001, p.18]

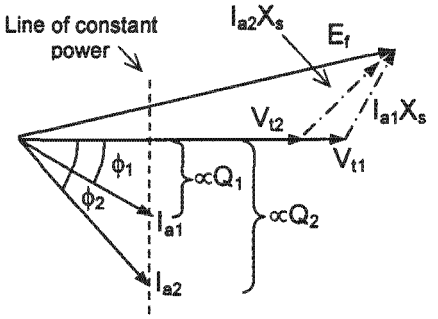

Fig. 5.6b. Phasor diagram used to understand the operation of voltage control mode.

The phasor diagram of Fig. 5.6b is constructed using the synchronous generator model of Section 5.1.1 and illustrates the relationship between the excitation voltage, E_f, and the terminal voltage, V_{t1}, for the given armature current I_{a1}. The armature current lags the terminal voltage by the power factor angle ϕ_1 corresponding to a reactive power generation of Q_1 MVAr.

Consider the case where the reactive power "load" is increased suddenly to Q_2 MVAr with no increase in the real power load. In Fig. 5.6b, this corresponds to a new armature current I_{a2} and an increased power factor angle ϕ_2. The excitation voltage, E_f, would initially remain unchanged, but the armature reaction term, I_aX_s would be altered as shown owing to the change in the magnitude and angle of the armature current. Thus, it is seen that the terminal voltage of the machine would decrease to a new value, V_{t2}. In voltage control mode, the excitation system would detect this low voltage condition, and would increase the field current to generate more reactive power and hence restore the voltage.

Voltage feedback control is the only available excitation control mode for generators operating independent from the grid, but can also be applied to grid-connected synchronous DG. In the former case, the generator capacity, at the design stage, is matched to the maximum apparent power to be supplied so that network voltage can be maintained under all loading conditions. This may not be true in the case of grid-connected generators, as the machine's capacity is often only a small fraction of the network load, and voltage feedback control may not be suitable for many DG applications as a result.

5.2.3.1 Limitations of voltage feedback control in DG applications

Recall from Section 4.1 that the magnitude of the voltage drop, ΔV_1, between busbars in an electrical network is proportional to the product of the branch reactance and reactive power flow, and the resistance and real power flow:

$$\Delta V_1 = -\frac{RP_1 + XQ_1}{V_1} \qquad (3.3a)$$

In passive networks, there is almost always a voltage drop between the source and load busbars as the flow of real and reactive power is from the source towards the load. It was discussed in Chapter 3 how the introduction of DG to such a network will tend to decrease the magnitude of the voltage drop, and hence increase the voltage in the vicinity of the generator. In the event that the DG only generates a small amount of real power (or the network is heavily loaded) this voltage rise may be small, and application of voltage control mode may burden the generator with supplying large amounts of reactive power such that the network voltage is raised to the preset value. Viewed on the machine's performance chart, this condition translates to operating in the lower right-hand corner of the "lagging" characteristic as illustrated in Fig. 5.7 below.

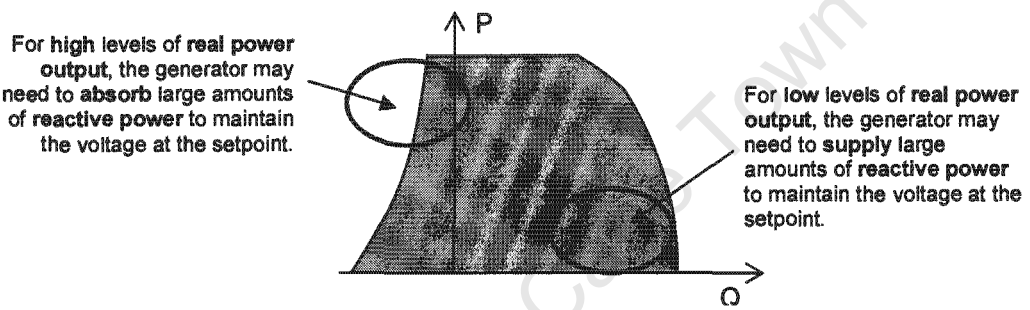

Fig. 5.7. Problems with using voltage control mode on grid-connected DG.

A second, more onerous condition in which voltage control mode may not be appropriate for DG is for high levels of real power generation onto a lightly loaded network. In this case, the voltage at the DG location may well be higher than at the source busbar, and the generator will be required to sink large amounts of reactive power to bring the voltage back to the setpoint value (as indicated by the ellipse at the top of Fig. 5.7).

In the previous section it was described how a synchronous generator's ability to absorb reactive power is limited by stability concerns and that this capability is reduced at high levels of power generation. Most modern excitation control systems include so-called "P-Q limitation" to prevent the machine from being forced to operate outside its performance chart, so it is unlikely that the generator would lose synchronism as a result of excessive VAR absorption, but this may not be true for older control systems.

5.2.4 Other generator control features

The advent of microprocessor-based excitation controllers such as those in the Unitrol range from ABB[5] has given rise to two additional control features that may prove useful in DG applications: automatic switching between PF/VAR control and voltage feedback control modes, and a VAR output "boost" function [Moor, 2001, p.21].

New-generation controllers include a feature whereby the excitation control mode can be automatically switched from PF/VAR mode to voltage feedback mode in the event that the terminal voltage deviates above or below settable thresholds. This feature can be used to ensure that the generator terminal voltage never exceeds a given limit, but permits the machine to operate in PF/ VAR mode until that threshold is reached. This function is used by Kiprakis et al. [2003] as the basis for a custom control strategy that serves to increase the penetration limits of DG.

A second new feature makes it possible for a generator to deliver reactive power beyond its specified capabilities for short periods of time. This is achieved via a stepped excitation current limiter that permits overloading of the field winding for short durations. This feature can be used to provide reactive power support to stressed networks, for example for the duration of network breaker auto-reclose cycles. Further discussion of this feature and its benefits is beyond the scope of this study, however.

5.2.5 Modelling generators using different control modes

A DG that operates in PF/VAR mode can be modelled as a negative load of variable power factor. For the purposes of this study, this representation is also suitable for DGs that operate in voltage control mode. In traditional load-flow studies, a generator operating in voltage control mode is modelled as a node with constant real power injection, constant terminal voltage and automatically-variable reactive power injection/drain [Weedy, 1994, p.225]. This approach need not be applied in this study, however, since we are only interested in voltage control mode so far as its maximum potential to limit the voltage rise phenomenon. This will occur with the machine operating at its reactive power/power factor limits and can be suitably modelled using the simpler constant P – constant Q node representation.

[5] In South Africa, "Unitrol" excitation controllers have been installed on several of the sugar mill-operated generators, and have been chosen by Eskom as the replacement technology for the old control systems on the Transkei hydro-generators. In recent times, a similar range of products from an American company, Basler Engineering, have become available in this country.

5.3 Implications of Control Mode Selection

The previous section included a discussion on the modes of excitation control that are commonly applied to synchronous generators. It was seen that for most synchronous DG applications, the choice must be made between constant PF/VAR control and voltage feedback control. This section describes the implications of selecting one mode in preference to the other. Specifically, the choice of control mode will be discussed in terms of tariff structures, network- and machine losses and generator stability.

5.3.1 Tariff implications

DG pricing in Eskom is described in the directive ESKPBAAG1 (Rev. 1) of March 2000. The following aspects taken from this document will have bearing on control mode selection for DG [Crous, 2000, p.5-6]:

1. The tariff offered to DG-operators reflects only the cost of energy supplied to Eskom. Thus, under normal circumstances no payment is made for reactive power delivered to the system by DGs. The exception to this is in cases where local circumstances require voltage support. Here the directive states that the value of the reactive energy will be determined by system operations, although the mechanism by which this should be calculated is not specified. It must be noted that the pricing directive does not outlaw the export of VARs to the network, but simply states that no monetary compensation will be provided to the DG operator for VARs supplied.

2. No stance is taken regarding reactive power charges for generators operating at leading power factors (absorbing reactive power). This is borne out in practice in the supply contracts for co-generation by two sugar mills where the tariff is specified purely as a three-part time-of-supply energy price with no mention of reactive power charges. The cost of the reactive power supplied to the generators in this case is ostensibly covered by the profit that Eskom will make from wheeling the DGs power to other customers at normal Eskom Distribution pricing rates.

The standpoint taken by Eskom regarding reactive power export by DG is closely aligned with European trends as reported by Cigré Task Force 38.06.03 [2002, p.22]. It is noted in the Cigré report that most European utilities place no value on VAR injections by DG and in most cases make no provision for the purchase of reactive power from DGs, even for the purposes of voltage support. The latter point is most likely a result of the fact that no method has been found to assign a monetary value to voltage support.

Unlike Eskom, many European utilities charge DGs for reactive power consumption. Here, the majority of utilities charge with respect to reactive power in excess of a certain percentage (normally 40-50%) of the total energy consumption for the month. Other utilities charge for the maximum reactive power demand in excess of forty percent of the peak energy demand

[Cigré, 2002, p.22]. It is noted in the Cigré report that reactive energy charges and the absence of payment structures for VAR export by DGs deter DG operators from participating in network voltage regulation.

Cigré Task Force 38.06.03 [2002, p.22] comments that the philosophy behind reactive power pricing as used by most utilities is based on that for a passive system, and is not appropriate for a distribution network with DG. In this regard, it is interesting to notice that reactive power tariffs offered to DG operators in Europe is similar to Eskom's "Ruraflex" tariff for non-generating customers. This tariff charges customers for reactive power drawn in excess of 30% of the total monthly energy consumption (i.e. consumption at an average power factor lower than 0.96 lagging).

Overall, the present tariff structures in South Africa and other countries encourage DG to operate at unity power factor. In South Africa, generation at a leading power factor can also be tolerated, but as discussed in the following sub-sections, network loss considerations and generator stability criteria may limit this in practice.

5.3.2 Effect on network and machine losses

Network losses arise as a result of the transfer of apparent power across the series resistances of transformers and lines, and are sometimes referred to as "I^2R losses". These losses may only be a small fraction of the real power that is transferred down the branch, yet Cigré Task Force 38.06.03 [2002, p.36] comment that their financial implications may be large. This is because network losses are greatest during periods of peak loading and this coincides with the highest per-unit electricity price.

The inclusion of DG on a distribution network alters the network power flows and hence the losses that would otherwise be incurred in transporting the power across the transmission and distribution networks. This reduction in losses is likely to be at its greatest when the DG operates at a lagging power factor, as the generator would then be a local source of both real and reactive power. It was discussed in the previous section, however, that no tariff incentive is given to generators for operating at lagging power factors, and it will be seen in the chapters to follow that this practice may also impose a constraint on the generator in terms of its maximum allowable real power generation limit.

Operation of DG at a leading power factor will give rise to increased network losses compared to operation at unity or lagging power factors. In fact, Cigré Task Force 38.06.03 [2002, p.42] comment that operation of a DG at leading power factors should not be considered without performing loss analysis. At present, however, DG operators in South Africa are not

incentivised to participate in network loss reduction or limitation, although this may change with future implementation of loss allocation practices[6].

For a synchronous generator, machine losses per kilowatt output are a minimum for unity power factor operation. This is because the armature current that gives rise to the losses[7] is a minimum in this operating mode. Power losses within a synchronous machine give rise to higher winding temperatures and result in accelerated degradation of the winding insulation and a shortened life span of the machine.

In summary, from the perspective of network loss reduction, it is preferable to operate DG at lagging power factors, whilst for minimal machine losses power generation by a DG should be controlled at unity power factor.

5.3.3 Implications for generator stability

Aspects of synchronous generator stability were discussed in Section 5.1.3. It was seen that a generator is more prone to transient instability when operating at a leading power factor prior to a network disturbance. From a stability perspective, it is thus preferable that a synchronous generator be operated at lagging power factors corresponding to operation with a small power angle.

5.3.4 Optimal excitation control mode for synchronous DG

Consideration of tariffs, network and machine losses and stability indicates that PF/VAR control is the optimal mode of excitation control for synchronous DG - specifically with a unity power factor/zero reactive power setpoint. From the utility perspective, it may be better that the generator operate at a lagging power factor, but methods to quantify the benefits of this are currently not available, and as a result no incentive is given to DG operators to operate in this way.

[6] The European practice of allocating losses to specific network customers is described by Jenkins et al. [2001, p240-6]. The discussion indicates that the allocation method used at present is not suitable in networks with DG and will have to be revised. No customer-specific loss allocation practice is currently applied in South Africa.

[7] Machine losses are calculated as $I_a^2 R_a$ where R_a is the resistance of the armature winding.

5.4 Chapter in Perspective

Through variation of its control mode or controller settings, a synchronous DG can be made to operate at leading or lagging power factors. The choice of operating mode – usually between PF/VAR control and voltage feedback control – and operating point is determined by consideration of tariffs, losses and stability. These factors indicate that DGs should be operated at or near unity power factor.

The network studies in Chapter 7 investigate the operation of DGs at leading power factors so as to mitigate against voltage rise, but the absence of a reactive power tariff and a procedure for loss allocation makes the evaluation of this option difficult. Prior to this, Chapter 6 describes the derivation and methods of solution of a network model that can be used for the generalised study of the voltage rise effect. The model includes representation of the DG as a negative load of variable power factor to simulate a machine operating at any point within its performance chart.

Chapter 6

A Generalised Method to assess Network Voltage Rise

The simple analysis of voltage regulation in Chapter 3 identified eleven factors that were expected to affect the voltage rise phenomenon in DG-installed systems. Thereafter, the discussions of Chapter 4 suggested a reduction of the original list. The present chapter serves to resolve a reduced set of factors into a representative network model. This model is then used to study the relative influence of the different network parameters on the voltage rise phenomenon. This "generalised" analysis is conducted by solving the network model under different system conditions to determine the limit of power generation that can be accepted before voltage regulation limits are exceeded.

Section 6.2 describes two methods by which the network model can be solved. The first, a simple algebraic approach, is seen in Chapter 7 to provide an intuitive "feel" of the nature of the voltage rise effect. The second, more rigorous Gauss-Seidel solution method is used in Chapter 8 to verify the accuracy of the simpler approach.

6.1 Derivation of a Network Model

The discussion of Chapter 4 identified three amendments that can be made to the original eleven factors that were thought, in Chapter 3, to influence network voltage rise. These simplifications are summarised in Section 6.1.1. Representation of the remaining eight factors in a generalised network model is complicated by the large number of variables required. The presence of load at different locations on the DG feeder, for example, requires a feeder model of many nodes, each with two independent input variables: load magnitude and power factor. Section 6.1.2 describes six further simplifying assumptions that can be applied to reduce the complexity of the required model. Thereafter, Section 6.1.3 describes a network model that is inclusive of all of the remaining study variables.

6.1.1 Voltage rise factors revisited

Section 4.4 identified that, under certain circumstances, three of the factors from Chapter 3 will not have an impact on the voltage rise effect. These findings are summarised below.

1. Source impedance can be neglected if the substation busbar voltage is regulated by OLTC action.

2. Substation HV and MV busbar loads (excluding load on the DG feeder) can be neglected if an OLTC is in operation at the source substation, and
3. Voltage regulators need not be modelled for their influence on the voltage rise effect to be studied.

Despite reduction of the number of influential factors, a complex network model is still required to accommodate the remaining list. To overcome this, Section 6.1.2 describes a number of assumptions that can be made to reduce the number of required variables to a manageable set while maintaining the ability to represent a wide variety of different network types.

6.1.2 Simplifying assumptions

Six assumptions are proposed to reduce the complexity of the network model:

1. *The source substation is equipped with an OLTC.* It is further assumed that the OLTC uses a conventional control strategy. The OLTC specifically does not use line drop compensation or negative reactance compounding techniques.

2. *The feeder load is uniformly distributed down the feeder.* This assumption is commonly made when considering voltage regulation on passive radial feeders with high load densities and is simulated by tapping the total feeder load from the centre of the line length [Weedy, 1994, p.199-200]. This assumption is applied to the present study, notwithstanding the fact that load densities on typical rural networks in South Africa are low. By the engineering principle of superposition, it is expected that the assumption is not particular to networks with only one source, but can be extended to interconnected systems and DG-installed networks.

3. *A single type of conductor is used along the entire feeder length.* It is common practice for distribution feeders to employ higher capacity conductors near to the source substation and to "taper" to lighter conductors farther away. Thinner conductors are also often used on spurs that tee-off the backbone. In this study, however, we will assume that only a single conductor type is used on the feeder.

4. *The feeder load is of the constant power type.* The power-voltage characteristic of a load depends on its type: motor loads tending to be of a constant real power nature (and variable reactive power response), whilst the power drawn by heating loads falls off rapidly at lower voltages. The behaviour of a composite load, a typical feeder load for example, is obtained by summing the characteristics of the constituent loads. Weedy [1994, p.140-1] comments, however, that detailed information regarding the make-up of such loads is seldom available and voltage studies are thus often completed under the assumption of constant impedance (heating-type) load. This corresponds to a $P,Q \propto V^2$

power-voltage relationship. Some authorities prefer to assume the P,Q $\propto$ V relationship that is characteristic of constant current type loads, as this, they say, gives a good approximation of practical conditions. In the present study, however, loads are modelled as constant-power consuming devices. This is expected to be the most onerous condition for network voltage rise, since, using the other load models, increased network voltages are restricted by a corresponding increase in feeder load.

5. *The DG is connected directly to the feeder backbone.* This assumption neglects the possibility of DGs being connected to lateral feeders. It also ignores the possibility of DGs being connected to sub-transmission or distribution networks via a generator transformer.

6. *The (synchronous) DG is not constrained to operate within a fixed capability curve.* It was seen in Chapter 5 that the capability curve of a synchronous generator is dependent on the machine size and its location on the network. These factors vary between applications. As the present study seeks a generalised analysis of the voltage rise phenomenon, it is thus not possible to confine the generator to operate within a given capability.

6.1.3 The network model

The simplifications and simplifying assumptions described above allow for the eight factors of influence to be represented by ten variables[1]:

1. OLTC setpoint;
2. Upper limit for steady-state network voltage;
3. Line length;
4. Conductor type;
5. Voltage level;
6. & 7. Total load on the DG feeder (magnitude and power factor);
8. Distance of the DG from the source substation; and
9. & 10. DG output (magnitude and power factor).

All of the above parameters are represented in the network model indicated in Fig. 6.1 below.

[1] Without the simplifying assumptions, many of the factors of influence from Chapter 3 would have required at least two different variables in the network model.

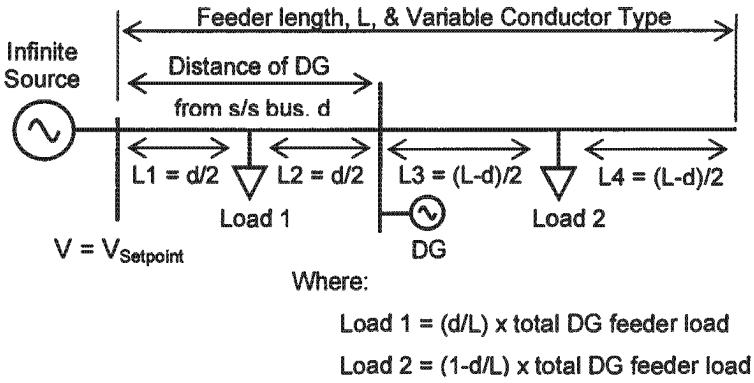

Fig. 6.1. Model network for the generalised evaluation of the voltage rise effect.

The model network of Fig. 6.1 includes an infinite voltage source of magnitude $V_{Setpoint}$ corresponding to the OLTC setpoint value. The DG feeder is of length L (km) and is strung with a conductor type that can be varied. The DG is installed directly onto the feeder backbone, a distance d (km) from the source substation. The total feeder load is split into two lumped values corresponding to load installed between the source substation and the DG (Load 1) and load connected downstream of the DG location (Load 2). The two formulae given in Fig. 6.1 are used to divide the total feeder load between the two load areas so as to simulate a uniform load distribution across the entire feeder length. The lumped loads are positioned in the centre of their respective line segments.

6.2 Solving the Network Model for allowable DG Penetration

In was found in Chapter 2 that the extent of the voltage rise effect can be studied by considering the maximum DG output (or penetration) that can be accepted at a given network location before the onset of an overvoltage condition. This section describes two methods whereby the network model of Section 6.1 can be solved to ascertain the maximum allowable DG output under different network conditions. The first approach, described in Section 6.2.1, is based on the simple voltage regulation equations from Chapter 3. A second, more rigorous method is described in Section 6.2.2.

6.2.1 Algebraic solution of the network model

An approximate algebraic solution of the network model can be achieved using the principle of superposition and one of the simple voltage regulation expressions derived in Chapter 3. In this derivation, the voltage constraint at maximum generation is assumed always to occur at the DG busbar, since load current is almost always of an inductive nature and voltage rise with respect to the DG busbar is not expected.

6.2.1.1 Derivation of the algebraic solution equation

By the principle of superposition, the total voltage drop or rise from the regulated substation busbar to the DG busbar in Fig 6.1 is given by the sum of three independent components:

1. The voltage drop caused by the load upstream of the DG location (Load 1 in Fig. 6.1),
2. The voltage drop caused by the load downstream of the DG location (Load 2), and
3. The voltage rise caused by the DG power export towards the source.

Each of the above expressions can be translated into mathematical equations using Eq. 3.4a of Chapter 3:

$$\Delta V_2 = -\frac{RP_2 + XQ_2}{V_2} \qquad (3.4a)$$

Recall that Eq. 3.4a is an approximate expression for the magnitude voltage change, ΔV_2, across an electrical network of per-unit branch resistance, R, and reactance, X, and whose receiving-end busbar draws $(P_2 + jQ_2)$pu of complex power, at voltage, V_2 pu. Equation 3.4a is only an approximate solution, since it neglects the contribution made to the magnitude of the voltage change by the quadrature term δV_2, as given by Eq. 3.4b.

Using Eq. 3.4a, the three voltage drop/rise expressions described above can be translated into mathematical formulae as follows:

1. *Voltage change, $\Delta V_{DG(1)}$, caused by Load 1*

   By Eq. 3.4a, the change in voltage magnitude along line section 1, ΔV_{L1}, resulting from Load 1, can be calculated as:

$$\Delta V_{L1} = -\frac{R_{L1} \times P_{L1} + X_{L1} Q_{L1}}{V_{L1}}$$

   Where: $R_{L1} + jX_{L1}$ = the impedance of line section 1;
   $P_{L1} + jQ_{L1}$ = the complex power drawn by Load 1 (expressed using the load convention: Q is positive for inductive loads); and
   V_{L1} = the voltage magnitude at Load Busbar 1.

   Since no load flows between Load Busbar 1 and the DG busbar in this scenario, $V_{L1} = V_{DG(1)}$, and the voltage drop across line section 2, ΔV_{L2} $(=V_{L1} - V_{DG(1)})$, is equal to zero. Further, the impedance of line section 1 is half of that of the line joining the DG to the source substation. The latter quantity is expressed as $(R_d + jX_d)$. Thus, the change in voltage between the source substation busbar and the DG busbar caused by Load 1, $\Delta V_{DG(1)}$, can be written as:

$$\Delta V_{DG(1)} = \Delta V_{L1} + \Delta V_{L2} = -\frac{R_d \times P_{L1} + X_d \times Q_{L1}}{2 \times V_{DG(1)}} \qquad (6.1a)$$

In Eq. 6.1a it is important to note that an identifier (1) is appended to the variable for the voltage at the DG busbar, V_{DG}, to identify this as the voltage under the scenario of only having Load 1 connected.

2. *Voltage change, $\Delta V_{DG(2)}$, caused by Load 2*

Neglecting the power losses on line section 3, the change in voltage at the DG busbar caused by Load 2 (downstream of the DG busbar) can be approximated as:

$$\Delta V_{DG(2)} = -\frac{R_d \times P_{L2} + X_d \times Q_{L2}}{V_{DG(2)}} \qquad (6.1b)$$

In Eq. 6.1b, as in case 1, the complex power drawn by Load 2 is expressed using the load convention. Note also that the voltage change up to the DG busbar, $\Delta V_{DG(2)}$ is influenced by the voltage at the DG busbar under this scenario. This is depicted as $V_{DG(2)}$ in Eq. 6.1b. The subscript (2) is added to differentiate this quantity from that used in scenario 1.

3. *Voltage change, $\Delta V_{DG(3)}$, caused by the DG output*

The voltage change at the DG busbar that is caused by the DG output has a similar form to Eq. 6.1b, except that the complex power, $P_{DG} + jQ_{DG}$, is expressed using the generator convention (i.e. P_{DG} and Q_{DG} are positive when the DG *exports* real and reactive power to the network) and depends on the voltage at the DG busbar, $V_{DG(3)}$:

$$\Delta V_{DG(3)} = \frac{R_d \times P_{DG} + X_d \times Q_{DG}}{V_{DG(3)}} \qquad (6.1c)$$

The overall variation of the DG busbar voltage with respect to that of the source busbar is given by the sum of Eqs. 6.1a, 6.1b and 6.1c:

$$\Delta V_{DG} = \Delta V_{DG(1)} + \Delta V_{DG(2)} + \Delta V_{DG(3)}$$

$$= \left[-\frac{R_d \times P_{L1} + X_d \times Q_{L1}}{2 \times V_{DG(1)}}\right] + \left[-\frac{R_d \times P_{L2} + X_d \times Q_{L2}}{V_{DG(2)}}\right] + \left[\frac{R_d \times P_{DG} + X_d \times Q_{DG}}{V_{DG(3)}}\right] \qquad (6.2)$$

Eq. 6.2 can be greatly simplified by making the assumption that $V_{DG(1)} = V_{DG(2)} = V_{DG(3)} = V_{DG(max)}$. The validity of this assumption is discussed in Section 6.2.1.2 to follow. The assumption allows Eq. 6.2 to be written as:

$$\Delta V_{DG} = \frac{R_d \times (P_{DG} - \frac{P_{L1}}{2} - P_{L2}) + X_d \times (Q_{DG} - \frac{Q_{L1}}{2} - Q_{L2})}{V_{DG(max)}} \qquad (6.3)$$

and, since we are interested in calculating the allowable real power output of the DG, solving Eq. 6.3 for P_{DG} yields:

$$P_{DG} = \left(\frac{V_{DG(max)} \times \Delta V_{DG}}{R_d}\right) + \left(\frac{P_{L1}}{2} + P_{L2}\right) + \frac{X_d}{R_d} \times \left(\frac{Q_{L1}}{2} + Q_{L2} - Q_{DG}\right) \quad (6.4)$$

Equation 6.4 can be written using the same variables as the network model of Fig. 6.1, by way of three substitutions:

1. R_d and X_d can be expressed in terms of the line length:

$$R_d = r \times d \quad \text{and} \quad X_d = x \times d \quad (6.5a - b)$$

where $r + jx$ = the line impedance per unit length (pu/km), and

d = the distance of the DG from the source substation (km).

2. ΔV_{DG}, the voltage change from the source busbar to the DG busbar under conditions of maximum generation, can be written as:

$$\Delta V_{DG} = V_{DG(max)} - V_{Setpoint} \quad (6.6)$$

3. P_{L1} and P_{L2} were defined in Fig. 6.1 as:

$$P_{L1} = \frac{d}{L} \times P_{Total} \quad \text{and} \quad P_{L2} = \left(1 - \frac{d}{L}\right) \times P_{Total} \quad (6.7a - b)$$

Similarly, $$Q_{L1} = \frac{d}{L} \times Q_{Total} \quad \text{and} \quad Q_{L2} = \left(1 - \frac{d}{L}\right) \times Q_{Total} \quad (6.7c - d)$$

Using Eqs. 6.5a – d and the identities:

$$P_{Total} = S_{Total} \times \cos\phi \quad \text{and} \quad Q_{Total} = S_{Total} \times \sin\phi$$

it is possible to prove the equality:

$$\left[\left(\frac{P_{L1}}{2} + P_{L2}\right) + \left(\frac{x}{r}\right) \times \left(\frac{Q_{L1}}{2} + Q_{L2}\right)\right] = \left[S_{Total} \times \left(1 - \frac{d}{2 \times L}\right) \times \left(\cos\phi + \frac{x}{r}\sin\phi\right)\right] \quad (6.8)$$

where S_{Total} = the total apparent power load on the DG feeder, and

ϕ = the load power factor angle [=arccos(Power factor)].

Finally, substitution of Eqs. 6.5a – b, 6.6 and 6.8 into Eq. 6.4 yields:

$$P_{DG} = \left[\frac{V_{DG(max)} \times (V_{DG(max)} - V_{Setpoint})}{r \times d}\right] + \left[S_{Total} \times \left(1 - \frac{d}{2 \times L}\right) \times \left(\cos\phi + \frac{x}{r}\sin\phi\right)\right] - \left[\frac{x}{r} \times Q_{DG}\right] \quad (6.9)$$

Where:

$V_{DG(Max)}$ = the upper voltage regulation limit on the network;

$V_{Setpoint}$ = the OLTC setpoint voltage;

$r + jx$ = the impedance per unit length of the line connecting the DG and the source busbars;

d = the distance of the DG from the source substation;

L = length of the DG feeder;

$S_{Total}\angle\phi$ = the total apparent power load on the feeder; and

Q_{DG} = reactive power export by the DG to the network.

The form of Eq. 6.9 is analysed in detail in the simulations of Chapter 7 and it is found to be useful in understanding the interaction of different network variables on the voltage rise problem. From the onset, however, it is important to stress that Eq. 6.9 is only an approximation to the allowable power output of DGs in different scenarios. This is on account of three assumptions that were made in the course of the equation's derivation.

6.2.1.2 Underlying assumptions

The three assumptions that were made in the derivation of Eq. 6.9 affect the accuracy of the results it yields. These assumptions and their expected effect on the solution accuracy are described below.

Assumption 1: $V_{DG(1)} = V_{DG(2)} = V_{DG(3)} = V_{DG(max)}$. This assumption was made in order to simplify Eq. 6.2. In fact, it is also a necessity in order that Eq. 6.4 (that follows from Eq. 6.2) can be solved non-iteratively. This is because the variables $V_{DG(1)}$, $V_{DG(2)}$ and $V_{DG(3)}$ in Eq. 6.2 are unknowns. Further, values for these variables cannot be calculated using a non-iterative method, since they depend on the voltage drop/rise terms $\Delta V_{DG(1)}$, $\Delta V_{DG(2)}$ and $\Delta V_{DG(3)}$ (from Eqs. 6.1a to 6.1c) of which they are coefficients. As a result, approximate values must be used for the three voltage terms, and in order to yield a simple equation, they are assumed to have the same value, termed V_{DG}.

Since Eq. 6.9 is to be used to determine the maximum DG output that will cause the DG busbar voltage to rise to the upper voltage regulation limit, termed $V_{DG(Max)}$, it is logical to assume $V_{DG} = V_{DG(Max)}$. The effect of this further assumption is understood by studying Eqs. 6.1a, 6.1b and 6.1c.

Eqs. 6.1a and 6.1b describe the voltage drops that are expected across a feeder as a result of connected load. In both of these cases, the voltage at the DG busbar (in the

absence of DG) will be less than that at the source substation (given as $V_{Setpoint}$). The assumption: $V_{DG(1)} = V_{DG(2)} = V_{DG(Max)} = V_{DG(max)} > V_{Setpoint}$ thus has the result that the voltage drops, $\Delta V_{DG(1)}$ and $\Delta V_{DG(2)}$, are underestimated. In Eq. 6.9, this translates into an underestimation of the influence of feeder load on the allowable DG output and renders P_{DG} a pessimistic result.

In the absence of feeder load, Eq. 6.2 simplifies to Eq. 6.1c and $V_{DG(3)} = V_{DG(max)}$ is a truth rather than an assumption[2]. The same statement *is*, however, an assumption in the presence of load. This is because at maximum generation, $V_{DG(3)}$ will exceed $V_{DG(max)}$, since the increased voltage rise will be countered by the load voltage drop. In the presence of load, the assumption that $V_{DG(3)} = V_{DG(max)}$ thus leads to an overestimation of the voltage rise caused by the DG and leads to a further underestimation of P_{DG} by Eq. 6.9.

Assumption 2: The quadrature voltage change term, δV, is neglected. The effect of this assumption on the accuracy of Eq. 6.9 is most readily understood using vector representations of Eq. 3.4. A similar representation for Eq. 3.4 was presented in Chapter 3 as Figs. 3.3a-b. These are re-presented as Fig 6.2a-b. Fig 6.2a is applicable in the event that bus 2 is a load busbar (assumed to be operating at a lagging power factor in the load convention). Fig. 6.2b represents the voltage phasors in the event that bus 2 exports both real and reactive power towards bus 1 and corresponds to a DG operating at a lagging power factor.

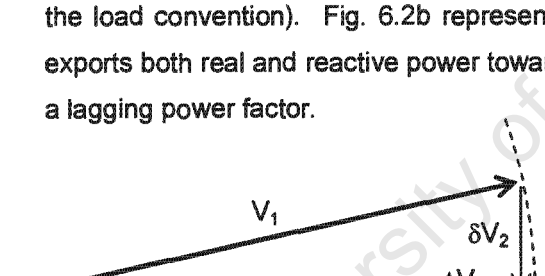

Fig. 6.2a. Vector diagram illustrating the voltage change across a feeder – Bus 2 is a Load bus.

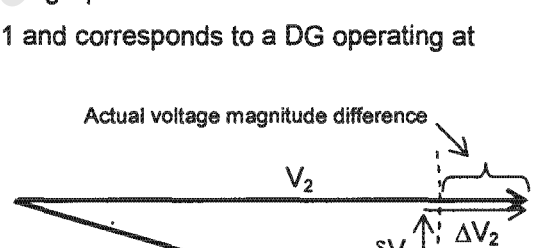

Fig. 6.2b. Vector diagram illustrating the voltage change across a feeder - Bus 2 is a Generator bus.

Significant from Fig. 6.2a is that, by taking the quadrature voltage change, δV_2, into account with bus 2 drawing load, the magnitude of the voltage drop between the sending- and the receiving-end busbars is greater than the magnitude of the in-phase voltage-change term ΔV_2 alone. It can thus be concluded that in neglecting the effect of the term

[2] In fact, this was the principal reason for using Eq. 3.4a as the basis of the derivation rather than Eq. 3.3a that uses the source busbar as reference. Use of sending-end quantities would dictate that assumptions be made under all network scenarios for the equations to be solved without iterations.

δV_2, Eq. 6.9 will underestimate the voltage drops caused by feeder load. As with Assumption 1, underestimation of the influence of feeder load will cause Eq. 6.9 to yield a conservative value for the allowable DG penetration in different networks.

Fig. 6.2b indicates that in the generation scenario, inclusion of the δV_2 term in the voltage rise calculation yields a lower result than the magnitude of the ΔV_2 term alone. Neglecting the δV_2 term in the voltage rise calculations of Eq 6.1c thus causes an overestimation of the voltage rise that will occur for a particular generator output. In Eq. 6.9, this translates into an underestimation of the allowable DG output before the upper voltage regulation limit is exceeded.

Assumption 3: Power losses on Line Section 3 are neglected. Neglecting the losses on line section 3 in the network model of Fig. 6.1 leads to a further underestimation of the allowable DG penetration. This is because power losses on line section 3 appear to the DG busbar as downstream load. From Eq. 6.4 it is clear that an increase in load downstream of the DG busbar adds directly to the allowable DG output.

The above discussion indicates that all of the assumptions that were made in the derivation of Eq. 6.9 lead to an underestimation of the allowable DG output before voltage regulation limits are exceeded. The qualitative analysis is not, however, sufficient to gauge the degree to which the assumptions affect the calculated results. Neither does it provide a clear indication regarding those network conditions that most affect the accuracy of the algebraic equation.

Uncertainty regarding the accuracy of Eq. 6.9 necessitates that a second, more rigorous solution to the model network be derived. To this end, Section 6.2.2 describes a computer-based load-flow program that was compiled to solve the model network.

6.2.2 Gauss-Seidel (iterative) solution of the network model

This section describes the method whereby the network model was solved for the maximum allowable DG penetration using the traditional Gauss-Seidel load-flow technique. The Gauss-Seidel method was identified in Section 2.1 as the most appropriate technique for the solution of load-flows of limited complexity.

6.2.2.1 Formulation of the load-flow problem

The model network of Fig 6.1 can be implemented as a traditional 4-bus load-flow problem as illustrated in Fig. 6.3 below.

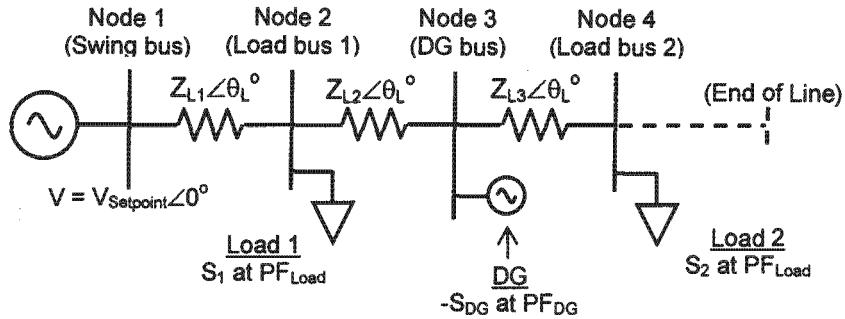

Note: load/generation is referenced as positive when flowing *away from* the respective busbars.

Where:

$Z_{L1} = Z_{L2}$ = (d/2) x Conductor impedance (Z_{pu}/ km);

Z_{L3} = (L-d)/2 x Conductor impedance (Z_{pu}/ km);

θ_L = Angle of Conductor impedance;

S_1 and S_2, the magnitudes of the apparent power loads, are calculated as in Fig. 6.1;

PF_{Load} and PF_{DG} are the load and DG power factors respectively;

S_{DG} = DG output power; and

$V_{Setpoint}$ = the setpoint voltage of the substation transformer OLTC

Fig. 6.3. Implementation of the model network as a load-flow problem.

In Fig. 6.3, the DG is modelled at Bus 4 and its output is represented as a negative load of variable power factor (as discussed in Section 5.2.5).

Bus 1 in Fig. 6.3 is the "Swing Bus". This node is specified as a constant voltage and phase angle and has no power constraint. It is used as a reference for other node voltages and supplies network loads and losses that are not supplied by the DG. Weedy [1994, p.211] describes how the swing bus in a load-flow can influence the complexity of the study and should be chosen as the node that most closely approximates an infinite busbar. In the case of this study, the source busbar *is* an infinite busbar and is thus the obvious choice of swing bus.

6.2.2.2 Application of the Gauss-Seidel algorithm using Microsoft Excel

Microsoft Excel was used for the implementation of the load-flow algorithm in preference to other programming tools, for example: C++ and Visual Basic. This decision was based on the following considerations:

1. *Ease of data handling.* The spreadsheet format of Excel provides a ready-made user-friendly interface for the entry and extraction of data from the load-flow program. Data

derived from the load-flow simulations can easily be represented graphically using the program's embedded graphing tool.

2. *Ease of programming.* Excel includes built-in functions for the representation of complex variables. Standard mathematical operators for complex variables are also provided. The program includes a built-in "goal seek" or feedback function that automatically varies one input variable such that a given output condition is attained. As seen in Fig 6.4 below, this function is required in order to determine the maximum DG output (input data to the simulation) that could be tolerated before the DG busbar voltage rises to the maximum allowable value (output condition).

A logic diagram of the load-flow program is presented as Fig. 6. Four sub-processes (**A** – **C**) are identified in the diagram. Details relating each sub-process are provided in the discussion to follow.

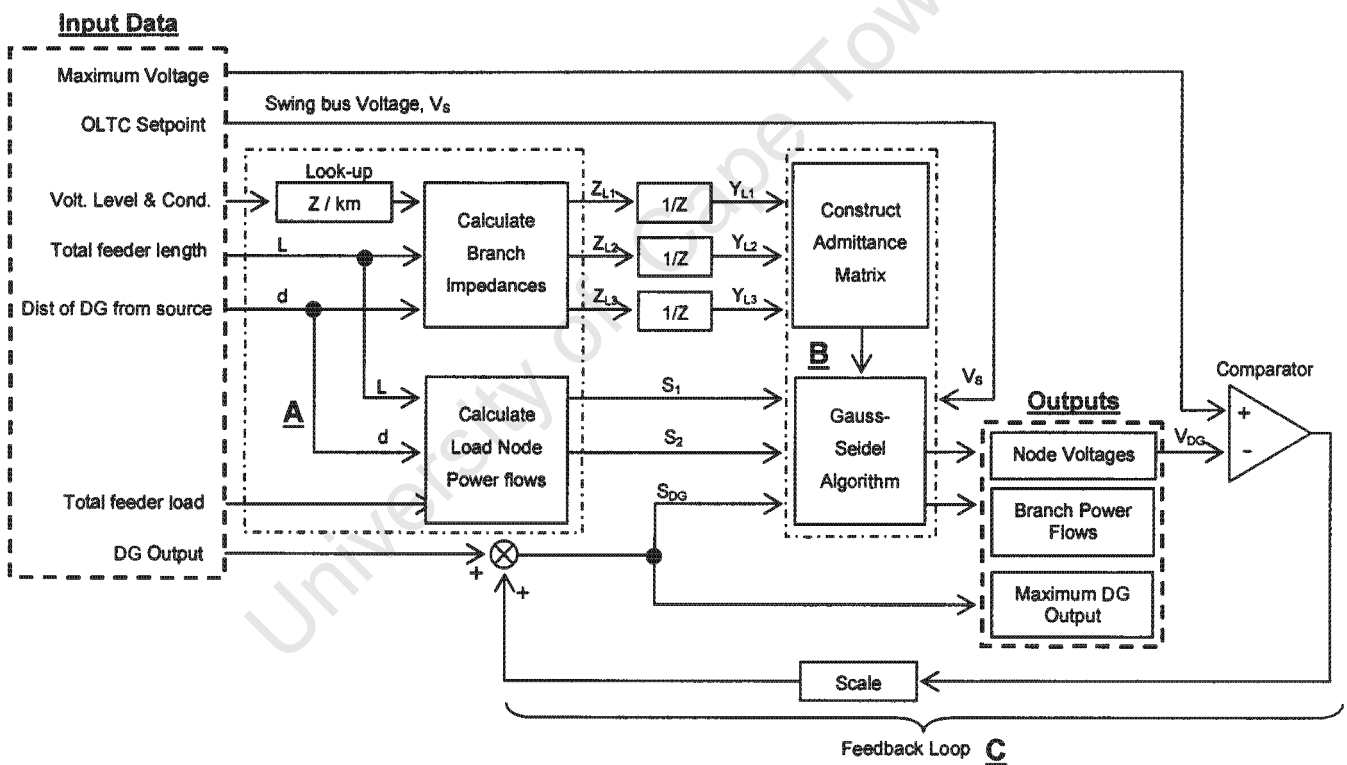

Fig. 6.4. Logic diagram of the load-flow program.

Sub-process A: Calculation of branch impedances and Load-Node Power flows. The calculation of the branch impedances Z_{L1}, Z_{L2} and Z_{L3} and the loads S_1 and S_2 at nodes 3 and 5 is based on formulae presented in Fig. 6.1 and Fig. 6.3. Data on line impedances per unit length (Z_{pu}/km) for the different conductor types at different voltage levels are derived from a look-up table. This information is derived from the standard Eskom table of line impedances and is presented in Table 7.1.

Sub-process B: Admittance Matrix construction and Gauss-Seidel solution process. Construction of the admittance matrices and the application of the Gauss-Seidel solution algorithm were performed as described in Appendix B. In contrast to the commonly used method where a variable number of iterations are used, the Excel-based load-flows use fixed numbers of iterations. This was done so as to simplify programming, but also afforded the advantage of being able to view the simulation's progress towards convergence. The latter feature was useful when determining the required tolerance for convergence, albeit at the expense of marginally increased computation times.

A figure of 1×10^{-5} pu was used for the tolerance of changes in the busbar voltages between iterations. This figure is 10 times smaller than the value suggested by Weedy [1994, p:225], but was required to achieve reliable convergence in simulations involving short line sections of low-impedance conductor and with little branch load. A second convergence criterion[3], the maximum change in branch power flows between iterations, was also applied with a tolerance of 1×10^{-6} pu. This provided solutions accurate to within 1kVA.

A minimum of 275 iterations was necessary to attain convergence in the worst case: a network with 2km sections of low-impedance conductor under light loading conditions, and the load-flow program thus used 310 iterations for each simulation. Notwithstanding the high number of iterations, when using a Pentium 4 desktop computer, a single load-flow solved in under half a second and DG penetration limits (requiring multiple load-flows) were calculated in under three seconds per case.

Sub-process C: Feedback loop. The feedback loop uses Excel's "Goal seek" function to determine that quantity of generation by a DG at a given network location that will cause the local busbar voltage to rise to the maximum allowable limit.

6.3 Chapter in Perspective

The voltage rise effect on DG-installed networks can be studied using a generalised 4-bus network model. The model network can be solved using a simple algebraic formula to ascertain the maximum penetration of DG that can be accepted at a given network location before the onset of overvoltage problems. The next chapter analyses the mathematical form of the algebraic solution equation to determine the relative influence of different network

[3] As described in Appendix B, this criteria is more onerous than the node voltage tolerance for networks with low impedance branches.

parameters on the voltage rise phenomenon. Chapter 8 investigates the limitations of the simple analysis that result from the assumptions made in the formulation of the network model and as a result the approximate solution method used. The latter analysis makes use of the Gauss-Seidel load-flow program that was developed in Section 6.2.2.

Chapter 7

Generalised Analysis of the Voltage Rise Effect

The discussion of Chapter 6 indicated that the mechanism of network voltage rise could be understood by considering the mathematical form of a simple algebraic expression for the allowable DG penetration into a generalised network. This discussion is developed further in the present chapter with an in-depth analysis of the form of the expression and through its application to four typical network scenarios. This serves to establish the usefulness of the algebraic equation as a tool for evaluating the voltage rise effect in different scenarios and for gauging the relative influence of different network parameters.

7.1 Approach

The relative influence of different network parameters on the severity of the voltage rise effect is studied by analysing the mathematical form of Eq. 6.9 and by entering typical parameter values into the equation. Results of the latter studies are plotted as a series of "DG location" vs. "DG penetration" curves.

Four types of feeders are used in the generalised analysis:

1. a 22kV line strung with ACSR "Rabbit" conductor: representative of distribution lines of low current carrying capacity,
2. a 22kV, ACSR "Hare" line: a high capacity distribution line,
3. an 88kV, ACSR "Hare" line: a low capacity sub-transmission line, and
4. an 88kV, ACSR "Wolf" line: a high capacity sub-transmission line.

Parameters for the different conductor types at the two voltage levels, as derived from Eskom's standard table of conductor data, are included in Table 7.1 below.

Table 7.1. Line impedance and rating data used in the generalised analysis.

Voltage	Conductor Type	Rating (75°)	R (pu/km)*	X (pu/km)*	X/R ratio
22kV	Single Rabbit	7.0MVA	0.12507	0.07987	0.639
22kV	Single Hare	10.2MVA	0.06703	0.07813	1.166
88kV	Single Hare	40.8MVA	0.00420	0.00598	1.424
88kV	Single Wolf	56.4MVA	0.00250	0.00524	2.096

*per-unit quantities are expressed on a 100MVA base.

The conductor types used in the sensitivity studies were selected such that the resistance of the low capacity type was approximately double that of the higher capacity conductor. The application of "Hare" conductor at both voltage levels is useful, as it allows for comparison between cases differing by voltage level alone.

Table 7.1 includes data on the MVA rating of each conductor type at the respective voltage levels. This is derived from each type's 75° thermal rating[1] and is used to place in context the penetration limits of the DG.

The feeder length was chosen as 50km in all simulations. This length represents a relatively long distribution line, and an average length sub-transmission line.

7.2 Impact of Network Parameters on the DG Voltage Rise Effect

Equation 6.9 from Section 6.2.1 indicates the maximum allowable DG penetration that can be accepted into a generalised network that is constrained only by voltage rise. As indicated below, Eq. 6.9 can be considered as the sum of three terms:

1. a "No-load" term that is independent of feeder load,
2. a term that is dependent on feeder loading – the "Load" term, and
3. a "Reactive Power Generation" term.

$$P_{DG} = \overbrace{\left[\frac{V_{DG(max)} \times (V_{DG(max)} - V_{Setpoint})}{r \times d}\right]}^{1\ \text{No-Load}} + \overbrace{\left[S_{Total} \times \left(1 - \frac{d}{2 \times L}\right) \times \left(\cos\phi + \frac{x}{r}\sin\phi\right)\right]}^{2\ \text{Load}} - \overbrace{\left[\frac{x}{r} \times Q_{DG}\right]}^{3\ \text{DG reactive power}} \quad (6.9)$$

Where:

$V_{DG(Max)}$ = the upper voltage regulation limit on the network;
$V_{Setpoint}$ = the OLTC setpoint voltage;
$r + jx$ = the impedance per-unit length of the line connecting the DG and the source busbars;
d = the distance of the DG from the source substation;
$S_{Total}\angle\phi$ = the total apparent power load on the feeder; and
Q_{DG} = reactive power export by the DG to the network.

[1] This is the maximum current-carrying capacity of the line such that, under the most onerous environmental conditions (highest ambient temperature and no crosswind), the conductor temperature will rise no higher than 75°C. This corresponds to a certain degree of conductor sagging. The 75° thermal limit of conductors has for many years been used in Eskom as the limit for continuous loading of a feeder under normal operating conditions.

Each of the three terms of Eq. 6.9 are analysed in the following sections to identify the relative influence of different network parameters on the voltage rise effect.

7.2.1 Analysis of the "No-Load" term

$$\text{No-Load term: } \left[\frac{V_{DG(max)} \times (V_{DG(max)} - V_{Setpoint})}{r \times d}\right]$$

Notice from Eq. 6.9 that the No-load term represents the total DG penetration limit for networks that are not loaded and where the DG operates at unity power factor.

The form of the No-load term indicates that in the absence of load the DG penetration limit is hyperbolic with respect to d, the distance of the DG from the source substation[2]. The limit of allowable DG penetration is thus halved as the distance of the DG from the source is doubled. This trend is illustrated for two typical 22kV feeders in the no-load curves of Fig 7.1 below[3].

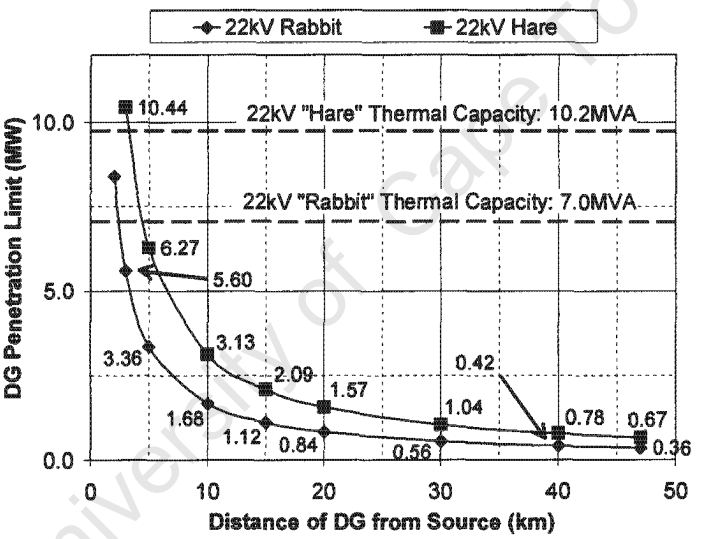

Fig. 7.1. DG penetration curves for typical 22kV feeders in the absence of load; generation at UPF.

The increase in allowable DG penetration on the higher capacity "Hare" feeder in Fig 7.1 is a result of its lower per-unit resistance. From Table 7.1, the upgrade of a 22kV "Rabbit" line to "Hare" conductor reduces the per-unit line resistance by 53.5%. By the No-load term this increases the penetration limit by a factor of 1.87 ($=0.535^{-1}$). A similar increase in the penetration limit is expected with a conductor upgrade from "Hare" to "Wolf" on an 88kV

[2] An equation in (x,y) is said to be hyperbolic if xy = c where c is a constant.

[3] The penetration curves of Figs. 7.1 and 7.2 are constructed under the assumption of a 1.03pu OLTC setpoint voltage and a maximum overvoltage limit of 1.05pu (as are commonly applicable to distribution networks in South Africa).

feeder. The type of conductor that is used on the DG feeder is thus seen to have a multiplicative effect on the No-load term of Eq. 6.9.

A second series of penetration curves in Fig. 7.2 demonstrates the effect of voltage level on the no-load DG penetration limits.

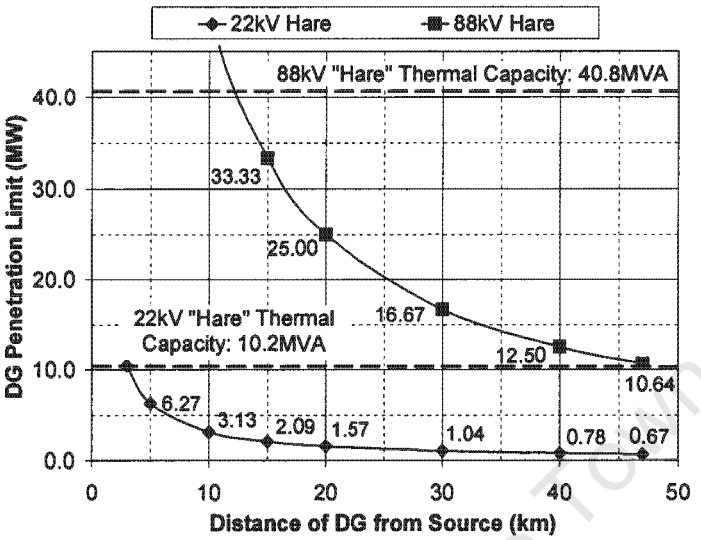

Fig. 7.2. Effect of voltage level on the no-load DG penetration curves; generation at UPF.

The curves in Fig. 7.2 indicate that the DG penetration limit on an 88kV "Hare" feeder is 16 times higher than that on a "Hare" line operated at 22kV. This effect is a result of the voltage dependency of the line resistance factor in the No-load term. Recall that the No-load term is expressed in per-unit values and that the per-unit resistance of a given conductor is inversely proportional to the square of the voltage level. By the No-load term then, the no-load DG penetration varies in proportion to the square of the voltage level.

The variation of no-load DG penetration limits with the square of the voltage level is particularly significant for lower voltage MV feeders. A "Hare" line operated at 11kV, for example, will accept one quarter of the power generation by DGs than one operated at 22kV. From Fig. 7.2, this suggests that an 11kV "Hare" line will accept less than 1MW of generation from any machine located further than 7km from the source substation.

The results of Figs. 7.1 and 7.2 indicate that DG feeders become increasingly voltage-constrained at lower voltage levels and with lower capacity conductors. This is evidenced by the fact that DGs within the first 13km of an 88kV "Hare" line are constrained by capacity limitations rather than the prevention of network overvoltages. On the 22kV "Rabbit" line, only machines closer than 2.4km to the source substation will be constrained by the conductor capacity. Also, a DG installed 40km down a 22kV "Rabbit" line can generate only up to 6% of the thermal capacity of the conductor, whereas the same machine on an 88kV "Hare" line can generate up to 31% of the conductor rating.

The form of the No-load term suggests that the DG penetration limit can be increased by lowering the OLTC setpoint at the source substation, or by increasing the limit for overvoltages on the network. In fact, the No-load term suggests that a 0.01pu reduction in the OLTC setpoint, or a 0.01pu increase in the limit for overvoltages, will give rise to a 50% increase in the penetration curves that were plotted in Figs. 7.1 and 7.2. This is because the figures were constructed under the assumption of a 0.02pu allowable voltage rise between the source and DG busbars. A 0.01pu increase to this represents a 50% increase in the $(V_{DG(Max)} - V_{Setpoint})$ term in the No-load term. Notice that a 0.01 to 0.03pu change in the limit for overvoltages (the maximum variation that is likely) represents a small percentage change in the variable $V_{DG(Max)}$, and the effect of the change on the multiplicative coefficient in the No-load term can thus be ignored.

A corollary of the above discussion is that an increase in the OLTC setpoint from 1.03pu to 1.04pu, or a decrease in the allowable limit for network overvoltages, to 1.04pu for example, will bring about a 50% reduction in the penetration limits of Figs. 7.1 and 7.2. This is a significant result in light of the discussions in Section 4.3 regarding the new approach to voltage drop apportionment on MV networks in the Eskom system. It was seen here that a reduction of the allowable overvoltage limit to 1.04pu is not uncommon.

7.2.2 Analysis of the "Load" term

$$\text{Load term: } \left[S_{Total} \times \left(1 - \frac{d}{2 \times L} \right) \times \overbrace{\left(\cos\phi + \frac{x}{r} \sin\phi \right)}^{\text{Power factor scaling factor}} \right]$$

Analysis of the Load term is considered in two parts: (i) the effect of unity power factor load and (ii) the effect of load power factor variations on DG penetration limits. Notice that the "power factor" scaling factor in the Load term equates to unity under the assumption of load at UPF (i.e. $\phi = 0^o$).

Expressed as a graph of "d" vs. "P_{DG}", the Load term at UPF represents a straight line having a maximum value of S_{Total} at the source substation busbar, and reaches a minimum of $\frac{S_{Total}}{2}$ at the line end. This is illustrated in Fig 7.3.

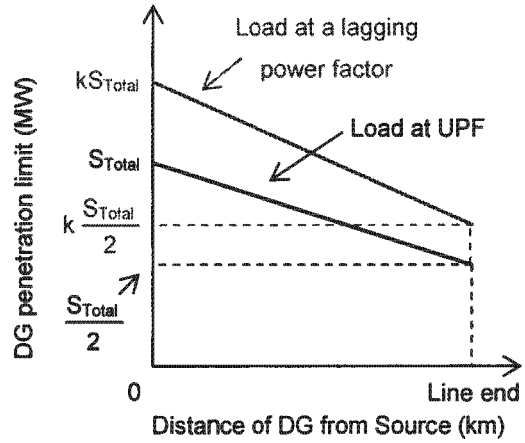

Fig. 7.3. Linear effect of feeder load on DG penetration limits.

Fig. 7.3 demonstrates that the effect of feeder load on DG penetration limits varies with the DG location. Significantly, however, the addition of S_{Total} of uniformly distributed load will increase the DG penetration at *all* locations by at least $\frac{S_{Total}}{2}$. This is in contrast to the hyperbolic No-load term that exhibits a much stronger bias towards DGs located near to the source substation.

The effect on the Load term of varying the load power factor is to multiply the linear UPF characteristic by a scaling factor, k. This is illustrated by the grey lines in Fig. 7.3. The scaling factor k is given by the expression: $\left(\cos\phi + \frac{x}{r}\sin\phi\right)$ in the Load term. The load scaling factor is plotted as a function of load power factor (i.e. cosϕ) for the four different types of networks in Fig. 7.4. Fig. 7.4 considers power factors from unity to 0.80 lagging.

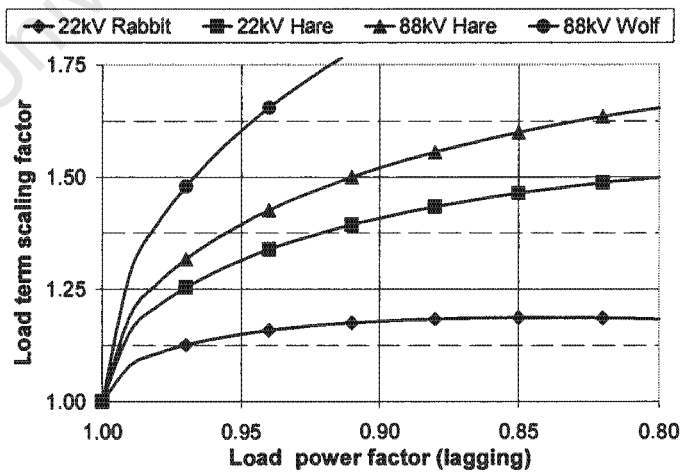

Fig. 7.4. The Load term scaling factor for varied load power factors on different networks.

The increase in the load scaling factor on higher voltage and higher capacity networks in Fig. 7.4 is a result of the increased X/R ratios of these feeders. This effect is countered to an extent, however, by the higher load power factors that are usually encountered on higher voltage feeders. Load power factors on distribution networks typically vary between 0.95 and 0.85 lagging, whilst on sub-transmission networks these range between 0.98 and 0.95[4]. This being the case, Table 7.2 lists the typical range of load scaling factors for the four networks considered in Fig. 7.4.

Table 7.2. Typical load scaling factor values for four different networks.

Network	Typical load scaling factor
22kV "Rabbit"	1.15 – 1.18
22kV "Hare"	1.31 – 1.46
88kV "Hare"	1.26 – 1.39
88kV "Wolf	1.39 – 1.60

The results of Table 7.2 indicate that even when considering the higher power factors on higher voltage networks, the load scaling factor generally increases with increased voltage levels and heavier conductor types. In this regard, Table 7.2 indicates a 40% increase in the load scaling factor between the 22kV "Rabbit" and 88kV "Wolf" networks.

The effect of load on DG penetration limits on stronger networks is increased further by the fact that high voltage, high capacity networks are usually loaded closer to their thermal limits than weaker systems. Recall from Chapter 3 that in the absence of DG, distribution networks in South Africa are often constrained by voltage-drop considerations that limit their capacities to values well below the thermal rating of the conductor. A simulation on a 50km 22kV "Rabbit" line, for example, reveals that the feeder can carry a maximum of 2.7MVA of uniformly-distributed load before the line-end voltage drops below 0.95pu. This compares with the 7.0MVA thermal rating of the conductor at this voltage level.

Despite the decreasing magnitude of Eq. 6.9's Load term in weaker systems, feeder load has a greater relative influence on DG penetration limits in weak networks. This is due to the swift decrease in the values of the No-load term in weaker systems. Figs. 7.5 a-b below indicate the increased overall DG penetration that is brought about on a 22kV "Rabbit" and an 88kV

[4] The highly reactive nature of sub-transmission and transmission line impedances dictates that voltage drops in these networks are more dependent on reactive power flows than on that of real power. Load power factors at these voltage levels are thus more tightly regulated through the application of tariff penalties to large power users that operate below a given power factor. Power factor correction devices are also commonly installed at sub-transmission voltage levels.

"Wolf" line with the addition of load to the value of 20% of the respective feeder's carrying capacity. The carrying capacity of the "Wolf" feeder is determined by the thermal rating of the conductor (56.4MVA), while that of the "Rabbit" line is constrained by voltage drop considerations in the absence of DG (2.7MVA).

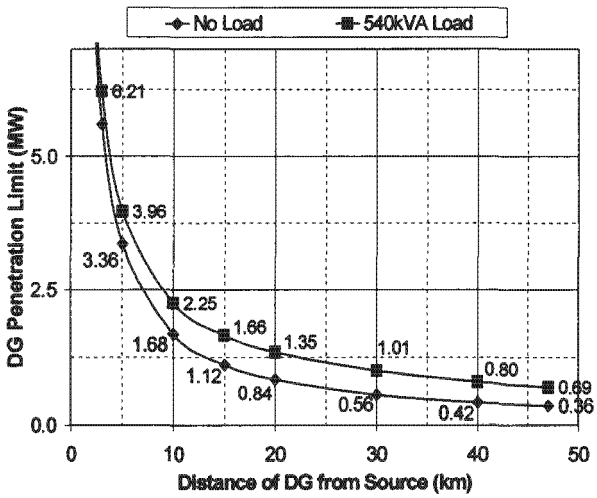

Fig. 7.5a. Increased DG penetration limit on a 22kV "Rabbit" line with the addition of feeder load.

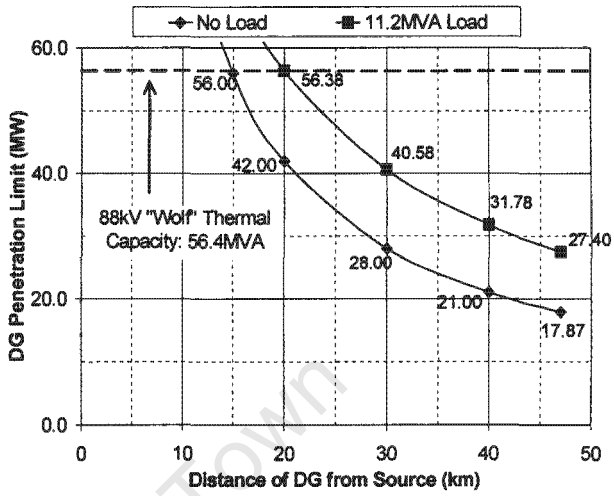

Fig. 7.5b. Increased DG penetration limit on an 88kV "Wolf" line with the addition of feeder load.

Notice from Fig 7.5a that the presence of 540kVA of load on the 22kV "Rabbit" line increases the allowable DG penetration 30km from the source substation by 80% when compared with the no-load threshold. On the 88kV feeder, the addition of 20% of rated load increases the penetration limit for a machine at the same location by 45%. It is also apparent from Figs. 7.5a-b that feeder load causes a greater percentage increase in the penetration limits for machines located farther from the source substation.

7.2.3 Analysis of the "Reactive Power Generation" term

$$\text{Reactive Power Generation term: } -\left[\frac{X}{r} \times Q_{DG}\right]$$

By the above term, reactive power absorption by the DG (in which case Q_{DG} is negative) has an additive effect on the DG penetration limit. The effect is, however, proportional to the X/R ratio of the feeder and is thus a more effective means of increasing DG penetration limits on higher voltage, higher capacity networks. To this end, the X/R data in Table 7.1 indicates that the absorption of 1MVAr by a DG will increase the allowable power export onto a 22kV "Rabbit" line by approximately 630kW, and by 2.10MW on an 88kV "Wolf" line.

It is significant that the effect of reactive power absorption (or generation) by a DG is independent of the machine's location. A fixed level of reactive power absorption thus gives

rise to the same increase in penetration limits for a DG located 2km from the source substation as it does for one located 47km away.

The "Reactive power generation" term can be reformulated to study the effect on DG penetration limits of operating the DG at a fixed power factor. This is achieved by substituting $Q_{DG} = P_{DG}\tan\theta$ into Eq. 6.9 and solving for P_{DG}.

$$P_{DG} = \underbrace{\left[\frac{V_{DG(max)} \times (V_{DG(max)} - V_{Setpoint})}{r \times d}\right]}_{(1)\ \text{No-Load}} + \underbrace{\left[S_{Total} \times \left(1 - \frac{d}{2 \times L}\right) \times \left(\cos\phi + \frac{x}{r}\sin\phi\right)\right]}_{(2)\ \text{Load}} \times \underbrace{\left(1 - \frac{X}{R} \times \tan\theta\right)^{-1}}_{(4)\ \text{DG power factor}} \qquad (7.1)$$

where θ is the leading power factor angle of the generator [= arccos(generator power factor)].

Notice in Eq. 7.1 that the "No-load" and "Load" terms have remained unchanged from Eq. 6.9, but that the "Reactive power generation" term has changed from an additive term into the multiplicative "DG power factor" term. The effect of operating a DG at a non-unity power factor is thus to multiply the results of the UPF studies by the scaling factor: $\left(1 - \frac{X}{R} \times \tan\phi\right)^{-1}$.

The form of scaling factor in Eq. 7.1 indicates that the effect of constant power factor operation by DGs is dependent on the X/R ratio of the feeder, and on the value of the generator power factor. The value of the scaling factor for four network types with DG power factors ranging from unity to 0.90 leading is shown in Fig. 7.6 below.

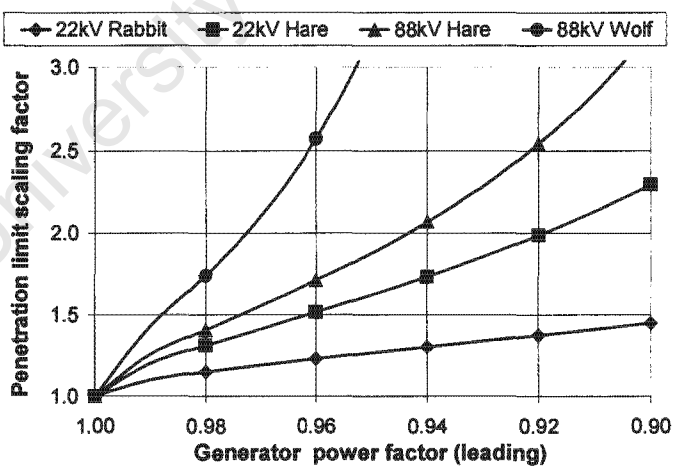

Fig. 7.6. Penetration limit scaling factors for DGs operating at leading power factors.

It is seen in Fig. 7.6 that the scaling factors for each of the four networks increase in a near-linear manner as the generator power factor is reduced. The increasing slopes of the curves with increased voltage levels and conductor sizes reinforce the finding earlier in this section that generation at lower power factors (corresponding to increased levels of reactive power absorption) is increasingly advantageous on stronger networks. Alternatively stated, the

effect of fixed power factor generation on the DG penetration limit is lowest on those networks that are most voltage constrained.

Notice from Eq. 7.1 that the presence of load on the feeder increases the benefits to be derived from fixed power factor generation. Specifically, the scaling factor in Eq. 7.1 is applied to the linear "Load" term as well as the hyperbolic "No-load" term. This is understood by the fact that the presence of load allows for an increase in DG penetration which, in turn, increases the level of reactive power absorption by the DG (since this operates at a fixed power factor). By the earlier discussion, an increase in reactive power demand by a generator increases the penetration limit further.

7.2.4 Summary: the influence of network parameters on DG penetration limits

The discussions of this section indicate that the DG-initiated voltage rise effect can be studied in terms of three terms:

1. A "No-load" term that is hyperbolic with respect to the distance of the DG from the source substation. The No-load term is proportional to the square of the voltage level and inversely proportional to the conductor resistance. Variations in the OLTC setpoint, and/or voltage regulation limits also have a multiplicative effect on the No-load term.

2. A "Load" term that is linear with respect to the distance of the DG from the source substation. This term is increased multiplicatively with increased load magnitudes and decreased load power factors, although the latter effect is dependent on the X/R ratio of the feeder.

3. A "Reactive Power Generation" (by the DG) term that is constant with respect to the distance of the DG from the source substation. This term is proportional to the X/R ratio of the feeder and the level of reactive power generation/absorption by the DG.

   OR

   A "DG power factor" term that forms a multiplier of the "No-load" and "Load" terms described above. The magnitude of the multiplier term is dependent on the generator power factor and the X/R ratio of the DG feeder.

The relative influence of variations in different network parameters was studied using the three-part analysis method outlined above. The results of these studies are summarised in Table 7.3 below.

Table 7.3. Relative influence of network parameter variations on DG penetration limits.

Network parameter	Affects Term*	Nature of effect	Summary
Voltage level	①②③④	Multiplicative	Has a significant effect on the no-load penetration limit. This is proportional to the square of the voltage level. Increased voltage levels also increase the effect of reactive power factor load (and generation) on account of the increased X/R ratios. Higher voltage lines are less voltage constrained, and can normally be loaded to a greater extent than lower voltage feeders.
Conductor type	①②③④	Multiplicative	The effect at No-load is inversely proportional to the conductor resistance. Has a similar effect on the load and reactive power generation terms as voltage level.
Feeder load	②	Additive	Has an additive effect on DG penetration. Effect decreases for machines located far from the source substation, but this decrease is not as significant as the decrease in the No-load component. The effect of the load term increases with decreasing lagging power factors, although this is dependent on the X/R ratio of the feeder.
OLTC Setpoint/ Voltage regulation limit	①	Multiplicative	Has a multiplicative effect on the No-load component. A 0.02pu decrease in the OLTC setpoint or a similar increase in the limit for overvoltages doubles the No-load factor.
Reactive power absorption by the DG	③④	Additive / Multiplicative	Fixed levels of reactive power absorption have an additive effect, but this is proportional to the X/R ratio of the conductor. Generation at a fixed power factor has a multiplicative effect on both the No-load and Load components of the penetration limit.

*Term references are as follows: ① "No-Load", ② "Load", ③ "Reactive power generation" and ④ "DG power factor".

7.3 Chapter in Perspective

The discussion in this chapter has revealed the algebraic solution equation to be a useful tool for the analysis of the voltage rise effect. This method of analysis is extended in Chapter 9 to describe the relative efficiencies of the voltage rise mitigation options that were outlined in Chapter 3. First, however, Chapter 8 investigates the accuracy of the equation's results given the number of core assumptions were made in the course of its derivation. This analysis serves to identify the limitations of the equation's applicability to the study of network voltage rise.

Chapter 8

Accuracy of the Generalised Analysis

Two sets of assumptions were described during the derivation of the algebraic solution equation (Eq. 6.9) in Chapter 6. These included:

1. assumptions made in the construction of the simple model network, and
2. assumptions required for the "linearisation" of the solution to the network model.

These assumptions are revisited in the present chapter. Section 8.1 identifies the limitations of the algebraic method as a solution to the network model. Thereafter, Section 8.2 revisits the assumptions that were made in Section 6.1 to determine whether or not the model network is adequately representative of real-life systems and can yield usable, practical results.

8.1 Accuracy of the Algebraic Solution of the Network Model

This section describes the results of a series of comparative studies that were performed to assess the accuracy of the algebraic method as a solution to the network model of Section 6.1.3. The results from the algebraic method are compared with those derived using the Gauss-Seidel load-flow program of Section 6.2.2 for simulations on different network types under varying load- and generation conditions.

8.1.1 Effect of variations in load, voltage level and conductor type

Twelve "DG location" vs. "DG penetration" curves were constructed to study the effect of DG location, voltage level, conductor type and network load variations on the accuracy of the algebraic solution method. The same four network types as were used in the analysis of Section 7.2 were applied for the present studies: 22kV "Rabbit", 22kV "Hare", 88kV "Hare" and 88kV "Wolf" networks (each 50km long). Simulations on the 22kV systems were performed at no load, and with 1MVA and 2MVA of load uniformly distributed down the feeder length. Studies at 88kV were conducted at no load and with 2MVA and 10MVA of feeder load respectively. These levels of loading were considered representative of the ranges that would typically be encountered in real-life applications, remembering that the voltage rise effect is most severe under the condition of lowest network loading. The load power factor was assumed at 0.95 lagging and the generation at UPF in all cases.

Simulation results for the three loading levels per network type are presented as Figs. 8.1a-d below. The results derived using the Gauss-Seidel technique are indicated by the solid curves, while curves derived using the algebraic method are indicated using dashed lines. In some cases, no dashed curves are visible, since they are overwritten by the respective Gauss-Seidel curves.

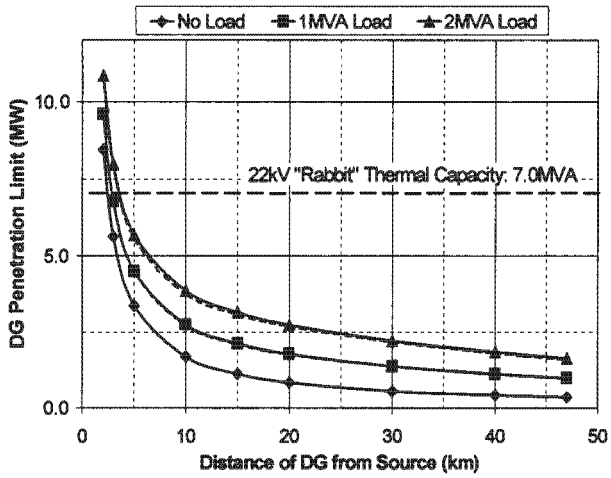

Fig. 8.1a. Accuracy of the algebraic solution under variable loading conditions on a 22kV "Rabbit" line.

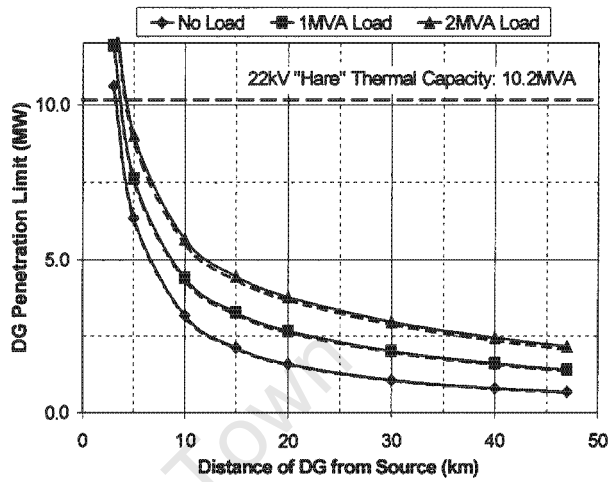

Fig. 8.1b. Accuracy of the algebraic solution under variable loading conditions on a 22kV "Hare" line.

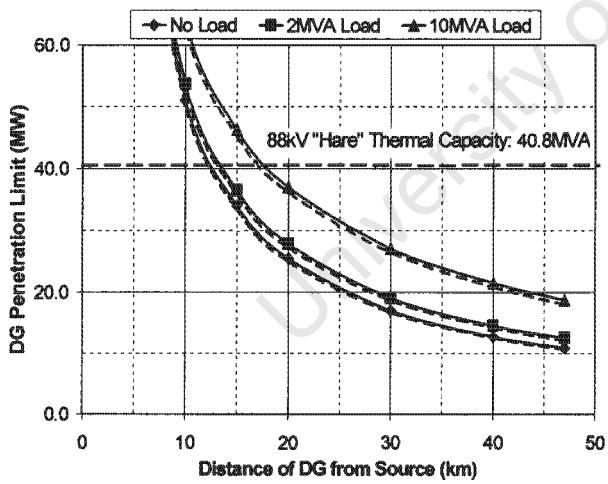

Fig. 8.1c. Accuracy of the algebraic solution under variable loading conditions on an 88kV "Hare" line.

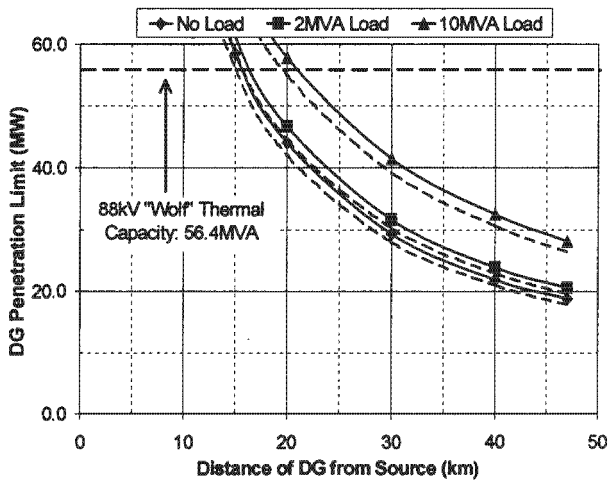

Fig. 8.1d. Accuracy of the algebraic solution under variable loading conditions on an 88kV "Wolf" line.

A notable trend from Figs. 8.1a-d is that the results from the algebraic method all fall below those derived using the Gauss-Seidel solution technique. This is to be expected given that all of the assumptions made in the derivation of Eq. 6.9 (as discussed in Section 6.2.1.2) lead to an underestimation of the allowable DG output.

Table 8.1 below describes the percentage underestimation of the allowable DG output by the algebraic solution method. Accuracy ranges are presented for all twelve of the curves in Figs. 8.1a-d. In all of the simulations, the algebraic method was most accurate for DGs located closest to the source substation. The starting figure of each accuracy range thus represents the accuracy for close-up machines, whilst the highest value is achieved for machines located at the end of the line.

Table 8.1. Percentage error of the algebraic solution under varying voltage level, conductor type and load conditions.

	Percentage underestimation by the algebraic solution method			
Case	**No load**	**1MVA load**	**2MVA load**	**10MVA load**
22kV Rabbit	0.6 - 0.7	0.7 – 2.4	1.8 – 3.9	-
22kV Hare	1.6 - 2.0	1.7 – 3.3	2.5 – 5.1	-
88kV Hare	2.0 - 2.5	-	2.0 – 3.1	2.1 - 3.5
88kV Wolf	4.6 - 5.2	-	4.4 – 4.9	4.7 - 6.1

It is apparent from Figs. 8.1a-d and Table 8.1 that the algebraic method is most accurate for DGs located closest to the source substation. This effect is a result of assumption 1 in Section 6.2.1.2 (i.e. that the DG busbar voltage remains fixed at 1.05pu under all conditions) being increasingly inaccurate for busbars located further from the source substation.

The accuracy of the algebraic solution method is reduced as the network load increases. This effect is particularly apparent from the results in Table 8.1 of the 22kV simulations for generators far from the source: the inaccuracy in the 22kV "Rabbit" simulations increases from 0.7% to 3.9% with the addition of 2MVA of feeder load. Notice that on an 88kV "Wolf" line, the change in accuracy is less than 1% with the addition of 10MVA of load. Deeper investigation reveals this phenomenon also to be a result of the first assumption in Section 6.2.1.2. The assumption that the DG busbar voltage remains fixed at 1.05pu is less valid as the load increases on account of the increased voltage drops across the conductor. The validity of the assumption is restored to an extent in higher voltage networks (with lower impedance conductors) since lower voltage drops are encountered for a comparable degree of feeder loading (i.e. a fixed percentage of the feeder's thermal capacity).

In Table 8.1, the 22kV no-load curves are very closely approximated by the algebraic solution method. Somewhat surprisingly, the accuracy of the no-load curves decreases at 88kV, and with the upsizing of the conductor. This effect can, however, be attributed to the second assumption of Section 6.2.1.2: that of neglecting the effect of the quadrature voltage change term, δV_2. By Eq. 3.4a and 3.4b, ΔV_2 and δV_2 are given as:

$$\Delta V_2 = -\frac{RP_2 + XQ_2}{V_2} \qquad \text{and} \qquad \delta V_2 = -\frac{XP_2 - RQ_2}{V_2} \qquad (3.4a\text{-}b)$$

The term magnitude of δV_2 is expected to increase relative to ΔV_2 as the X/R ratio of the line increases, since P_2 is usually greater than Q_2. Neglecting the δV_2 term in the derivation of Eq. 6.9 thus gives rise to greater inaccuracies on higher voltage lines, since these exhibit higher X/R ratios than reticulation-type networks.

A second series of simulations, described in Appendix C, were conducted to determine the effect of load power factor on the accuracy of the algebraic solution method. These simulations reveal that in the worst case of load at low (0.85) lagging power factors, the accuracy of the algebraic method drops by less than one percent compared to the studies with 0.95 lagging power factor load.

Overall, the algebraic solution method is found to be accurate to within 7% of the Gauss-Seidel method under typical network conditions. The approach is most accurate at lower voltage levels and under light loading conditions. From the previous chapter recall that these are the conditions under which the constraint on the DG output is most severe, and thus the conditions under which most accuracy is required.

8.1.2 Effect of reactive power generation

A further series of simulations were performed to establish the accuracy of the algebraic solution method under the condition of generation at leading power factors. Simulations were performed at no-load on each of the four network types for DG power factors of unity, 0.975, 0.95 and 0.925 leading.

The results of the simulations on the 22kV "Hare" network are illustrated in Fig 8.2 overleaf. As in Figs. 8.1a-d, results derived using the Gauss-Seidel technique are indicated in using solid lines, whilst those derived using the algebraic method are indicated using dashed lines. Note that the base case described as "Gen UPF" corresponds to the "No-Load" curve in Fig. 8.1b.

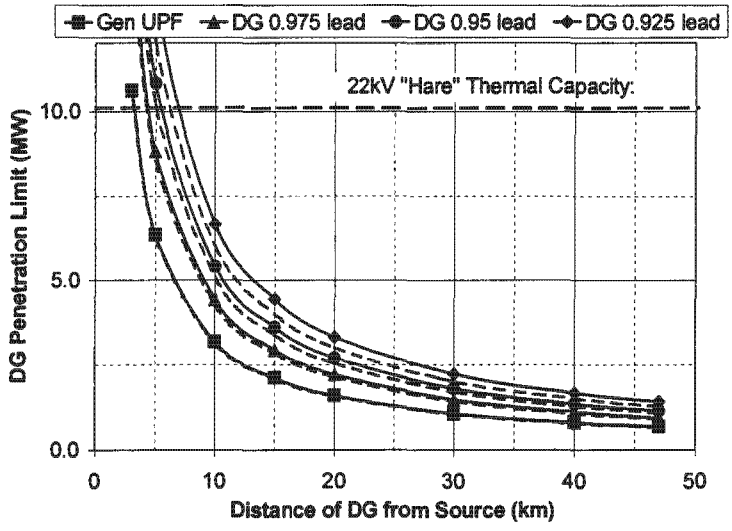

Fig. 8.2. Accuracy of the algebraic solution for various leading DG power factors on a 22kV "Hare" line.

Fig. 8.2 demonstrates a trend of decreasing accuracy of the algebraic method at lower leading DG power factors. It is also apparent from the figure that the percentage underestimation of the DG penetration limit remains relatively constant with increased distance of the DG from the source substation. In fact, analysis of the raw data reveals that the accuracy *is* constant across the length of the feeder. Percentage inaccuracy statistics for all the sixteen different scenarios are presented in Table 8.2 below.

Table 8.2. Percentage error of the algebraic solution for different DG power factors.

	Percentage underestimation by the linear solution method.			
Case	**UPF**	**0.975 lead**	**0.950 lead**	**0.925 lead**
22kV "Rabbit"	0.6	1.2	1.5	1.8
22kV "Hare"	1.5	3.4	6.2	9.7
88kV "Hare"	2.0	6.3	12.1	25.6
88kV "Wolf"	4.8	26.1	77 – 100*	100**

*Load-flow program determines very high penetration limits, but does not converge reliably.

** Load-flow program does not solve (i.e. the DG penetration limit approaches infinity).

The increased inaccuracy of the algebraic solution method for lower leading DG power factors can be attributed to assumption 2 from Section 6.2.1.2: the fact that the δV_2 term was

neglected in the derivation of the linear solution formula[1]. Recall that ΔV_2 and δV_2 are given by the expressions:

$$\Delta V_2 = -\frac{RP_2 + XQ_2}{V_2} \qquad \text{and} \qquad \delta V_2 = -\frac{XP_2 - RQ_2}{V_2} \qquad (3.4a\text{-}b)$$

Notice from Eq. 3.4b that the magnitude of δV_2 is greatest when P_2 and Q_2 are of opposite sign. This is the case when the DG operates at a leading power factor (absorbing reactive power whilst generating real power). Notice also by the form of Eq. 3.4a that ΔV_2 is smallest in the event of generation at a leading power factor. Generation at lower leading power factors thus causes large increases the relative size of δV_2 with respect to ΔV_2, and gives rise to the increased underestimation of the DG penetration limit that is observed in Table 8.2. Notice also from Eqs. 3.4a-b that the relative size of δV_2 and ΔV_2 is not affected by the distance of the DG from the source substation, but rather by the X/R ratio of the feeder. This explains the constant error percentages across the feeder lengths that are observed in Table 8.2.

Table 8.2 indicates a sharp decrease in the accuracy of the algebraic solution method for leading DG power factors on higher voltage and higher capacity networks[2]. This effect can again be understood by studying the form of Eqs. 3.4a-b. Specifically, the increased X/R ratios of the higher voltage/capacity feeders further increase the size of δV_2 relative to ΔV_2 and hence the degree of underestimation by the algebraic solution (that neglects the δV_2 term). Interestingly, a more qualitative analysis of the raw data for these simulations (and those in Appendix C.2) indicates a correlation between the decay in the accuracy of the algebraic solution and the increase in line losses on the network. The mechanism by which this occurs is not fully understood, but the result is very significant in the context of this section, since it indicates that underestimation of the DG penetration limit by the algebraic solution method may not be an *inaccuracy*. Rather, it may be that the algebraic method, through its having neglected the effect of the δV_2 term, is constrained in a way that tends to limit the extent of line losses. In this way, the results of the algebraic solution method may be more practical than those derived using the Gauss-Seidel technique, since the latter method does not consider line losses. This trend is suggested as a topic of further research.

---

[1] Note that Assumptions 1 and 3 from the discussion of Section 6.2.1.2 are not applicable in simulations performed without feeder load.

[2] A similar trend is noticed in a series of simulations on 22kV and 88kV "Hare" feeders with DGs operating at low leading power factors in the presence of low lagging power factor load. This study is described in Appendix C.2.

The results of this section, as in the previous section, indicate that the algebraic solution equation is most accurate on weak systems. The simulations at 22kV indicate that the method is accurate to within 5% of the Gauss-Seidel results for machines that are constrained to power factors higher than 0.95 leading. The "accuracy" of the algebraic solution is diminished dramatically in the event of heavy reactive power loading on the networks, a phenomenon that appears to be related to increasing line losses on the feeder.

8.2 Accuracy of the Network Model in representing Real-life Systems

The ability of the network model to represent real-life systems is evaluated in this section by revisiting the assumptions of Section 6.1.2. The assumptions were made in an endeavour to reduce the complexity of the model that was required to represent typical DG networks.

8.2.1 Model assumptions revisited

1. *The source substation is equipped with an OLTC.* Eq. 6.9 was derived under the assumption that the substation busbar voltage was regulated by OLTC action. In fact, the derivation of Eq. 6.9 can be easily modified for applications where this is not the case. In this event, the source impedance as seen from the substation busbar (at the same voltage level as the DG feeder) can be added to the impedance of line section 1 in Fig. 6.1, and Eq. 6.4 can be reformulated as:

$$P_{DG} = \left(\frac{V_{DG(max)} \times \Delta V_{DG}}{R_d + R_S}\right) + \left(\left(1 + \frac{R_S}{R_d + R_S}\right) \times \frac{P_{L1}}{2} + P_{L2}\right) + \left(\frac{X_d + X_S}{R_d + R_S}\right) \times \left(\left(1 + \frac{X_S}{X_d + X_S}\right) \times \frac{Q_{L1}}{2} + Q_{L2} - Q_{DG}\right) \quad (8.1)$$

where $R_d + jX_d$ = the impedance of the conductor connecting the source substation to the DG busbar
$R_S + jX_S$ = the source impedance seen from the source busbar

The magnitude and angle of the source impedances in Eq. 8.1 can be derived from the fault level statistics presented in Table 4.1 and Fig. 4.4 of Chapter 4.

Using Eq. 8.1, and comparing the magnitudes of typical busbar source impedances in South Africa with per unit length conductor impedances (from Table 7.1), indicates that the absence of a substation OLTC is unlikely to impose a significant constraint on DG penetration limits. From Table 4.1, for example, it is seen that the 50th percentile fault level for 22kV busbars is 84MVA. Assuming a typical source impedance angle of 84°, this fault level translates into a source impedance of 0.008 + j0.118 pu. Notice from Table 7.1 that the resistance of the source impedance in this case is only 12% of the per-unit resistance of 1km of "Hare" conductor at 22kV. By the first term in Eq. 8.1, it can thus be concluded that the absence of a substation OLTC will give rise to only a 6% change in the no-load DG penetration limit for DGs located 2km from the source. Recall from the

discussion of Chapter 7 that DGs located close to the source substation are often constrained by the thermal rating of the conductor rather than by voltage-rise issues, so the absence of an OLTC may actually have no effect on the no-load penetration limits at all.

Notice also from the form of Eq. 8.1 that the absence of a substation OLTC does not significantly alter the effect of load on DG penetration limits. From Fig. 6.1, the load P_{L1} is small for DGs located close to the source and so the multiplier $\left(1+\frac{R_S}{R_d+R_S}\right)$ will thus not have a large effect on the DG penetration limit. For DGs located farther from source substation, $R_d >> R_S$ and the multiplier term tends to unity.

The discussion above indicates that the network model of Section 6.1 is not constrained by the assumption of an OLTC being operational at the source substation. In fact, the algebraic solution equation is easily reformulated to allow the study of networks not fitted with OLTCs.

2. *The feeder load is uniformly distributed down the feeder length.* Notice from the form of Eq. 6.4 that the effect of feeder load on DG penetration limits can be divided into the effect of load downstream of the DG busbar (P_{L2}, Q_{L2}) and that of upstream load (P_{L1}, Q_{L1}). By Eq. 6.4, only half of the upstream load is added to the DG penetration limit. This is a result of the assumption that the load was uniformly distributed down the feeder's length and that the upstream load centre is halfway between the DG busbar and the source. In reality, practical experience suggests that the load centre from any point on a distribution line is located approximately 30% from the source busbar. This takes into account the distribution and lengths of spurs that tee-off the feeder backbone. This finding suggests that a more accurate formulation of Eq. 6.4 for application on distribution networks might be to reduce the multipliers of P_{L1} and Q_{L1} from 50% to 30%. In this way, Eq. 6.4 can be made to more closely represent practical networks.

3. *A single type of conductor is used along the entire feeder length.* The common design practice for distribution lines of reducing the conductor size along the backbone and spurs leads to non-uniform conductor impedance. This can, however, be accommodated into the network model of Chapter 6 by entering the average conductor impedance per unit length, and varying the location of the upstream load centre. The mechanism by which this is achieved is best understood by example.

   Scenario. Suppose that a DG is to be connected 10km from the source substation on a 22kV feeder. The first 2km of the feeder is strung with "Hare" conductor, whilst the

remainder of the feeder uses "Rabbit" conductor. As described above, the upstream load centre is located 3km from the source substation busbar.

Calculation of the DG penetration limit. From Table 7.1, the average impedance per unit length of the composite conductor can be calculated as $\left(\frac{2\times Z_{Hare}+8\times Z_{Rabbit}}{10}=\right)$ 0.1124 + j0.7952pu/km. This figure can be used as the uniform conductor impedance in the network model. Now, the impedance from the source busbar to the upstream load centre in this example is $(2\times Z_{Hare}+1\times Z_{Rabbit}=)$ 0.2591 + j0.2361pu. The resistive component of this figure corresponds to 23% of the line resistance from the source to the DG busbar, whilst the reactive component is 30% of the line reactance up to the DG busbar. The effect of the composite conductor can thus be represented by moving the real power load centre to 2.3km from the source busbar on the model feeder of uniform conductor type. As described in the previous section, this is achieved by reducing the multiplicative factor for P_{L1} in Eq. 6.4 to 0.23. Notice that the use of different conductor types on the same feeder has almost no effect on the location of the reactive power load centre, since the per-unit reactance of a line is hardly affected by the size of the conductor. Notice also that the use of multiple conductor types on the DG feeder will also give rise to a change in position of the downstream load centre. The position of the downstream load centre is not relevant in Eq. 6.4, however, on account of the assumption that power losses on the downstream line are neglected (as described in Section 6.2.1).

The example above demonstrates that the assumption of a single conductor type being used on the DG feeder will not limit the application of the algebraic solution method to real-life networks.

4. *The feeder load is of the constant power type.* The total range of allowable voltage rise resulting from the application of DGs is of the order of 0.01 to 0.03pu. It can thus be accepted that the voltage characteristics of the network load will have a negligible influence on the penetration limits that are derived using Eqs. 6.4 or 6.9. The voltage characteristics of loads are more significant in classical voltage drop studies where the range of voltage variation is of the order of 10%, and in transient studies where larger voltage deviations can be encountered.

5. *The DG is connected directly to the feeder backbone.* The possibility of DGs being connected to lateral feeders on distribution networks can be accommodated in the network model of Chapter 6 by shifting the location of the upstream load centre. Alternatively, the upstream load might be split into upstream load that is downstream of the tee-off point of the lateral on the backbone, and load upstream of this location.

"Scaling factors" for these loads in a reformulation of Eq. 6.4 can be calculated based on the location of the load relative to the source and DG busbars.

One of the primary concerns regarding the application of generator transformers in DG applications is the possibility of worse overvoltages arising on the DG-side bushings of the transformer. Generator transformers are, however, normally fitted with OLTCs. From the discussion of Chapter 4, these should be capable of bucking the source (i.e. utility-side) voltage by at least 5%. If the utility-side busbar voltage is restricted to a maximum of 1.05pu, adequate voltage regulation on the DG-side can thus be maintained via OLTC action of the generator transformer. Since transformers have very low series resistances, operation of DGs via a transformer should not give rise to significant voltage rise across the transformer itself. It thus appears that the presence of a DG transformer will have little effect on voltage rise studies conducted using Eqs. 6.4 or 6.9. The present study has, however, not considered the interaction between the generator transformer OLTC controller and the DG excitation controller. This topic should be similar to the application of generator transformers in traditional power station applications, but is suggested as an area for future investigation with particular reference to DG applications.

6. *The (synchronous) DG is not constrained to operate within in a fixed capability curve.* Detailed knowledge of a synchronous DG's capability curve (in terms of steady-state voltage studies) is required when the DG is to be made to operate at a leading power factor. This may be done in an effort to curb network voltage rise. In this case, Eq. 6.4 can be used to determine the required reactive power absorption capacity of the DG at a particular real power output if busbar voltages are to be maintained within the regulatory limit. This can be achieved by solving Eq. 6.4 for Q_{DG}.

   It was described in Chapter 5 how the optimal operating point within the DG's capability curve is influenced by considerations of generator stability, machine and network losses and reactive power tariffs. None of these factors are considered in the network model of Chapter 6 or in the "DG penetration" equations that followed therefrom. Indeed, it was seen in Section 8.1.2 how some "solutions" to the network model for DGs operating at leading power factors can give rise to extreme levels of power losses across the network. Further discussion in Section 8.1.2 indicated that the algebraic equation for the solution of the network model takes into consideration the reduction of losses in its solution process, although the mechanism by which this is achieved is not fully understood. Overall, the simple network model and the related algebraic solution equations must be applied with caution to DG applications at leading power factors. The necessity to consider machine stability, losses and tariffs indicates that detailed application-specific studies will be required in these cases. The simple analysis equations identified in this study are, however, useful in identifying the potential for the application of different generator control modes for the mitigation of network voltage rise.

8.3 Chapter in Perspective

The algebraic method for the study of DG-initiated network voltage rise is most accurate for applications on weak networks: those of low voltage level, X/R ratio and load. This is advantageous since, as described in Chapter 7, voltage rise is more of a constraint to DGs in this type of network. The algebraic method is also useful for the study of network voltage rise in stronger systems. The slightly reduced accuracy of the solution method in these networks is not likely to be significant, since voltage rise is less of a constraint for DG applications.

The discussion of Section 8.2 indicated that, with minor modifications, the algebraic approach could be applied to most real-life systems. The scope of application of the method is demonstrated in two case studies in Chapter 9. The method is also applied to the evaluation of the voltage rise mitigation options from Chapter 3. The discussion of the present chapter found that the algebraic approach is not sufficient on its own to study one of the mitigation options, namely that of reactive power absorption by DGs. The approach is, however, found to be useful in identifying network conditions that most suit this option.

Chapter 9
Application of the Analysis Technique

The discussion of Chapter 7 regarding the relative influence of different network parameters on the voltage rise effect is extended in the first section of the present chapter to identify the relative efficiency of the six voltage rise mitigation options from Chapter 3. Thereafter, the algebraic analysis technique is used as the basis for a generalised approach for the evaluation and resolution of voltage rise problems in DG applications. This method is compared with two generalised evaluation methods that are used in other countries and which were introduced in Chapter 1. The application of the generalised approach is demonstrated on two South African case studies in the final section of this chapter.

9.1 Assessing the Mitigation Options

The six options for the mitigation of the voltage rise effect from Section 3.2.3 are revisited in the present section. The relative efficiency of each option is established following the discussion of Chapter 7 regarding the effect of different network parameters on network voltage rise.

9.1.1 Upgrading the network

An upgrade of the conductor on the DG feeder to one of larger cross-section increases the DG penetration limit by way of the reduction in conductor resistance, r. This has a multiplicative effect on the No-load term in Eq. 6.9. A reduction in conductor resistance also affects the reactive power load and generation terms in Eq. 6.9 through the increase brought about on the X/R ratio of the feeder.

A study of Eskom's standard table of line impedances reveals that the maximum possible reduction in line resistance that can be effected by a conductor upgrade is of the order of 85%. This figure corresponds to a 22kV feeder being up-rated from "Mink" to "Kingbird" conductor, or at 88kV from single "Hare" conductor to a twin "Kingbird" bundled arrangement. Such drastic reductions in line resistance will, however, usually require that the line be entirely rebuilt for the towers to carry the extra conductor weight. This constraint is likely to limit the practical maximum reduction in line resistance by between 35 to 50%. These figures correspond to a 50 to 100% increase in the no-load DG penetration limit. A 50% decrease in conductor resistance will typically increase the X/R ratio by 75 – 100% on a reticulation line, and from 50 – 75% on a sub-transmission network.

The hyperbolic characteristic of the no-load DG penetration limit with increased distance of the DG from the source (as described in Section 7.2.1) has serious implications for the efficiency of network upgrading as a mitigation option. The multiplicative effect of this option on the penetration limit dictates that its efficiency (in terms of MW generation) will decrease in proportion to the distance between the DG and source busbars. The cost of a conductor upgrade, on the other hand, increases in proportion to the line length.

Costs for re-conductoring distribution and sub-transmission networks in South Africa vary in the region of R150 000 to 200 000/km. This makes the network upgrade option an expensive prospect for all but those DGs located very close to the source substation – typically closer than 4 or 5km away. In Chapter 7, it was seen that DGs located close-in are often constrained by the thermal capacity of the conductor (or that of the substation transformer), rather than by voltage rise. Network upgrading might thus be the best prospect in these select applications. This option has the added benefit of increasing the effect of reactive power absorption by the DG as a mitigation option as described in Section 9.1.4. Overall, however, DGs located farther from the source substation will usually benefit more from the option of installing a voltage regulator as described below.

9.1.2 Installing a voltage regulator

The discussion of Section 4.2.4 indicated that the application of a voltage regulator to a DG feeder can be approximated by considering voltage rise in terms of two separate systems: the networks upstream and downstream of the regulator installation. In this way, installing a voltage regulator on the DG feeder reduces the effective distance of the generator from the source busbar (represented by the variable "d" in Eq. 6.9). At best, the application of a voltage regulator midway between the source and DG busbars can halve the value of "d", and can give rise to a 100% increase in the no-load DG penetration limit. As with the previous option, however, this has a multiplicative effect on the hyperbolic no-load characteristic, and the efficiency of this solution method is reduced for machines located farther from the source substation.

A two-can voltage regulator installation can be installed at a cost of approximately R500 000. For DGs located further than 5km from the source substation, this option thus has a much lower cost/benefit ratio than a possible network upgrade. This option is less viable for DGs located close the source substation, since the application of a voltage regulator does not increase the thermal carrying capacity of the network. Voltage regulators are also only available for application at distribution voltage levels.

In the discussion above, it was assumed that the voltage regulator could be installed at the midpoint between the source and DG busbars. In fact, the placement of regulator installations is a more complex topic, and includes an analysis of load magnitudes and

positions, as well as the accessibility of the proposed site [Carter-Brown, 2002b, p.45-6]. This discussion is beyond the scope of this study. A further aspect that could influence the optimal location of a regulator installation is, however, described in Section 9.1.3.

9.1.3 Reducing the sending-end voltage

The discussion of Chapter 7 indicated that reduction of the source voltage setpoint (as with the previous mitigation options) has a multiplicative effect on the no-load DG penetration limits. From Section 4.2.3, this mitigation option can be realised through the application of "Line Drop Compensation" (LDC) to the OLTC or regulator control strategy. This same discussion indicated, however, that LDC is often limited to applications with regulators, or with OLTCs whose transformers supply only a single feeder. The option of applying LDC to reduce the sending-end voltage on the DG feeder can thus mostly be considered as an extension of the previous mitigation option. Section 4.2.3 indicated that the presence of DG can negatively influence the operation of the LDC controller. The possible application of LDC to DG-installed networks will thus require detailed study, and is beyond the scope of the generalised analysis technique.

9.1.4 Reactive power absorption by the DG

The studies of Section 7.2.3 demonstrated the potential of having the DG absorb reactive power in order to mitigate against network voltage rise. The effect of reactive power absorption was seen to depend on the X/R ratio of the feeder and is thus a less effective option in weaker networks. In fact, the decrease in efficiency is such as to make this option unviable for application on many 22kV and 11kV networks. It is, however, a viable option on higher voltage, higher capacity systems.

The extent to which this mitigation option can be applied is reliant on the tariff for reactive power consumption and the extent of allowable network losses. At present, however, no charge is levied for reactive power consumed by DGs in South Africa and no consideration is given to the losses that might be incurred as a result of the generator's control strategy. Until such time as these structures are developed, it is difficult to further assess the efficiency of this option for voltage rise mitigation. At present, this option is the most favourable from the DG operator's perspective on account of the avoided capital expenditure as compared to the other mitigation techniques. This will undoubtedly change if a reactive power tariff is instituted with respect to DG.

A future reactive power tariff that includes a charge for VArs drawn in excess of a given power factor (similar to the tariffs presently offered to non-generating customers) will encourage DGs to operate at a fixed power factor. This was seen in Chapter 7 to give rise to a multiplicative increase in the DG penetration limits. As with the previous mitigation options, operation of the

DG at a fixed leading power factor will be less effective for machines located far from the source substation.

Section 2.2 described a study by Salman et al. [1996] that concluded that the effectiveness of this mitigation option can be increased by connecting the DG to the network via a generator transformer. This premise on which this is based is that a transformer has a high series reactance, and that this will increase "x" in Eq. 6.9. This logic is flawed, however, since the transformer is a lumped reactance, and although its presence will reduce the voltage on the DG-side busbar as a result of reactive power drawn through the transformer, an overvoltage condition will still exist on the network-side of the transformer.

The possible application of a shunt reactor to reduce the extent of network voltage rise was introduced in Section 2.2. The mechanism by which voltage reduction is achieved in this case can be understood using Eq. 6.9. Shunt reactor applications will, however, be equally constrained by the lack of a reactive power tariff and loss allocation practice, as is the option of reactive power absorption by the generator itself.

9.1.5 Back-feeding an adjacent network

Back-feeding an adjacent network is an effective means of increasing the load on the DG feeder. From Chapter 7, feeder load has an additive effect on the DG penetration limit, although its effectiveness is reduced if the load is situated far upstream of the DG location. The additive effect of feeder load is particularly significant for the mitigation of voltage rise caused by DGs located far from the source substation. All of the mitigation options described previously have a multiplicative effect on the penetration limit. Penetration limits for machines far from the source substation are low, however, and multiplicative solutions thus have a very limited influence.

The option of using the DG feeder to supply an adjacent network has implications for the reliability and quality of supply of both networks. It may also cause difficulties with the grading of the protection on line-installed switchgear and may cause voltage drop problems in the event that the DG is out of service. Application of this solution option will require that a detailed study be performed and cannot be adequately evaluated using the simple voltage rise studies alone.

9.1.6 Constraining the generator

Constraining the DG to operate during periods of heavier network loading is a second load-based method for mitigating against voltage rise. This may be the only viable option for small DG operators whose machines are located far from the source substation, since this solution requires no extra capital investment. The effect on the DG operator of constraining the

generator to operate during periods of heavier loading is limited by the fact that the energy price will be highest at this time. For operators of MW-sized machines the cost of undelivered energy may, however, justify the capital outlay required by one of the other mitigation options.

9.2 Generalised Approaches for the Evaluation of Network Voltage Rise

Section 3.3 introduced two generalised methods for the evaluation of DG-initiated network voltage rise: standard penetration limits based on DG location and voltage level, or expressed as a multiple of the three-phase fault level at the point of connection. The present study has identified a third method by which the voltage rise phenomenon can be studied. This method is developed into a formal evaluation procedure in Section 9.2.1. Thereafter the "new" generalised approach is compared with the two previous methods.

9.2.1 A new generalised approach

The discussion of Chapters 7 and 8 indicates that the voltage rise phenomenon in DG-installed networks can be studied using Eq. 9.1 below. This equation is similar in form to Eq. 6.9, but includes discrete terms for the apparent power load that is situated upstream and downstream of the DG busbar. A discrete variable, n, is also included for the upstream load scaling factor that, as described in Section 8.2, can be varied to represent networks of non-uniform load distribution and/or conductor type.

$$P_{DG} = \overbrace{\left[\frac{V_{DG(max)} \times (V_{DG(max)} - V_{Setpoint})}{r \times d}\right]}^{1} + \overbrace{\left[(n \times S_{Up} + S_{Down}) \times \left(\cos\phi + \frac{x}{r}\sin\phi\right)\right]}^{2} - \overbrace{\left[\frac{x}{r} \times Q_{DG}\right]}^{3} \quad (9.1)$$

Where: $V_{DG(max)}$ = the maximum allowable busbar voltage on the DG feeder (pu)

$V_{Setpoint}$ = the setpoint voltage of the substation OLTC controller or the line-installed voltage regulator (pu)

x,r = the average resistance/reactance per-unit length of the conductor connecting the DG to the source substation (pu/km)

d = the electrical distance of the DG from the source substation (km)

S_{Up} = the total apparent power load on the line section between the source substation and DG busbar (pu).

S_{Down} = the total apparent power load at, or downstream of, the DG busbar (pu).

n = upstream load scaling factor. On networks of uniform conductor type n is calculated as the distance of the load centre of the upstream load from the source substation, expressed as a percentage of d. If the load centre is k km from the source substation then $n = \frac{k}{d}$. Where the position of the upstream load centre is not known, use n = 0.3.

ϕ = the load power factor angle [=arccos(load power factor)].

Q_{DG} = reactive power delivered by the DG to the network.

Notice that Eq. 9.1 is applicable to DG feeders whose source busbar voltage is regulated by OLTC or voltage regulator action. The same equation can, however, be used in the event that no OLTC or regulator is installed at the source if the DG is located further than 5km from the source substation. Failing this, an equation of the form of Eq. 8.1 should be used.

Eq. 9.1 is used as the basis for a generalised procedure for the evaluation of the voltage rise effect in DG projects as described the flow diagram of Fig. 9.1 below.

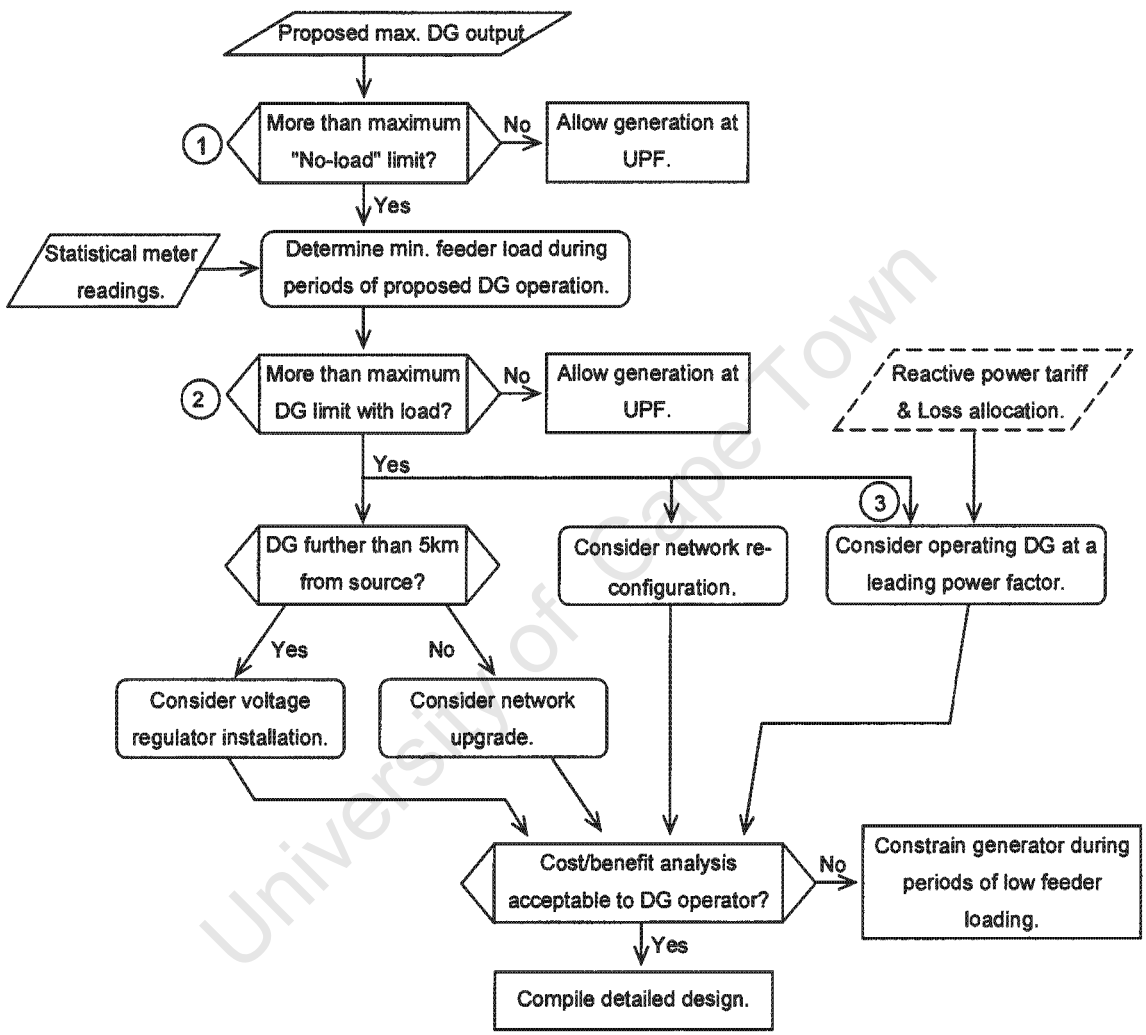

Fig. 9.1. Decision tree for the evaluation and solution of network voltage rise problems.

In Fig. 9.1, decision ① requires only basic information regarding the DG proposal: maximum planned power output, location, and voltage level and conductor type. This information is used to determine the No-load DG penetration limit via term① in Eq. 9.1. Decision 2 requires that statistical metering data is available for the DG feeder, and the simple study is repeated, but with information on the magnitude and power factor of the "standing" load included via term② in Eq. 9.1. Note that this term requires knowledge of the load that is located upstream and downstream of the DG location. If this is not known, the upstream and downstream loads

can be approximated using the assumption of uniform load distribution. In this case S_{Up} and S_{Down} are given by:

$$S_{Up} = \frac{d}{L} \times S_{Total} \quad \text{and} \quad S_{Down} = \left(1 - \frac{d}{L}\right) \times S_{Total} \tag{9.2}$$

Where:

d = the distance of the DG from the source substation;
L = length of the DG feeder; and
S_{Total} = the total apparent power load on the feeder.

Eq. 9.1 can be used as the basis for a screening study of the possible mitigation options in the event the allowable penetration limit at the DG location is not sufficient to cater for the proposed machine output. Term ③ in Eq. 9.1 can be used to gauge the effect of reactive power absorption by the DG, or, re-writing the term as a function of generator power factor as in Eq. 7.1, the effect of operation at a fixed power factor. As described in Section 9.1, proper evaluation of DG control mode variation as a solution of the voltage rise effect is dependent on the reactive power tariff and the loss allocation philosophy, neither of which are currently defined in South Africa. As described earlier in this chapter, Eq. 9.1 can also be used to gauge the relative efficiency of other solutions to the voltage rise problem: voltage regulator installation, conductor upgrade and network re-configuration.

9.2.2 Comparison of generalised methods

The "new" generalised approach to the evaluation of network voltage rise is here compared to the two international methods that were introduced in Section 1.3. Recall that the first of these methods employs a table of generalised DG penetration limits based on the voltage level of the DG feeder and a rough indication of the DG's location: at a source busbar, or elsewhere on the network. The second method uses the three-phase fault level at the DG busbar to calculate the allowable DG penetration limit.

The first international method

Table 1.1 in Chapter 1 listed the generalised DG penetration limits that are applicable when using the first international method. This table is re-presented in part as Table 9.1 below and includes comparative penetration limits for four of the voltage level/DG location categories as derived using the "new" generalised approach.

Table 9.1. Comparison of DG penetration limits derived using the first international method and the "new" generalised approach.

Cat.	*DG location*	*Int. Method 1*[1]	*"New" Method*
1	Anywhere on a 63kV – 90kV network	10-40MVA	10-40MVA*
2	Anywhere on a 15kV – 20kV	6.5-10MVA	500kVA – 7MVA†
3	At an 11kV or 11.5kV busbar	8MVA	8.2MVA‡
4	Elsewhere on an 11kV or 11.5kV network	2-3MVA	125kVA – 3.5MVA**

* Based on the results for the 88kV "Hare" line in Fig. 7.2

† Based on the results for the 22kV "Rabbit" line in Fig. 7.1

‡ Based on the 20th percentile fault level for 11kV busbars in South Africa with an assumed source impedance angle of 84°. This corresponds to a source resistance of 0.118pu.

** Calculated from the results of the 22kV "Rabbit" line, using the (halved) thermal capacity as the upper limit and the voltage-rise related lower limit. The latter figure is four times smaller than that at 22kV on account of the no-load DG penetration limit varying with the square of the voltage level.

Notice in Table 9.1 that the upper limit of DG penetration limits in categories 1,2 and 4 for the "new" method are based on the thermal capacity of the respective lines and not on a voltage constraint. The generalised equation has the penetration limits (that are based purely on the study of network voltage regulation) approaching infinity near to the source busbar. The international method presumably also considers thermal capacity limits for the upper bound of the listed penetration limits.

Table 9.1 indicates a close correlation between the ranges of penetration limits in category 1. This correlation may, however, be misleading, since entry for the "new" method is based on an 88kV network. The discussion of Chapter 7 indicated that the penetration limit varies with the square of the voltage level. It may thus have been more realistic to list penetration figures for a typical 66kV network. These would have been in the range of 5MVA – 40MVA. The results of the two methods are nevertheless still in good agreement.

There is a large discrepancy between the lower values of the penetration limit ranges in categories 2 and 4 in Table 9.1. This may be partly due to the results of the "new" method having neglected the possible presence of load on the DG feeder. Even so, the addition of typical "standing" loading values (2MVA on a 22kV network and 1MVA on an 11kV system) by Eq. 9.1 will only add 1MVA and 500kV to the respective penetration limits. The results of the "new" method will thus still be significantly lower than those listed for the international method. This can be related to the relative strength of the electrical networks in the countries where

[1] Penetration limits derived from this method are tabulated in Cigré [2002, p.10].

the methods are applied. The 6.5MVA penetration limit that is listed by the international method, for example, corresponds to a figure derived using the "new" method if the length of the "Hare" line is limited to 5km. The same lower penetration limit is obtained if a higher capacity conductor is used on a slightly longer line: a 15km "Kingbird" line, for example. Comparison of the results of Table 9.1 thus provides confirmation of the results of Sections 3.2.2 and 4.1 regarding the comparative weakness of South African distribution networks with respect to those in other countries. The "new" method can be used for voltage rise analysis on weak and strong networks.

There is a close correlation in Table 9.1 between the results from the two methods for the DG penetration limit on 11kV busbars. The result of the "new" method is representative of the penetration limit for DGs that are located near to a typical 22/11kV reticulation substation whose transformer is not fitted with an OLTC. Note, however, that this result does not consider (as is likely) the restriction that is placed on DGs by the limited transformer capacity. It is possible, on the other hand, that the figure for the international method is based on the consideration of typical 11kV transformer sizes in other countries.

The second international method

An alternative generalised method of evaluating DG penetration limits, as used in Spain and other countries, is to specify that the DG penetration does not exceed a given percentage of the three-phase fault level at the proposed point of connection. Section 4.1 described how the fault level at a given network location provides an indication of the source impedance at that point, but that it neglects the effect of network load[2]. This suggests that the origins of the second international method can be understood by considering the No-load term in Eq. 6.4.

It was seen in Section 2.2 that the per-unit three-phase fault level at a particular network location can be inverted to provide a value for the per-unit source impedance. This suggests that the per-unit source resistance, $R_{Source(pu)}$, as seen from a DG busbar, can be calculated using the expression:

$$R_{Source(pu)} = \frac{\cos\varphi}{S_{Fault(pu)}} \qquad (9.2)$$

Where: $S_{Fault(pu)}$ = the three-phase fault MVA expressed in the per-unit system; and
φ = the fault level or source impedance angle.

[2] It also neglects the effect of OLTC action at the upstream substation that acts to mask the impedance of the higher voltage networks. This is not likely to lead to great inaccuracies, however, since the source impedance from the point of DG connection will be dominated by the line and transformer impedances at that voltage level.

Eq. 9.2 can be substituted for R_d into the first term of Eq. 6.4 to yield the following approximate expression for the allowable per-unit DG penetration limit at a given network location:

$$P_{DG} \approx \left(\frac{k}{\cos\varphi} \right) \times S_{Fault(pu)} \qquad (9.3)$$

Where: k = a constant given by the expression $V_{DG(Max)} \times (V_{DG(Max)} - V_{Setpoint})$. For networks with a 1.03pu voltage setpoint, and a maximum allowable busbar voltage of 1.05pu, k = 0.021.

Equation 9.3 can be used to understand the stipulation in some countries that the DG penetration must not exceed one twenty-fifth of the three-phase fault level at that location. This amounts to assuming a fault level angle of 58° and that k = 0.021 in Eq. 9.3. The more lenient stipulation in Spain, that the DG penetration can be as high as 10% of the fault level, is equivalent to assuming a fault level angle of 78°. The discussion of Section 4.1 indicated that source impedance angles in the characteristically weak distribution networks in South Africa approach 45° on account of the high conductor resistances. This suggests that, expressed using the second international method, DG penetration on MV networks in this country should be limited to one thirty-fourth of the fault level at the point of connection.

The discussion above indicates that the second international method for the generalised evaluation of network voltage rise can be well understood using the "new" generalised method. The international method is seen to be more pessimistic than the new approach, since it makes no provision for representing network load, or of the different DG control modes on DG penetration limits. The present study has shown the significance of the load term in Eq. 9.1 on the overall DG penetration limits, especially in weak networks where the fault levels (and hence no-load penetration limits) are lowest.

9.3 Case Studies

The application of the generalised approach to evaluating network voltage rise of Fig. 9.1 is demonstrated using two South African DG case studies.

CASE 1: Sugar mill A co-generation

A sugar mill in the Mpumalanga Province applied for co-generation rights in April 2002. The mill planned to generate up to 4MW onto the local 22kV network using one of its 8MVA (6.4MW) synchronous generators (refer to Fig. 9.2).

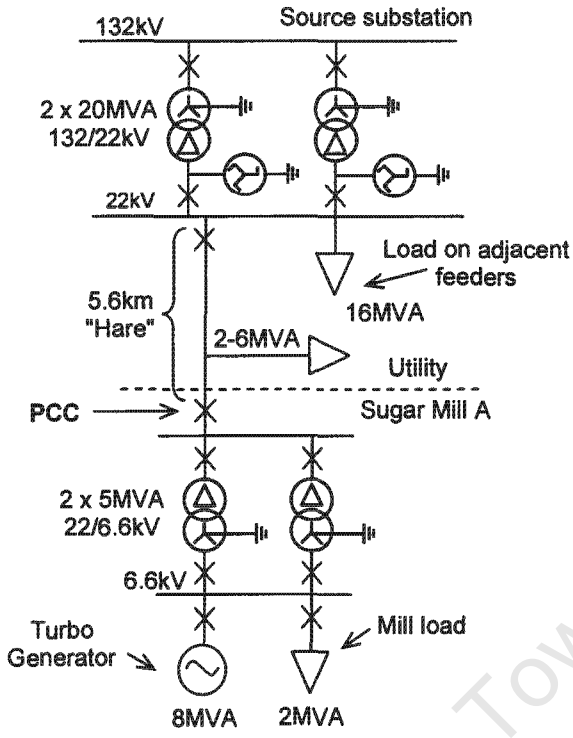

Fig. 9.2. Electrical network for Case 1: Sugar Mill A co-generation.

In Fig. 9.2, the maximum load on the mill feeder under normal operating conditions is 2MVA at a power factor of 0.87 lagging, although this is increased by up to 4MW when back-feeding an adjacent feeder. The load is tapped off the backbone two spans before the DG busbar, and to good approximation can be modelled at the DG busbar. The transformers at the source and mill substations are all fitted with OLTC functionality.

The first step of the generalised procedure of Fig. 9.1 reveals that the no-load DG penetration for this application is 5.6MW and thus that no overvoltage problems should be encountered for the proposed generator output. The DG proposal, with respect to voltage regulation, can thus be approved for generation at unity power factor. In practice, the co-generator would operate at a high lagging power factor so as to supply the reactive power load of the mill processes, but maintain the power factor at the Point of Common Coupling (PCC) close to unity.

Note that, by considering the effect of feeder load (given by term② in Eq. 9.1), the DG penetration limit can be increased to 6.2MW under normal operating conditions[3] and up to

[3] This figure is calculated under the assumption of a 20% load ratio (the ratio between maximum and minimum loading). This indicates that the standing load on the feeder is 400kVA. The load scaling factor for this feeder at a load power factor of 0.87 lagging can be calculated as 1.44 and thus load will add 580kW to the no-load penetration limit.

7.3MW in the event that the tie-point to the adjacent network is closed. Notice that as described in Section 4.4, the load that is drawn from the source substation busbar has no effect on the penetration limits on the DG feeder.

CASE 2: Sugar mill B co-generation

A second sugar mill has been co-generating up to 5MW onto the utility's 22kV network since 1996, although the generation is limited to 3MW under conditions of normal mill operation. Mill B is supplied via a dedicated 10.3km lateral that branches off the backbone 5.1km outside the source substation (refer to Fig. 9.3). Most of the 6MVA feeder load (at 0.9 lagging power factor) is situated downstream of the tee-off point of the lateral. As in Case 1, the source substation and mill transformers are fitted with OLTCs.

Operating experience with the co-generator indicated that the machine had a better chance of remaining on-line following the operation of the anti-islanding protection (that tripped the PCC breaker) in the event it was operated at a 0.95 *lagging* power factor with respect to the PCC. This operating mode was also favoured owing to ambiguity in the reactive power pricing tariff that lead the operator to believe that he would be charged for reactive power drawn during periods of co-generation.

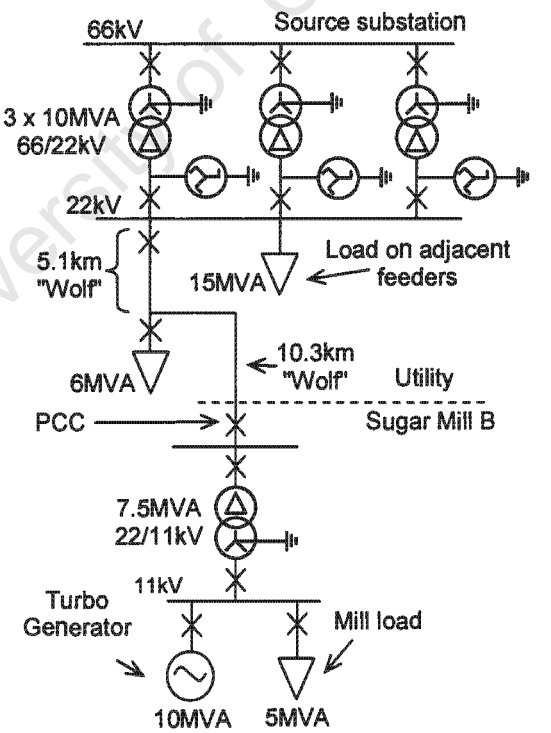

Fig. 9.3. Electrical network for Case 2: Sugar Mill B co-generation.

The no-load study for a DG located 15km from the source substation on a "Wolf" line indicates that up to 3.5MW of generation can be tolerated at UPF before the voltage at the PCC rises to 105% of nominal. The generation limit at UPF is increased by 1MW when 1.2MVA of load (corresponding to a 20% load ratio) is added 5.1km from the source substation in Eq. 9.1. This simple analysis indicates that up to 4.5MW of generation can be accepted from the Mill before the onset of an overvoltage condition at the PCC. Further analysis using Eq. 9.1 reveals that absorption of 300kVAr of reactive power by the mill's generator will raise the allowable penetration limit to 5MW. This corresponds to operation at a 0.998 leading power. The reactive power absorption of reactive power by the DG in this application is a particularly effective means of limiting network voltage rise on account of the uncharacteristically high (for a 22kV network) X/R ratio of the "Wolf" line.

Operation of the DG at a 0.95 lagging power factor, as occurred in practice, reduces the penetration limit to 3.7MW under minimum loading conditions and indicates that the busbar voltage at the PCC would have exceeded the 1.05pu limit under some operating conditions.

9.4 Chapter in Perspective

The "new" generalised method of voltage rise evaluation in DG applications is a practical tool that can be used in real-life projects. The method compares well with the two previously identified evaluation methods in terms of simplicity of application. It is an improvement on the existing methods by way of its ability to discretely represent different network parameters. This attribute allows the approach to be applied at different levels of complexity, depending on the solution accuracy required. The method also allows for the evaluation of the applicable voltage rise mitigation options.

Chapter 10
Lessons Learned

The answers to research questions posed in Chapter 1 were expected to facilitate the evaluation of the main hypothesis that an improved generalised method for the evaluation of DG-initiated voltage rise could be developed. Answers to these questions were developed over the course of the study, and are summarised in the first section of the present chapter. Thereafter, the hypothesis is assessed in the light of the research findings, and the scope for further research is identified.

10.1 Research questions answered

A number of questions relating to the main hypothesis of the research were raised in Chapter 1. Preliminary answers to these questions were found in the literature survey of Chapter 2 and were developed in the discussions of subsequent chapters. The answers to the questions are summarised below.

Which methods can be used to study the voltage rise effect?

A number of authors use complex, detailed network models to study DG-initiated voltage rise. Possibly as a result of the large number of variables required, no other studies were found that considered the generalised effect in a wider range of network types.

A simple 2-node model is used in a number of published studies to understand the basic mechanism of voltage rise. Limitations in the application of this method, however, have restricted its use to placing the voltage rise studies in context. The present study overcame these limitations by making three assumptions and applied the simple analysis technique to a more complex 4-node model. Comparison of the results with those from a traditional load-flow based method indicate that the "algebraic" approach is sufficiently accurate for most planning studies.

What is the limit of allowable voltage rise in electrical networks?

The extent of allowable voltage rise on a given network is governed by the setpoint voltage that is applied to the nearest upstream voltage regulator or OLTC, and by the limit for overvoltages on the network. In South Africa, setpoint voltages of 1.03 or 1.04pu are commonly applied, and network voltages in excess of 1.05pu are accepted only in emergency conditions. This gives rise to a narrow band of allowable voltage rise – typically 0.01 to

0.02pu, but most commonly 0.02pu. Similar ranges of allowable voltage rise are used in published studies from other countries.

Significantly, a new approach to voltage drop apportionment and MV/LV transformer OCTS setting in the Eskom's distribution system will restrict the extent of the allowable voltage rise in some MV networks. The new planning philosophy allows for significant savings in installation costs and/or increases in the carrying capacities of voltage-constrained MV and LV feeders. The increased voltage profile of the feeder that results from the application of DG can jeopardise the application of the new philosophy, however, and in these cases could lead to a decrease in the overall carrying capacity of the feeder or extra costs to upgrade the network. It is unlikely that the new Eskom planning philosophy, or an equivalent, has been applied in other countries and it would thus appear that this constraint on DG is unique to South Africa.

To what extent can the fault level at a busbar be used to determine the degree of the voltage rise problem at that location?

The three-phase fault level at a busbar provides a good indication of the source impedance seen from that point. In this way, the fault level indicates the relative "strength" or "stiffness" of the network and can be used as an indicator of the maximum amount of load of a given type that can be connected at a certain location without causing quality of supply problems. The fault level-based approach to calculating DG penetration limits appears to be based on a similar principle, although no information could be found regarding the calculation of the limits specified by either approach. The "new" approach to studying voltage rise that was developed in this thesis can, however, be used to understand the origins of the fault level based limits of DG penetration, and could possibly also be used to understand the broader application of the approach.

The use of the three-phase fault level as an indication of the allowable DG penetration limit at a given location is pessimistic on account of the fact that it neglects the influence of network load. The studies of Chapter 7 indicate that the presence of load on the DG feeder can bring about large percentage increases in the no-load DG penetration limits (or those based on the fault level at the DG's point of connection).

How is adequate regulation of voltage attained in passive distribution systems?

Voltage control in distribution networks is principally achieved through the application of transformer tap changers (OLTCs and OCTSs), voltage regulators and shunt- and series capacitors or reactors. Shunt reactors could be applied in an effort to curb DG-initiated voltage rise, but bring about an increase in network losses. This option is similar to that of having a synchronous DG operate at a leading power factor. Series reactors are unlikely to find application in DG-installed networks, since they would have to be removed from service during periods of non-operation of the DG.

To what extent are classical voltage regulation methods appropriate for the mitigation of voltage rise in DG-installed networks?

Voltage regulators and OLTCs using traditional fixed setpoint control can successfully regulate the voltage at the chosen busbar, irrespective of the direction of power flow. This is a result of the grid dictating the source voltage. Advanced control algorithms such as Line-Drop Compensation (LDC) and Negative Reactance Compounding (NRC) will be negatively affected by the presence of DG. This can be minimised in the case of NRC through having the DG operate at a lagging power factor, although this is not supported by tariff structures, and may give rise to overvoltages on the network.

The presence of an OLTC at the source substation does not significantly increase the penetration limits for DGs on its feeders. This is because, although high with respect to those in other countries, the source impedances seen from substation busbars in South Africa are low relative to the impedances of the lines connecting DGs to the source substation. Also, the highly reactive nature of source impedances dictate that relatively little voltage rise will be experienced in the event that the DG,s real power output is exported back through the source substation transformers. It is thus not critical that the source substation be fitted with OLTC functionality for DG applications on the feeders to be viable.

Voltage regulators are a good prospect for the mitigation of DG-initiated voltage rise. LDC techniques that are not often viable in substation OLTC applications can more readily be applied to voltage regulators, and can lead to further mitigation of the voltage rise phenomenon.

What control mode options are available to synchronous DG operators?

Although others are available, the most commonly-applied control modes for synchronous DGs are constant power factor or constant reactive power (PF/VAR) mode and voltage feedback control. Modern excitation control relays include a number of additional features that may be beneficial in DG applications, including the ability to automatically switch between control modes, and the ability to operate outside the machine's capability limits for short periods.

What factors influence the choice of DG control mode?

Control mode selection for synchronous DGs must include consideration of the tariff for reactive power generation or absorption by the DG, generator stability, and machine and network losses. Worldwide, there is currently little clarity regarding the optimal form of a reactive power tariff for DGs, and most are inappropriately based on tariffs for passive networks. There is no clear ruling regarding reactive power pricing for DGs in South Africa apart from disallowing reactive power generation. Generation at lagging power factors is, however, advantageous from the utility's perspective in minimising network losses and

minimising the influence of the DG on OLTCs using the NRC parallel control technique, although it can give rise to overvoltages in the network.

The absence of a tariff for reactive power absorption by DGs indirectly encourages generators in South Africa to operate at leading power factors so as to mitigate against voltage rise. This practice will, however, increase machine and network losses and may jeopardise the stability of the machine during fault conditions on the network. The ability of a generator to maintain the DG busbar voltage within limits using voltage control mode may also be constrained by its limited capability to absorb reactive power.

Neglecting the possible participation of the DG in network voltage control, the optimal control mode for DGs is at constant, unity power factor. In this regard, co-generators commonly operate at high lagging power factors so as to supply embedded reactive power load, but generate at unity power factor with respect to the point of connection to the distribution network.

10.2 Assessing the Hypothesis

Answers to the research questions above facilitated the evaluation of the main hypothesis that was proposed in Chapter 1. The hypothesis stated that:

> *It is possible to improve the existing generalised methods for the evaluation of the influence of synchronous DGs on the steady-state voltage regulation of radial distribution networks to which they are connected. By design, the improved process should remain simple to implement; relying on data that is readily available, yet its results should not be overly conservative. The method should be useful in seeking realistic solutions to the voltage rise problem.*

The "new" approach to evaluating voltage rise that was developed in this thesis was based on a 4-node network model. Despite its simplicity, the model is representative of a wide range of DG applications on radial feeders, including feeders with "tapering" conductors and non-homogenous load distribution.

Algebraic solution of the model network revealed that the allowable DG penetration at any location on the feeder (based on the voltage rise constraint) could be calculated as the sum of three terms. These include (i) a term that is independent of network load, (ii) a load term, and (iii) a term representing the reactive power generation or absorption by the DG. The algebraic solution equation forms the basis for a procedure to evaluate voltage rise in DG-installed networks. The three-part format of the equation allows the DG penetration limit to

be calculated to an increasing degree of accuracy, depending on the amount of data available, and the objective of the study.

Simplicity of application. Even at the most detailed level, the input data required by the "new" voltage rise evaluation process is limited to summated statistical metering data for the DG feeder and basic information regarding the voltage level, conductor type and location and proposed output of the DG. The method can also be used to study the effect of various voltage rise mitigation options, including the possible application of a voltage regulator on the DG feeder. In the latter case, the generalised method is, however, limited to a regulator that uses conventional fixed setpoint control.

Accuracy of results. The results of the "new" generalised method were compared with those derived using a traditional load-flow technique and were found to be accurate to within 7% under most network conditions. Significantly, the "new" method was most accurate for studies on networks with low X/R ratios and under light loading conditions. These are two characteristics typical of rural feeders in South Africa, and corresponds to the network types that are most constrained by the voltage rise phenomenon.

Improvement on existing generalised methods. The "new" generalised method can be used to understand the origin of the fault-level based approach to voltage rise evaluation. In making provision for the effect of network load and DG control mode on penetration limits, the "new" method is also an improvement over the existing approach. Simulations have shown the importance of representing the influence of feeder load, particularly on weak networks where the "no-load" penetration term is small.

The results of the "new" method compare well with the tabulated penetration limits of the existing voltage level/location-based generalised method. The "new" method can, however, be better adapted to specific DG applications and will provide more realistic penetration figures as a result.

The "new" voltage rise evaluation method is unique in its ability to determine the influence of specific network parameters on the voltage rise phenomenon and is able to provide answers to two of the remaining questions from Chapter 1:

Which network parameters are most important in determining the extent of the voltage rise problem in DG applications?

The voltage level at which the DG is connected is the most significant factor determining the extent of network voltage rise. DG penetration limits for non-loaded feeders increase with the square of the voltage level. This is in contrast to the thermal ratings of feeders that increase in proportion to a single power of the voltage level and indicate that feeders become less voltage constrained (and more constrained by the thermal limits of their conductors) at higher voltage levels. No-load penetration limits for DG also vary in proportion to the allowable limit

for voltage rise on the feeder, and in an inverse relationship with the resistance per-unit length of the conductor and the distance of the DG from the source substation. The latter property results in the no-load DG penetration limits being halved as the distance of the machine from the source is doubled.

Load on the DG feeder has an additive effect on DG penetration limits, although its influence is dependent on the load's location. Load located at or downstream of the DG has the greatest effect. Significantly, load on adjacent feeders (to the DG feeder) at the source substation has no effect on DG penetration limits where the source busbar is regulated by OLTC action, and little effect where no OLTC or regulator is installed. Reducing the (lagging) load power factor has a multiplicative effect on the load term, with lagging power factor loads having the greatest effect on DG applications on higher voltage and higher capacity feeders. Overall, however, the effect of load on DG penetration limits is most pronounced on weaker networks since the no-load term is reduced significantly with respect to that on stronger systems. It must be borne in mind, however, that the extent of allowable loading on weak networks is limited by voltage drop considerations in the absence of DG, and that these are affected by the same parameters that govern voltage rise in the presence of DG.

Reactive power absorption by the DG has an additive effect on the DG penetration limit, although this varies in proportion to the X/R ratio of the feeder. Operation of the DG at a leading power factor has a multiplicative effect on the overall penetration limit, but again is dependent on the X/R ratio of the feeder and is thus more effective on DG applications on higher voltage, higher capacity feeders.

Which is the optimal method for the mitigation of network voltage rise in typical DG applications?

The optimal method of voltage rise mitigation varies between applications. The option of re-conductoring a portion of the feeder is attractive for applications on MV networks where the DG is located within 5km of the source substation, or in the less likely event of voltage rise problems with applications on HV networks. This option has the added benefit of increasing the thermal capacity of the network, as well as raising the voltage-based penetration limits.

Operation of the DG at a leading power factor is an effective method of voltage rise mitigation on higher voltage, higher capacity feeders. This option will, however, give rise to increased network losses and is difficult to evaluate in the absence of clear policies regarding loss allocation between the utility's customers and pricing of reactive power absorption by DGs.

The option of increasing feeder load by using the DG feeder to back-feed an adjacent network is an effective means of increasing DG penetration limits. This option may, however, give rise to quality of supply and protection grading problems and may result in low voltages at customer supply points during times when the DG is out of operation.

DG applications on MV networks where the generator is located at an intermediate location from the source substation – between 5km and 20km on a 22kV network, and closer-in on a lower voltage feeder – will benefit most from the application of a voltage regulator. This solution is advantageous as a result of the fixed cost of a voltage regulator installation compared with the price of a network upgrade that varies with the length of the affected line section.

Installing a voltage regulator on the DG feeder, or upgrading the conductor to one of heavier gauge has a multiplicative effect on the no-load DG penetration limits on the feeder. These methods will thus be significantly less effective in DG applications on 22kV networks where the generator is located farther than 15km or 20km from the source substation. On 11kV systems, this limit is reduced to between 7km and 10km from the source substation. This is on account of the low no-load penetration limits encountered at these locations. Constraining the generator to operate during periods of heavier feeder loading is probably the only viable mitigation option available to DGs located this far and further from the source substation. This option might in any case be optimal for operators of smaller capacity machines, since voltage rise mitigation is achieved without capital expenditure, and the DG is only constrained during off-peak periods where the market price for power generation is at its lowest.

10.3 DG-initiated Voltage Rise in South Africa

This research has confirmed the initial suspicion that the extent of DG-initiated voltage rise will be exaggerated under typical South African network conditions – long, sparsely loaded feeders of relatively thin-gauge conductor. Ominously, the research also indicates that the options for voltage rise mitigation are less effective under these conditions and, as a result, the output of many DGs may need to be constrained to prevent excessive voltage rise. It is concluded the voltage rise phenomenon will form a key constraint in many local DG applications.

It is fortunate that most co-generation schemes currently in service on South African distribution networks appear to be connected to relatively strong feeders. This is on account of their notified load requirements in event of loss of generation. Even so, Case Study 2 from Chapter 9 demonstrates that generation to the machine's capability can raise busbar voltages very near to, or above the limit statutory value.

The results of this study demonstrate the importance of considering the effect of DG operation on the steady-state voltage regulation of the feeder when evaluating proposals for DG. While it is standard practice for planners to consider feeder voltage drops when evaluating plans for the connection of new loads, there is no record of voltage rise studies having been performed in the evaluation of similar scale proposals for generation onto the networks. Some co-

generator operators also appear to be unsure of the effect of real and reactive power generation on busbar voltages in the distribution network to which they are connected.

10.4 Scope for further Research

This research into the extent of the DG-initiated voltage rise effect and the options for its mitigation has identified a number of areas requiring further research. These include:

- developing a reactive power tariff for DGs. This tariff should reflect the cost of increased network losses when DGs operate at leading power factors, and should consider the possibility of overvoltages arising from lagging power factor generation. The development of a reactive power tariff is closely related to that of loss allocation between customers as applied in some European countries;

- investigating the apparent correlation between neglecting the quadrature voltage change term δV and restricting allowable network losses in the derivation and application of the "new" generalised method;

- extending the generalised evaluation method to include alternative generator technologies and meshed network topologies;

- developing an understanding of the interaction of a generator transformer OLTC controller and the excitation control system of a synchronous DG in regulating the reactive power output of a DG installation; and

- investigating the possible application of LDC techniques to voltage regulators that are installed on DG feeders as a means to further mitigate network voltage rise.

10.5 Conclusion

The extent of the voltage rise problem in weak distribution networks has implications for DGs, not only in South Africa, but also in other countries. The phenomenon is likely to be especially prevalent in DG projects in other African countries whose networks are expected to be significantly weaker and more sparsely loaded than those in South Africa. The reduced efficiencies of the voltage rise mitigation options under these network conditions also bodes poorly for the widespread application of DG that is often also limited by high installation and operational costs.

Co-generators appear to be less affected by voltage rise on account of their being supplied from relatively strong feeders. These applications should nevertheless also be carefully evaluated in terms of possible steady-state voltage problems arising from their operation.

References

Beukes, H.J.; Stephen, R.; Meyer, B.; Van der Merwe, F.S. (2001). "Innovative Opportunities in Distribution Network Planning and Design", course notes from the University of Stellenbosh, South Africa, November.

Cacioli, L.; Invernizzi, G.; Lionetto, P.F. (2001). "Relaying Problems in the Connection of Dispersed Generation Plant to the 132kV Network" in Proc. of the IEEE Developments in Power System Protection Conf., Conference publication No.469, April 2001, pp86-9.

Carter-Brown, C.G. (2002a). "Optimal Voltage Regulation Limits and Voltage Drop Apportionment in Distribution Systems" in Proc. of the Eleventh Southern African Universities Power Engineering Conf., SAUPEC 2002, Vaal Triangle Technikon, Vanderbijlpark, 31 Jan.

Carter-Brown, C.G. (2002b). "Eskom Standard: SCSAGAAU7 rev 0 – Reticulation planning Guideline: Step-voltage regulators", February.

Carter-Brown, C.G. (2002c). "Eskom Standard: SCSASACN7 rev 0 – Distribution voltage regulation and apportionment limits", October.

Carter-Brown, C.G.; Gaunt, C.T. (2003). "Increasing Network Capacity by Optimising Voltage Regulation on Medium and Low Voltage Feeders" in Proc. 17th International Conf. on Electricity Distribution (CIRED), Paper No. 5-27.

Cigré (1999). "Impact of Increasing Contribution of Dispersed Generation on the Power System", Final Report by Cigré Working Group 37.23, February.

Cigré (2002). "Economic and Technical Interaction between Dispersed Generation and Power System", Draft Report by Cigré Task Force 38.06.03, August.

Crous, J. (2000). "Eskom directive: ESKPBAAG1 rev 1 – Pricing of self-dispatched non-Eskom generation", March.

De Jongh, A. (2001). "Eskom Standard: SCSASAAU3 rev 0 – Protection Standard: Substation automatic voltage regulation philosophy", September.

Ferguson, I.A. (2003). "Draft Eskom Standard: SCSASACP2 – Network Planning Philosophies and Criteria", February.

Gaunt, C.T.; Van Zyl, S.J.; Mabuza, S.; Simelane, S. (2002). "Definition and scope of application of Distributed Generation in South Africa", Eskom Research report.

Glover, J.D.; Sarma, M. (1994). "Power System Analysis & Design", PWS Publishish Company, Boston.

Heathcote, M.J. (1998). "J&P Transformer Book", 12th Ed, Newnes, Oxford.

IEEE P1547/D07 (2001). "Draft Standard for Interconnecting Distributed Resources with Electric Power Systems", IEEE Standards Co-ordinating Committee 21, February.

Ippolito, M. G.; Morana, G.; Riva Sanseverino, E.; Vuinovich, F. (2003). "Risk Based Optimization for Strategical Planning of Electrical Distribution Systems with Dispersed Generation" in Proc. of IEEE PowerTech 2003 Conf., Paper No. BPT03-27, Bologna, Italy, pp1-8.

Jenkins, N.; Allan, R.; Crossley, P.; Kirschen, D.; Strbac, G. (2000). "Embedded Generation", IEE Power and Energy Series 31, Institute of Electrical Engineers, London.

Kiprakis, A.E.; Wallace, A.R. (2003). "Hybrid Control of Distributed Generators connected to Weak rural Networks to Mitigate Voltage Variation" in Proc. 17th International Conf. on Electricity Distribution (CIRED), Paper No. 4-44.

Mabuza, S.; Gaunt, C.T. (2002). "Stability of Distribution networks connected with Distributed Generation", Eskom Research report RES/RR/02/19752.

Masters, C.L. (2002). "Voltage rise: the big issue when connecting embedded generation to long 11kV overhead lines", IEE Power Engineering Journal, February, Vol 16 No.1, pp5-12.

McCann, G.D. (1950). *Regulation and Losses of Transmission Lines* in "Electrical Transmission and Distribution Reference Book", 4th Ed, Rev. by Lawrence, R.F., Westinghouse Electric Corporation, Pennsylvania.

Moor, P. (2001). "Unitrol 1000 Automatic Voltage Regulator User's Manual", Revision 2, ABB Industrie AG document no 3BHS121514 E80, 30 Aug pp1-71.

NRS 048 (1996). "NRS048: Electricity Supply – Quality of Supply. Part 2: Minimum Standards," South African Bureau of Standards.

Pandiaraj, K.; Hodgkinson, G.; Fox, B. (2000). "Use of Embedded Generators for Voltage Support in Rural Distribution Networks" in Proc. of the 35nd Universities Power Engineering Conf., Queens University, Belfast, Ireland, pp1-4.

Persaud, B.; Fox, B.; Flynn, D. (1999). "The Effects of Embedded Wind Generation on Automatic Voltage Control in Radial Distribution Networks" in Proc. of the 34th Universities Power Engineering Conf., University of Leichester, UK, pp365-8.

Redfern, M.A.; Checkersfield, M.J. (1998). "A new solution for the problems experienced with pole slipping protection", IEEE Transactions on Power Delivery, Vol 13, No.2, April. pp394-405.

Repo, S.; Laaksonen, H.; Järventausta, P.; Huhtala, O.; Mickelsson; M. (2003). "A Case Study of a Voltage Rise Problem due to a Large Amount of Distributed Generation on a Weak Distribution Network" in Proc. of IEEE PowerTech 2003 Conf., Paper No. BPT03-51, Bologna, Italy, pp1-6.

Salman, S.K.; Jiang, F.; Rogers, W.J.S. (1996). "Investigation of the operating strategies of remotely connected Embedded Generators to help regulating local Network Voltage", Opportunities and Advances in International Power Generation, 18-20th March. IEE Conf. Publication No. 419, pp180-5.

Sellick, N. (1998). "Financial Analysis - Standby generators for load management", Eskom Research report TRR/NGE98/003.

Sen, P.C. (1989). "Principles of Electric Machines and Power Electronics", John Wiley and Sons, New York.

Thomson, M. (2000a). "Automatic-voltage-control relays and embedded generation Part 1", Power Engineering Journal, April, pp71-76.

Thomson, M. (2000b). "Automatic-voltage-control relays and embedded generation Part 2", Power Engineering Journal, June, pp93-99.

Topham, G.H. (1995). "Eskom Guide: ESKAGAAG2 rev 1 – Minimum Requirements for the connection of non-Eskom generating plant to the Eskom electrical networks", September.

Weedy, B.M. (1994). "Electric Power Systems", 3rd Edition revised. John Wiley and Sons, New York.

Index of Figures

Index of Tables

Appendix A
The Per-Unit System

In this thesis, as is common when analysing power networks, electrical parameters are expressed in the per-unit (pu) system rather than using the actual values (in SI units, for example).

A.1 The Per-Unit System [Weedy, 1994, p.72-4]

In the per-unit system, network parameters are expressed as fractions of reference or "base" quantities:

$$\text{per - unit quantity} = \frac{\text{actual quantity}}{\text{base value of quantity}}$$

This is done for three principle reasons:

1. By choosing appropriate voltage bases, the solution of networks containing transformers is greatly simplified,
2. The use of root-three coefficients in calculations is reduced (as in the equation for apparent power described below), and
3. Per-unit values lend themselves more readily for automatic computation (as in the Gauss-Seidel load-flow program described in Chapter 6).

When using the per-unit system, it is common to select a fixed three-phase power base, $S_{Base(3\phi)}$, for the network under study and differing phase-to-phase voltage bases, $V_{Base(\phi-\phi)}$, corresponding to the nominal voltage levels of the different sections of network (where applicable). As is common practice in the industry, a 100MVA power base is used throughout this thesis. Base values for line currents, I_{Base} and branch or load impedances, Z_{Base}, are then calculated as follows:

$$I_{Base} = \frac{S_{Base(3\phi)}}{\sqrt{3} \times V_{Base(\phi-\phi)}} \qquad (A.1)$$

and

$$Z_{Base} = \frac{V^2_{Base(\phi-\phi)}}{S_{Base(3\phi)}} \qquad (A.2)$$

Equation A.1 can be used to prove that the following identity that is used in Section 3.1.1 in the derivation of the voltage regulation equations:

$$S_{Actual} = \sqrt{3} \times V_{Actual} \times I_{Actual} \quad \Leftrightarrow \quad S_{pu} = V_{pu} \times I_{pu}$$

Notice that the customary root three co-efficient is neglected when working with per-unit quantities rather than actual values.

Appendix B

The Gauss-Seidel technique of Load-Flow Solution

The Gauss-Seidel method of load-flow solution was used in this study to provide an accurate solution of the 4-bus model network of Section 6.1.3. Details regarding the application of the Gauss-Seidel technique are provided below.

B.1 The Gauss-Seidel Method of Load-Flow Solution [Weedy, 1994, p.223-5]

In the Gauss-Seidel method, the network branch impedances are resolved into a matrix of admittances. The voltages at all nodes other than that at the swing bus (that is already known) are assumed at some initial value. The load-flow equation presented as Eq. B.1 below is then applied successively to each node (excluding the swing bus) to obtain a better approximation of the node voltages.

The load-flow equation for the $(p\text{-}1)^{th}$ recalculation of the voltage at node k with real (P_k) and reactive (Q_k) load/generation specified, and based on the latest calculated voltage values at the other nodes, i, is stated here without proof as[1]:

$$\overline{V}_k^{(p+1)} = \frac{1}{\overline{Y}_{kk}}\left[\frac{P_k - jQ_k}{\overline{V}_k^{*(p)}} - \sum_{\substack{i<k \\ (i\neq k)}} \overline{V}_i^{(p+1)} \times \overline{Y}_{ki} - \sum_{\substack{i>k \\ (i\neq k)}} \overline{V}_i^{(p)} \times \overline{Y}_{ki}\right] \qquad (B.1)$$

where the admittance matrix, $[\overline{Y}]$, is derived as follows:

Diagonal elements: $\overline{Y}_{ii}$ = the sum of all admittances terminating at bus i; and

Off-diagonal elements: $\overline{Y}_{ij}$ = the negative of the series admittance between buses i and j.

The variables P_k and Q_k represent the real and reactive power load connected at node k. The term (p) or (p+1) that is presented as a superscript on all the voltage variables indicates the version of the node voltage approximation to use and are shown in parenthesis to distinguish them from powers.

The application of Eq. B.1 to the solution of the radial 4-bus load-flow problem of Fig. B.2 is demonstrated by way of example below.

---

[1] Details regarding the derivation of Eq. 6.1 are included in Weedy [1994, p223-5].

Step 1: Derivation of the Admittance matrix

The elements of the complex 4 x 4 admittance are calculated as described above. The third diagonal element, $\overline{Y}_{33}$, for example, is:

$$\overline{Y}_{33} = \frac{1}{Z_{L1}\angle\theta_L^\circ} + \frac{1}{Z_{L2}\angle\theta_L^\circ}$$

and the off-diagonal elements, $\overline{Y}_{34}$ and $\overline{Y}_{43}$ are calculated as follows:

$$\overline{Y}_{34} = \overline{Y}_{43} = -\frac{1}{Z_{L2}\angle\theta_L^\circ}$$

In a radial network, each node is connected to only one predecessor- and one successor node. Thus, all matrix elements that do not neighbour a diagonal element, and which are not diagonal elements themselves have value zero i.e. for $i \in [1,2]$, $\overline{Y}_{i(i+2)} = \overline{Y}_{(i+2)i} = 0$

Step 2: First recalculation of the node voltages, V_k

The voltage at node 2 is recalculated using Eq. B.1. For the 4-bus system described above, this can be expressed as:

$$\overline{V}_2^{(1)} = \frac{1}{\overline{Y}_{22}}\left[\frac{P_2 - jQ_2}{\overline{V}_2^{*(0)}} - \overline{V}_1^{(1)}\overline{Y}_{21} - \left(\overline{V}_3^{(0)}\overline{Y}_{23} + \overline{V}_4^{(0)}\overline{Y}_{24}\right)\right]$$

Since $\overline{Y}_{24} = 0$, this simplifies to:

$$\overline{V}_2^{(1)} = \frac{1}{\overline{Y}_{22}}\left[\frac{P_2 - jQ_2}{\overline{V}_2^{*(0)}} - \overline{V}_1^{(1)}\overline{Y}_{21} - \overline{V}_3^{(0)}\overline{Y}_{23}\right]$$

The first recalculation of the node 2 voltage uses the assumed values for the voltages at the downstream nodes. Node 1 is the swing bus and its voltage is fixed. Thus $\overline{V}_1^{(0)} = \overline{V}_1^{(1)} = \overline{V}_1^{(n)}$. The voltage at node 3 is recalculated in a similar manner, but uses the updated node 2 voltage value:

$$\overline{V}_3^{(1)} = \frac{1}{\overline{Y}_{33}}\left[\frac{P_3 - jQ_3}{\overline{V}_3^{*(0)}} - \overline{V}_2^{(1)}\overline{Y}_{32} - \overline{V}_4^{(0)}\overline{Y}_{34}\right]$$

The same procedure is followed to recalculate the voltage at node 4. The recalculation of the entire set of busbar voltages in this manner constitutes a single iteration of the solution process.

Step 3: Perform further iterations of node voltage calculations

The procedure of Step 2 is repeated, but using the latest estimates for the node voltages. Weedy [1994, p.225] describes how it is normal for the iteration process to be continued until the value of $\overline{V}^{(p+1)}$ at every node differs from the corresponding value from the previous iteration, $\overline{V}^{(p)}$, by less than a specified amount. The figure 0.0001pu is commonly used as this tolerance of convergence. In this way, the iteration procedure yields values for the magnitude and angle of the voltage at each node relative to that at the swing bus.

In networks that include low impedance branches, a more onerous convergence criterion is to consider the difference in calculated branch power flows between iterations. With the approximate node voltages known, branch power flows within the model network can be calculated using simple linear analysis similar to that described in Chapter 3. Equations 3.1 and 3.2 from Section 3.1 can be combined to yield the following equation for the apparent power, $\overline{S}_{ij}^{(p)}$, that flows between nodes i and j, based on the latest approximation of the node voltages, $\overline{V}^{(p)}$, and the branch impedance, $\overline{Z}_{ij}$:

$$\overline{S}_{ij}^{(p)} = \left[\frac{\overline{V}_i^{*(p)} \times \left(\overline{V}_i^{(p)} - \overline{V}_j^{(p)}\right)}{\overline{Z}_{ij}}\right]^* \qquad \text{(B.2)}$$

A convergence criterion of $\left|\overline{S}_{ij}^{(p+1)} - \overline{S}_{ij}^{(p)}\right| < 1\times10^{-6}$pu (for all $[i,j] \leq 4$) was used in the load-flow program of Section 6.2.2. The convergence tolerance of 1×10^{-6}pu corresponds to a power flow variance of less than 100VA between iterations, and provides accurate network solutions to within 1kVA.

B.2 Application of "Acceleration factors" to the Gauss-Seidel method

[Weedy, 1994, p.225]

The number of Gauss-Seidel iterations required to reach convergence can be reduced through the use of acceleration factors in the calculation procedure. By this method, termed "successive over-relaxation", each re-calculated node voltage is brought closer to its final value by adding a factor based on the difference in voltages between iterations. This is achieved using Eq. B.3 below.

$$^1\overline{V}_i^{(p+1)} = \overline{V}_i^{(p)} + \omega\left(\overline{V}_i^{(p+1)} - \overline{V}_i^{(p)}\right) \qquad \text{(B.3)}$$

In Eq. 6.3, ${}^{1}\overline{V}_i^{(p+1)}$ is the accelerated "new" voltage that is used in subsequent calculations instead of $\overline{V}_i^{(p+1)}$ and ω is the acceleration factor. Weedy describes how ω is usually specified as a real number and that a value of 1.6 is commonly used.

The method of successive over-relaxation could not, however, be applied on the 4-bus radial network of this study. This is because the application of acceleration factors quickly caused a previously convergent load-flow to diverge. Various different solutions to this were sought, including introducing the acceleration only after a given number of "standard" iterations, and using reduced acceleration factors. These measures were not able to curb the divergence of the accelerated load-flow, however, and it was concluded that acceleration factors are not appropriate for application on multi-node radial networks.

Appendix C

Further studies into the Accuracy of the Generalised Analysis

This section describes two series of simulations that were conducted to determine the accuracy of the algebraic solution of the network model of Section 6.1.3 relative to the more rigorous Gauss-Seidel load-flow program. The results of these studies are mentioned in Section 8.1 as part of the broader accuracy analysis of the algebraic method.

C.1 Effect of variable load power factor

Simulations were conducted on the four network types from Section 8.1.1 to determine the effect of variable load power factor on the accuracy of the algebraic solution method. The load magnitude in these simulations was assumed to be 2MVA in the 22kV simulations and 10MVA at 88kV. The load power factor was assumed at 0.95, 0.90 and 0.85 lagging for each network type. Simulations were conducted with high load magnitudes since, from the studies in Section 8.1.1, this increases the discrepancy between the algebraic and Gauss-Seidel solution methods and would make more noticeable variations in their relative accuracy with varied power factor.

Figures indicating the percentage accuracy of the algebraic solution method as compared to the Gauss-Seidel results for varying load power factor are presented in Table C.1 below. Notice that the data in the "0.95 lagging" power factor column is the same as that presented in the "2MVA" and "10MVA" load columns in Table 8.1 for 22kV and 88kV simulations respectively.

Table C.1. Percentage error of the algebraic solution for different load power factors.

	Percentage underestimation by the algebraic solution method		
Case	**0.95 lagging**	**0.90 lagging**	**0.85 lagging**
22kV Rabbit	1.8 - 3.9	1.8 – 4.5	2.0 – 4.8
22kV Hare	2.5 - 5.1	2.2 – 5.7	2.5 – 5.8
88kV Hare	2.1 - 3.5	2.2 – 3.7	2.3 – 3.9
88kV Wolf	4.7 - 6.1	4.7 – 6.6	4.7 – 7.0

It is clear from the results in Table C.1 that variation of the load power factor has only a slight effect on the accuracy of the algebraic solution method. In all of the study cases, the change in accuracy is less than one percent and it can be concluded that the algebraic method

remains an accurate approximation to the Gauss-Seidel method for a wide range of load power factors.

C.2 Composite accuracy of the algebraic solution method

A further two studies were conducted in an effort to identify the worst-case accuracy statistics for the algebraic solution method. This was to be achieved by combining the most onerous network conditions from the discussions of Sections 8.1.1 and 8.1.2. These sections identified high load magnitude, low lagging load power factor, low leading generator power factor and high feeder X/R ratios as the most onerous network conditions for the accuracy of the algebraic solution method. The following networks can thus be considered as comprising the worst-case conditions for the accuracy of the algebraic solution method:

1. A 22kV "Hare" line, 50km long, with 2MVA of uniformly distributed load at 0.85 lagging power factor and with the DG operating at a fixed leading power factor of 0.95.

2. An 88kV "Hare" line, 50km long, with 10MVA of uniformly distributed load at a lagging power factor of 0.90. The DG operates at a fixed leading power factor of 0.95.

Percentage error statistics for the results of the algebraic solution from the two worst-case networks are presented in Table C.2 below. Also presented for comparison in Table C.2, are the results from Appendix C.1 and Section 8.2.2 for the studies considering separately the effect of lagging power factor load and leading power factor generation on solution accuracy.

Table C.2. Worst-Case error of the algebraic solution method.

	Percentage underestimation by the algebraic solution method.		
Case	**Load only***	**Gen pf only****	**Composite Network**
22kV "Hare"	2.5 – 5.8	6.2	8.4 – 26.6
88kV "Hare"	2.2 – 3.7	12.1	13.0 – 23.7

*Data derived from Table C.1.

** Data from Table 8.2.

The results in Table C.2 indicate that the underestimation of the DG penetration limit by the algebraic solution method is comparable the results of Table 8.2 for machines located near to the source substation. The accuracy of the algebraic method is greatly diminished for machines located near the end of the line, however. Deeper analysis indicates that this effect corresponds to a drastic increase in line losses as the DG moves farther from the source substation, and is similar to that noted with leading power factor generation onto high voltage networks in Section 8.1.2.